Lotus japonicus SYMREM1 is a novel signalling component involved in symbiotic nitrogen fixation

A thesis submitted for the degree of Doctor of Philosophy
of Eötvös Loránd University

Katalin Tóth

Doctorate School in Biology, Head of the School: Prof. Dr. Anna Erdei, PhD
Member of Hungarian Academy of Sciences

Classical and Molecular Genetics Ph.D. Program,
Head of the Program: Prof. Dr. László Orosz, DSc
Member of Hungarian Academy of Sciences

Ph.D. advisers:

Zsuzsanna Buzás, PhD
National Institute of Pharmacy, Budapest, Hungary

Thomas Ott, PhD
Institute of Genetics, Faculty of Biology, University of Munich, Germany

Eötvös Loránd University, Faculty of Science, Department of Genetics
Budapest, Hungary

2012

Table of Contents

Abbreviations

3-AT – 3-amino-1,2,4-triazole
aa – amino acid(s)
Ade – adenine sulphate
Alg5 – yeast resident ER (control) protein for SUS
AM – arbuscular mycorrhiza
BiFC – Bimolecular Fluorescence Complementation
BLAST – Basic Local Alignment Search Tool
bp – nucleic acid base pair(s)
CaMV 35S – cauliflower mosaic virus constitutive 35S promoter
ccdB – toxin targeting DNA gyrase
CDS – coding sequence
CFP – Cyan Fluorescent Protein
CLSM – Confocal Laser Scanning Microscopy
Cub – C-terminal half of the Ubiquitin molecule
DMI2 – Does not Make Infection 2
dpi – day(s) post infiltration/infection
DsRed – Red fluorescent protein from *Discosoma sp.*
FL – full-length
FLIM-FRET – Fluorescence Lifetime Imaging Microscopy-Förster Resonance Energy Transfer
GFP – Green Fluorescence Protein
GUS – *beta-glucuronidase*
H – histidine
hpi – hours post inoculation
hyg – hygromycin
ID – identifier/identity/identification
IT(s) – infection thread(s)
kb – nucleic acid kilo base pair(s)
kDa – kiloDalton
L – leucine
LTS – Lotus Transformation Service, Institute of Genetics LMU
NF – Nodulation Factor
NFP – Nod Factor Perception
NFR1 – Nod factor receptor 1
NFR5 – Nod factor receptor 5
nm – nanometre(s)
No. – number
NubG – mutated N-terminal half of the Ubiquitin molecule
NubI – native N-terminal half of the Ubiquitin molecule
OD – optical density
ON – overnight

PIT – pre-infection thread
PM – plasma membrane
pUb –polyubiquitin promoter
Rcf – relative centrifugal force
RLK(s) – Receptor-like kinase(s)
RNS – root nodule symbiosis
Rpm – rotations per minute
RT – room temperature
SD – synthetic drop-out medium
SM – symbiosome membrane
SUS – split-ubiquitin (yeast) system
SV – sand-vermiculite
SYMRK – SYMbiosis Receptor-like Kinase
T-DNA – transferred DNA
TF – transcription factor
Tg – teragram (e.g. 1Tg=1Megatonne)
TILLING – Targeting Induced Local Lesions IN Genomes
TM - transmembrane
UBP – ubiquitin-specific protease
W – tryptophan
wpi – week(s) post infection
wt – wild-type
X-Gluc – 5-bromo-4-chloro-3-indolyl-β-D-glucuronic acid
YFP – Yellow Fluorescent Protein
YFP_C – C-terminal domain of YFP
YFP_N - N-terminal domain of YFP

1. Introduction

1.1. The phenomenon of root nodule symbiosis

Beside water, plants require significant amounts of carbon dioxide, oxygen and further 14 elements for full nutrition. Insufficient availability of any of these elements results in drastically reduced plant growth and yield. Six out of the fourteen mineral elements (the macronutrients), N (nitrogen), P (phosphorus), Ca (calcium), K (potassium), S (sulphur) and Mg (magnesium) are necessary in larger amount for plants (White and Brown, 2010). Nitrogen together with carbon (C) represents essential nutrients for basic processes of the plant cell. Both serve as key components of amino acids and proteins and thus serve as building blocks of the whole cell machinery. Therefore supply of both nutrients is crucial for plant growth, development and life cycle (Zheng 2009). While C is obtained via photosynthesis, sources of N are limited. Plants can uptake N in form of nitrate (NO_3^-) and/or NH_4^+ (ammonium) via their root system (Zheng 2009), if they are available in the soil. Plants are able to form symbiotic associations with soil bacteria and fungi, by the help of which they can overcome nitrogen and other nutritional deficiency.

In nature symbiotic relationships are established when organisms of two different species live together and form an association. These interactions can be beneficial for both organisms (mutualism), "half"-beneficial when only one of the symbionts profits from the interaction (commensalism) or harmful for one of the partners (parasitism) as well (Burnie, 1994). A widely spread beneficial relationship is arbuscular mycorrhizae (AM) symbiosis that supply plants with P, N and S and further micronutrients. It represents probably the most widespread terrestrial symbiosis (Fitter, 2005; Kistner and Parniske, 2002) on which 70-90% of land plants participate and form endosymbiosis with fungi belonging to Glomeromycota (Schüßler *et al*., 2001; Parniske, 2008). In AM symbiosis the symbiotic fungi penetrates with their hyphae into the root cells maintaining endomycorrhiza. In contrast, in ectomycorrhiza the symbiotic fungi remain extraradial forming a tight network on the root surface (Parniske, 2008). AM-like symbiosis has been observed already in early land plants. Whereas the other well-known mutualistic association, the root nodule symbiosis (RNS) developed later within orders Fabales, Fagales, Cucurbitales and Rosales (Fa Fa Cu Ro) belonging to the Eurosids I (Kistner and Parniske, 2002).

RNS adds up to a total of approximately 200 million tons of nitrogen per year (Graham and Vance, 2003) that supply the majority of terrestrial biological nitrogen fixation (Zhang *et al*., 2009). It has not only ecological significance but it is also of outstanding agronomical importance. The symbiosis has been used for crop rotations in many agricultural traditions to enrich soils with organic nitrogen, and today it represents a significant part of sustainable agriculture. A broad range of agriculturally important plants possesses the ability forming RNS. Therefore, they do not have to be treated with fertilizer. Currently agricultural consumption of nitrogen fertilizers is around 90 Tg (teragram) per year (Good *et al*., 2004) that probably will be increased about 40 Tg in the next few decades to meet a condition of enough food production for the growing Earth´s population (Vance 2001).

In nitrogen-deficient soils, plants initiate and undergo RNS with their host-compatible bacteria (Hirsch, 1992). In the process of symbiotic nitrogen fixation (SNF), bacteria fix atmospheric nitrogen and supply the plants with ammonia (a form utilized by plants) and therefore they receive photosynthetic products (carbon and energy source) from their host (Ferguson *et al*., 2010). Plants belonging to the family of *Fabaceae* (legumes) establish such a symbiotic association with bacteria involving the genera: *Rhizobium*, *Mesorhizobium*, *Sinorhizobium*, *Bradyrhizobium*, and *Azorhizobium* collectively named rhizobia (Gage 2004). The tropical tree, *Parasponia* (family: *Ulmaceae*) is able to form symbiotic interaction with rhizobia as well (Appleby *et al*., 1983; Gualtieri and Bisseling, 2000). Other bacteria that belong to the actinomycetes and are called *Frankia* have also the ability to form root symbiosis with non-leguminous plants of families *Betulaceae*, *Elaegnaceae*, *Casuarinaceae*, *Rhamnaceae*, *Myricaceae*, *Coriariaceae*, *Datisticaceae* and *Rosaceae* also called ‘actinorhizal plants’ (Benson and Silvester, 1993). Both types of relationship result in formation of a new organ, called nodules that harbour the symbiotic bacteria and SNF takes place. However, nodules of these two interactions differ significantly in their anatomy and morphology (Benson and Silvester, 1993).

1.2. First dialogues between interacting partners of the legume-rhizobia symbiosis

Legumes under nitrogen starving conditions initiate the first steps of RNS, by attracting their symbiotic bacteria to enter the symbiosis. Secretion of plant exudates

(flavonoids) into the rhizosphere (Peters et al., 1986; Redmond et al., 1986) initiates molecular dialogues between the symbiotic partners. These compounds specify rhizobia, to select compatible bacteria from pathogens. Flavonoids attract bacteria to the host root and perception of them induces in rhizobia expression of a number of genes, called nodulation genes (*nod* genes). Binding flavonoids to the bacterial NodD protein activates transcription of the other, downstream *nod* genes (Mulligan and Long, 1985; Fisher *et al*., 1988; Fisher and Long, 1992; Perret *et al*., 2000). Common *nod* genes that are widely conserved among rhizobia (nod ABC; Lerouge *et al*., 1990) and host-specific *nod* genes (*nod H* and *nodQ*; Lerouge *et al*., 1990) can be distinguished. Products of host-specific *nod* genes determine nodulation of particular plants (Long, 1996). Activation of *nod* genes leads to catalyzing biosynthesis of the so-called nodulation factors (Mulligan and Long, 1989; Broughton et al., 2000; Perret *et al*., 2000), the rhizobial response elicited by the plant flavonoids (Schultze and Kondorosi, 1998; Broughton et al., 2000). Nod factors (NF) are lipochitooligosaccharide molecules comprised of an N-acetylglucosamine backbone. Strain-specific side-chains decorate the reducing and non-reducing end residues of this backbone (Lerouge *et al*., 1990; Dazzo *et al*., 1991; Long, 1996; D'Haeze and Holsters, 2002). These decorations determine the host range that can be infected by the individual rhizobial strains (Roche *et al*., 1991; Long, 1996). Perception of rhizobia and rhizobial NFs elicit a series of molecular, biochemical, cellular, physiological, morphological and developmental processes that lead to establishment of RNS.

1.3. Bacterial infection and nodule formation

After the first exchange of the plant (flavonoids) and bacterial signal molecules (NFs), formation of RNS continues with bacterial entry into the root cells and subsequent invasion of the newly formed root organ, the nodule. Following morphological and developmental changes can be observed microscopically: root hair deformation and curling, infection, primordium formation and subsequent nodule formation (Nap and Bisseling, 1990; Figure 1.1).

Rhizobia invade the root cells usually by intracellular root hair infection, more rarely, by an intercellular ‘crack-entry‘ invasion or by infections between epidermal cells (Oldroyd *et al*., 2011). In the case of root hair infection, bacteria attach to the root hair tip

(Figure 1.1A). It is assumed that root lectins might promote the adhesion of bacteria to the root hair (Diaz *et al*., 1995; Kijne *et al*., 1997). Attachment of bacteria causes early physiological events as responses to the compatible rhizobia/NF. Changes in calcium level (Ca^{+} flux) are accompanied by membrane depolarization and later on calcium oscillation (Ehrhardt *et al*., 1992; Ehrhardt *et al*., 1996; Downie and Walker, 1999; Oldroyd and Downie, 2004). Subsequent rearrangement of the root hair cytoskeleton (Timmers *et al*., 1999; Sieberer *et al*., 2005) includes rearrangements of actin filaments (Allen *at el*., 1994) and increased cytoplasmic streaming (Heidstra *et al*., 1994; Mylona *et al*., 1995). Membrane depolarization of root hairs is associated with an extra- and intracellular alkalinisation (Felle *et al*., 1996; Downie and Walker, 1999) as well. These physiological changes lead to root hair deformation (Figure 1.1A). Root hair formation and swelling on the root of *Vicia faba* leading to formation of so called tubercle (nodules) were already observed by Prof. H. Marshall Ward in 1887 (Ward, 1887; reviewed in Bauer 1981). Root hairs curl and capture bacteria attached to the tips (root hair curling) and form so called *shepherd's crooks* (tightly curled root hairs) containing a rhizobial microcolony (Esseling *et al*., 2003; Gage, 2004; Figure 1.1B).

At the site of entrapment, bacteria enter the root hair through the curl by degradation of the root hair wall starting infection of the epidermal root hair cell (Callaham and Torrey, 1981). As next step, infection thread (IT) growth is initiated by invagination of the plasma membrane at the site of infection (Figure 1.1B). Observations of bacterial entry via infection threads (root hair infection) were already made in the first decades of the 20th century (Thornton, 1930). Infection threads are tubular structures that distribute rhizobia from the root surface (epidermal root hair cell) into the cortex (Thornton, 1930; Dixon, 1964) that gives rise to the newly formed nodule primordia (Figure 1.1C).

During steps of the infection process in the epidermis, cortical cell layers below the infection site undergo cytological and morphological alterations. These alterations include cell division when mitosis of outer cortical cells is re-activated, following pericycle activation and subsequent activation of inner cortical cell divisions (Gage, 2004). As a result, nodule primordia are formed by newly divided cortical cells and nodule organogenesis is initiated (Figure 1.1C).

Determinate and indeterminate type of nodules can be distinguished within the legume-rhizobia symbiosis. Figure 1.1 summarizes the steps of infection and nodule formation in both types of nodules. In legumes that develop indeterminate nodules (like the

model organism *Medicago truncatula*, or pea/*Pisum sativum* and vetch/*Vicia sp*.), NF perception induces periclinal cell divisions in the pericycle followed by inner cortical cell proliferation (Brewin, 1991). While in legumes forming determinate nodules (like model organism *Lotus japonicus* or soybean/*Glycine max* and common bean/*Phaseolus vulgaris*), nodule primordium can be formed either in the middle root cortex (*L. japonicus*) or in the outer root cortex (*P. vulgaris*) (van Spronsen *et al*., 2001).

While the root cortex undergoes mitotic activity, infection threads grow towards emerging nodule primordia delivering the first rhizobia (Figure 1.1C). The penetration progress of infection threads is prepared by so-called pre-infection thread (PIT) formation, cellular structures also known as cytoplasmic bridges, which join the inner and outer periclinal cell walls of outer cortical cells (van Brussel *et al*., 1992; Timmers *et al*., 1999). Cytoplasmic bridges were observed in legumes with indeterminate nodules. Among the legumes with determinate nodules, PITs has been found in *L. japonicus*, since the IT has to get to the middle cortex, through the outer cortical cell layer, where nodule primordia form (Figure 1.1C). No such structures have been found in common bean (*P. vulgaris*), which develops nodule primordia in the outer cortex (van Spronsen *et al*., 2001). In the root cortex bacteria are released from the infection thread into the cytoplasm of the nodule primordia cells. These remain encapsulated by a plant-derived membrane (called peribacteroid membrane; Whitehead and Day, 1997) constituting the so-called symbiosome (Roth *et al*., 1988). Within this organelle-like structure, bacteria differentiate into nitrogen fixing bacteroids (Bergersen, 1955; Whitehead and Day, 1997). In determinate nodules, bacteria divide within the symbiosome membrane and form a certain population of cells. Internalized bacteria divide parallel with the symbiosome membrane before bacteroid differentiation in the indeterminate nodules (Prell and Pool, 2006; Jones *et al*., 2007).

For development of indeterminate nodules outer, inner and middle cortical cells are re-activated and undergo mitosis as well as cells in endodermis and pericycle (Figure 1.1B-C). Those cells of the middle cortex that will not become infected will form the nodule meristem (Gage 2004). Cells neighbouring the primordium will produce a persistent nodule meristem that consists of actively dividing cells and keeps growing outward from the root (Foucher and Kondorosi; 2000). First cell divisions in determinate nodules occur sub-epidermally in the cells of outer or middle cortex (van Spronsen *et al*., 2001; Figure 1.1B-C). Nodules are usually spherical and have a certain life span, since they omit

meristematic activity (Figure 1.1D). The inner nodule cells proliferate, differentiate, fix and undergo senescence synchronously (Mergaert *et al*., 2006; Newcomb *et al*., 1979).

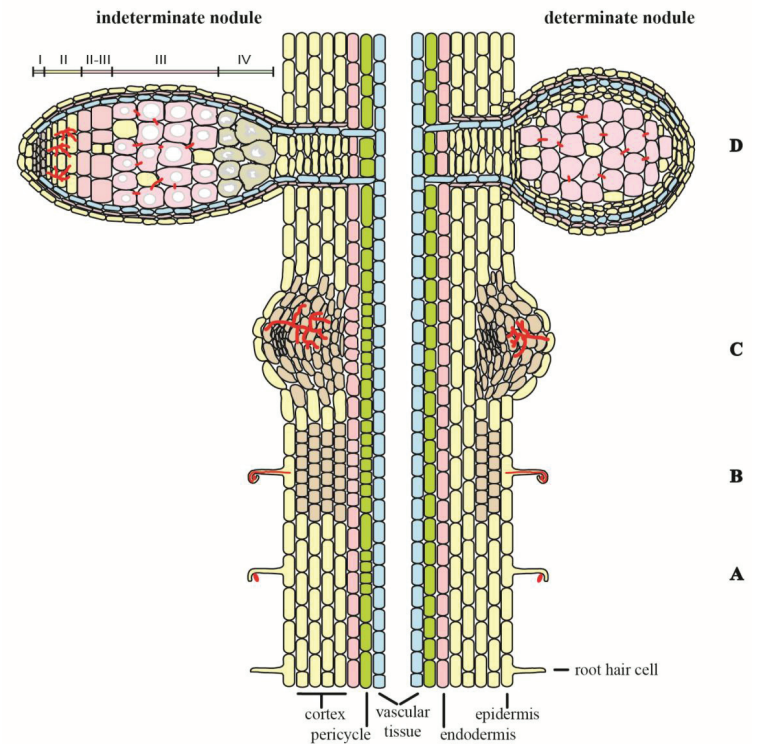

Figure 1.1 Development of indeterminate and determinate root nodules
The figure describes the two types of root nodules developed by legumes in symbiotic association with rhizobia. (A) Bacteria attach to the root hair tip when they invade the root via root hair infection. (B) Root hair curling and infection thread (IT) formation. IT serves to deliver rhizobia into developing nodule tissue. Recognition of bacteria triggers several cytological and morphological processes that differ in the two types (determinate and indeterminate) of legume nodules. In legumes forming determinate nodules, underneath the epidermal root hair cell (perceiving bacteria) the outer and middle cortical cells start to divide. Whereas in legumes developing indeterminate nodules, cells of the entire cortical layer and of the pericycle undergo cell proliferation. (C) Emerging nodule primordium and branching IT. Development of the nodule primordium is accompanied by the presence of a persistent meristem. (D) Zonation of the indeterminate nodule with the meristem (zone I), the infection zone (II), an interzone (II-III), the fixation zone (III) and the senescence zone (IV). In contrast, determinate nodules derive from cell divisions in the outer root cortex where meristematic activity is lost in mature nodules. Modified from Popp and Ott (2011).

Since indeterminate nodules grow and are infected continuously, they have an elongated shape that can be divided into four zones: I meristematic zone, free of bacteria; II infection zone; III nitrogen-fixing zone and IV senescent zone (Vasse *et al*., 1990; Figure 1.1D).

The role of the nodule is to provide a physiologically appropriate environment for biological nitrogen fixation. This requires oxygen concentration balance for the activity of the rhizobial nitrogenase enzymes. Nodule tissue of the infected cells insures a free oxygen concentration less than 1% of the atmospheric one that is required for the obligate aerobe bacteria to carry out the biological nitrogen fixation process (Studer *et al*., 1987; Brewin, 1991). Such micro-oxic environment is maintained by the existence of an oxygen diffusion barrier at the nodule endodermis (Dalton *et al*., 1998). Furthermore, the expression of legume-specific haemoglobins (leghemoglobins) ensures sufficient quenching and transport of free oxygen to the site of consumption (mainly the bacteroids) (Ott *et al*., 2005).

1.4. Molecular players in the signalling of root-nodule symbiosis

Morphological and developmental changes during pre-infection, infection and nodule formation follow diverse players on genetic, molecular and biochemical level. At least two different signalling cascades/events responsible for a successful root nodule establishment can be distinguished. Initial signalling events occur at the root epidermis maintaining bacterial infection and another giving rise to nodule development (Madsen *et al*., 2010; Oldroyd *et al*., 2011). Figure 1.2 illustrates the two parallel pathways.

Nod factor perception by LysM-type receptor-like kinases such as NFR5/NFP (in *L. japonicus*/*M. truncatula*) and NFR1/LYK3 (Amor *et al*., 2003; Limpens *et al*., 2003; Madsen *et al*., 2003; Radutoiu *et al*., 2003) represents the initial step of this molecular dialogue. Mutations in the corresponding genes result in the entire loss of cellular responses towards NFs and the lack of induction of infection threads or nodule primordia in both *nfr1* and *nfr5* mutants (Madsen *et al*., 2003; Radutoiu *et al*., 2003) in *L. japonicus*. Both RLKs are required for the initiation of the infection (infection thread formation) and nodule organogenesis as well (Figure 1.2; Madsen *et al*., 2010). The *M. truncatula nfp* mutant also does not exhibit any of the early responses (like root hair deformation, calcium spiking or early nodulin gene expression) to NF application (Amor *et al*., 2003). In

contrast, the *hcl-1* (lyk3) mutant is able to respond to NFs by root hair deformation while no infections can be observed. Interestingly, root hairs of the *hcl-1* mutant branch rather than curl because of impaired cytoskeletal (microtubule) rearrangement. Therefore, mutants do not form cytoplasmic bridges to create PITs in activated cortical cells (Catoira *et al*., 2001). Weak *hcl* alleles such as *hcl-4* shows blocked infection at the stage of infection thread (IT) formation but bacteria were still able to elicit root hair curling while ITs show aberrant morphology (Limpens *et al*., 2003).

Both *L. japonicus* receptors exhibit three extracellular LysM domains, which were shown to be required for determining host specificity towards the rhizobial NF (Radutoiu *et al*., 2007). The LysM domains are anchored by simple pass transmembrane domain to serine/threonine kinase domains (Madsen *et al*., 2003; Radutoiu *et al*., 2003). It was shown *in planta* that NFR5 and NFR1 localize to plasma membrane and form a heterocomplex triggering downstream signalling. Furthermore, a posphorylation site that was detected *in vitro*, is required for NFR1 function in NF-signalling and for its kinase activity (Madsen *et al*., 2011). Three threonine residues (1 in the juxtamembrane region and 2 in the kinase domain) were identified in LYK3 to be indispensible for the biological function of the protein but not for kinase activity (Klaus-Heisen *et al*., 2011). NFP and NFR5 did not show kinase activity (Arrighi *et al*., 2006; Madsen *et al*., 2011).

Interestingly both, AM symbiosis and RNS share a common set of signalling proteins (common '*sym*' genes) during initial signal perception and downstream activation of cellular signalling. A Leucine-Rich Repeat (LRR) containing receptor-like kinase SYMRK/DMI2/NORK (in *L. japonicus*, *M. truncatula* and *M. sativa*, respectively; Stracke *et al*., 2002; Endre *et al*., 2002; Catoira *et al*., 2000) downstream of the LysM-type RLKs represents the first, shared component of RNS and AM symbiosis signalling (Kistner *et al*., 2005; Parniske 2008). SYMRK was found to exist in at least three different structural versions, of which the shorter forms from rice and tomato are sufficient for AM, but not for functional RNS in the legume *L. japonicus*. These data indicate that SYMRK sequence evolution was involved in the recruitment of a pre-existing signalling network from AM symbiosis for the evolution of RNS (Markmann *et al*., 2008). Its function remains to be clarified, however, plants carrying mutation in *SYMRK* locus show an impaired calcium spiking elicited by NF perception, and therefore it might serve as a link between the upstream NF receptors and the downstream physiological calcium-related events (Stracke *et al*., 2002). Three Ser/Thr residues were found in the SYMRK intracellular region that

are responsible for full kinase activity of the protein and its function involved in both endosymbiosis (Yoshida and Parniske, 2005). A mutation in the SYMRK extracellular domain (*symRK-14*) affected normal infection in epidermal cells by fungal or bacterial symbionts. Epidermal responses of *symRK-14* to bacterial signalling, including calcium spiking, *NIN* gene expression and infection thread formation, were significantly reduced. However, negative effects on nodule primordia formation and cortical infection were not detected (Kosuta *et al*., 2011).

NF perception leads to calcium oscillations in and around the nucleus, molecular players involved in calcium-related occurrence represent the so-called common *SYM* genes (like SYMRK, involved in the common symbiosis pathway; Figure 1.3), since each mutant shows an altered phenotype in both endosymbiosis. Downstream SYMRK two potassium-channel proteins CASTOR and POLLUX (Figure 1.3) were identified in *Lotus* while in *Medicago* it was found only one protein of the same function, DMI1/POLLUX (Ané *et al*. 2004). The symbiosis-defective *castor* and *pollux* mutants show impairment in perinuclear calcium spiking (Miwa et al. 2006; Charpentier et al., 2008). Mutations in these genes and in further three components of the nuclear pore complex NUP85, NUP133 and NENA (described so far in *L. japonicus)* are accompanied with impairment in calcium spiking in response to NF (Saito *et al*., 2007; Kanamori *et al*., 2006; Groth *et al*., 2010; Figure 1.3). All these mutants (*castor*, *pollux*, *nup85*, *nup133*, *nena*) show nodulation and AM symbiosis affected phenotypes and thus represent common *sym* genes.

A molecular component downstream of the calcium spiking, and it is thought to be act as a decoder of the calcium signature, is a calcium-calmodulin-dependent protein kinase, CCaMK in *L. japonicus* and DMI3 in *M. truncatula* (Lévy, *et al*., 2004; Mitra *et al*., 2004). It interacts with CYCLOPS (IPD3) a phosphorylation substrate of CCaMK in the nucleus (Yano *et al*., 2008; Messinese *et al*., 2007). Auto-active mutations in CCaMK (*snf1*) in *L. japonicus* and expression of the DMI3$^{1\text{-}311}$ in *M. truncatula* are able to trigger a spontaneous nodule formation in the absence of rhizobia (Tirichine *et al*., 2006; Gleason *et al*., 2006). At this point, the pathway bifurcates (Figure 1.2), CCaMK initiates nodule organogenesis, whereas CCaMK-CYCLOPS interaction (Yano *et al*., 2008) leads to intracellular infection (Madsen *et al*., 2010). Expression of a gain-of-function mutant of CCaMK in different *Lotus* symbiotic mutant backgrounds also supports this hypothesis (Hayashi *et al*., 2010; Popp and Ott, 2011). Cross-talk between the infection and the

organogenesis pathway (or bifurcation of them) was shown by Madsen and colleagues (2010) as well.

Another common *sym* gene has been identified recently in *M. truncatula*, a plasma membrane resident ankyrin protein, VAPYRIN. Mutation in this protein causes phenotypical aberration in both endosymbiosis. *Vapyrin* mutant plants do not show impairment in calcium spiking in response to NF application, therefore it can be concluded that it acts downstream of the calcium spiking events (Murray *et al*., 2011). Orthologous protein of the NENA in *M. truncatula* and of the VAPYRIN protein in *L. japonicus* has not been identified so far.

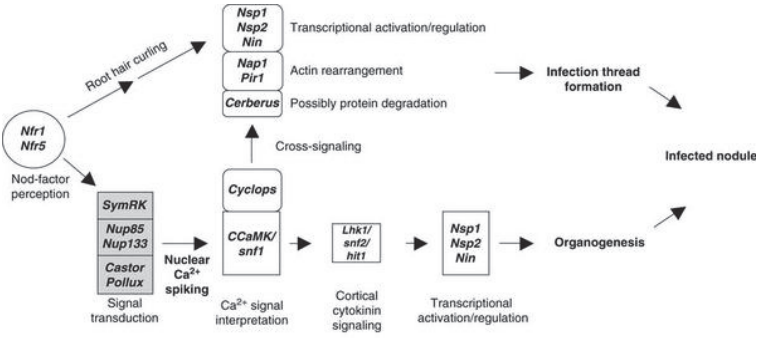

Figure 1.2 Symbiotic signalling pathways mediating infection and nodule organogenesis
NF perception induces two parallel signalling transduction pathways to establish root nodule symbiosis. Recognition of NF via NFR1 and NFR5 receptor complex induces infection processes in the epidermis via deformation and root hair curling of epidermal root hair cells. The parallel pathway facilitating nodule organogenesis bifurcates at the CCaMK. One site of the pathway is involved in infection thread formation upon CCaMK interaction with its substrate Cyclops via Cerberus, Nap1, Pir1 proteins in epidermis and subsequent activation of the transcription regulators Nin, Nsp1 and Nsp2. While in cortex cytokinin signalling pathway activated via CCaMK induces nodule organogenesis. Modified from Madsen *et al*., 2010.

Transcriptional regulators NIN (nodule inception; Schauser et al., 1999), NSP1 (nodulation signalling pathway 1) and NSP2 (Catoira *et al*., 2000; Oldroyd and Long, 2003; Kaló *et al*., 2005; Heckmann *et al*., 2006) are involved in both infection and nodule organogenesis as well (Madsen *et al*., 2010; Figure 1.2). NSP1 and NSP2 belong to the GRAS protein family. *Nin* mutants exhibit root hair deformation indicating that the gene is not involved in early NF-signalling. Furthermore, it was found to be responsible for infection thread formation since *nin* mutants are defective in root hair curling (inordinate

curling) and rhizobial infection is blocked in epidermis while in cortex they are aberrant in cell division and nodule primordium formation (Schauser *et al*., 1999).

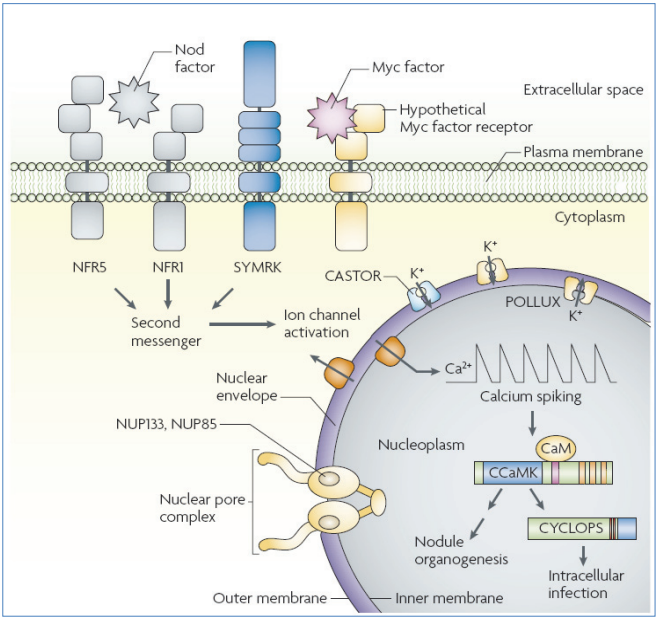

Figure 1.3 Common components of AM and RNS signalling pathway
Signal perception of rhizobial or AM fungal signals triggers a signal transduction that shares at least nine (7 on the figure) common component: SYMRK (DMI2), CASTOR (no ortholog in *Medicago*), POLLUX (DMI1), NUP133, NUP85, NENA (in *L. japonicus*, Groth *et al*., 2010), CCaMK (DMI3), CYCLOPS (IPD3) and VAPYRIN (in *M. truncatula*, Murray *et al*., 2011). SYMRK kinase acts downstream of the Nod factor receptors (NFR1 and NFR5) and a hypothetical Myc factor receptor, but upstream of the calcium signalling that occurs in and around the nucleus. CASTOR and POLLUX are potassium-permeable channels while NUP85, NUP133 and NENA (not on the figure, it can be placed as component of the nuclear pore complex) are components of the nucleopore complex and required for calcium spiking. CCaMK forms a complex with CYCLOPS that activates further downstream elements. The ninth component VAPYRIN can be placed downstream of CYCLOPS and CCaMK (from Parniske, 2008; with modifications in text).

The *L. japonicus* mutants *nsp1* and *nsp2* are impaired in nodule cortical cell division indicating their role in nodule organogenesis (Heckmann *et al*., 2006). Activation of these transcription factors (NSP1, NSP2 and NIN) via CCaMK and subsequent cytokinin signalling in the cortical cell layers induces expression of late nodulins (genes specifically induced in nodulation and they can be grouped as early and late nodulins; Nap

and Bisseling, 1990) and organogenesis (Madsen et al., 2010). CCaMK-CYCLOPS interaction triggered signalling involves further molecular components like CERBERUS (Yano *et al*., 2009), PIR1 and NAP1 (Yokota *et al*., 2009) that activate NSP1, NSP2 and NIN transcription regulators in epidermal cell layer participating in the infection process (Madsen *et al*., 2010; Figure 1.2). *Cerberus* mutants showed impairment in both infection (defects in IT formation) and nodule organogenesis (Yano *et al*., 2009), whereas *pir1* and *nap1* mutants were aberrant in rearrangement of the actin cytoskeleton (Yokota *et al*., 2009). While the abovementioned transcription regulators have not been shown to bind directly DNA. In *Medicago* was found an ERF transcription factor, ERN (EFR Required for Nodulation) that directly binds DNA. Plants carrying mutation in this gene show IT aberrations and it assumed to act downstream DMI3/CCaMK in NF induced gene expression (Middleton *et al*., 2007).

Recently a novel component of the symbiotic signalling pathway, the remorin protein MtSYMREM1 in *M. truncatula* was described (Lefebvre *et al.*, 2010).

1.5. Remorins, a protein family of unknown function

Remorins represent a plant-specific protein family of unknown function that are present in all land plants including ferns and mosses (Figure 1.4). The proteins consist of a C-terminal domain that is highly conserved among the whole family and an N-terminal region with highly variable sequence. Remorins were ordered into six groups based on phylogenetic analysis that were combined with domain features (Figure 1.4). Group 3 remorins stands for exception because of the lack of the N-terminal domain (Raffaele *et al*., 2007). Figure 1.4 illustrates phylogenetic analysis and clustering of the remorin proteins. Remorins represent a novel family with coiled-coil forming filamentous proteins that were localized to apical and vascular tissue and leaf primordia (Bariola *et al*., 2004).

A member of a plant-specific protein family has been described just two decades ago that later was designated as remorins (Farmer *et al*., 1989; Reymond *et al*., 1996). It was described as a plasma membrane (PM) associated protein, phosphorylated upon treatment with polygalacturonic acid (a proteinase inhibitor inducing factor; Farmer *et al*., 1989) and it was suggested to play a role in cell-to-cell communication and plant defence because of its features similar to viral proteins (Reymond *et al*., 1996).

Recently, Raffaele and colleagues (2009) showed that a group 1 remorin, SlREM1.3 in tomato interacts with a movement protein TGBp1 of potato virus X (PVX) and inhibits movement of the virus through the plasmodesmata that are used by viruses for intercellular movement.

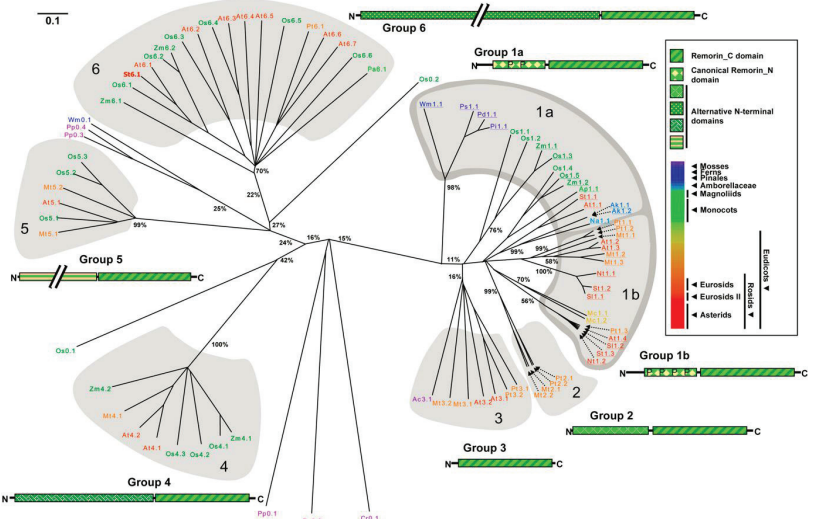

Figure 1.4 Phylogenetic and domain organization of the remorin family based on their protein sequences. The right box shows the color code used to indicate evolutionary positions within the plant kingdom (according to the Angiosperm Phylogeny Group, 2003) and domain elements used for classification. In the diagrams domain lengths are proportional to the average protein sequence length (except for groups 5 and 6, for which the representation of the N-terminal region is intercepted by ‘‘//,’’indicating a variable length of this module within these two groups). Underlined sequences contain Remorin_N domains identified by InterProScan. Bootstrap values (%) are given along the most important branch points. True branch lengths were inferred by maximum-likelihood analysis; the upper-left scale represents a probability of 0.1 amino acid changes per site. The tree was reconstructed using parsimony analysis. For clarity of the figure, a shortened nomenclature was used (e.g. At1.1 for AtRem1.1) the first number in the proposed name indicates the corresponding group (e.g. At1.3 is the third member of group 1). Abbreviations: Ac, *Adiantum capillus-veneris*; Ak, *Amborella trichopoda*; Ap, *Allium cepa*; At, *Arabidopsis thaliana*; Cr, *C. richardii*; Mc, *Mesembryanthemum crystallinum*; Mt, *M. truncatula*; Na, *Nuphar advena*; Nt, tobacco; Os, rice; Pa, *Persea americana*; Pd, *Pinus taeda*; Pi, *Pinus pinaster*; Pp, *P. patens*; Ps, *Picea sitchensis*; Pt, *P. trichocarpa*; Sl, tomato; St, *Solanum tuberosum*; Wm, *Welwitschia mirabilis*; Zm, *Zea mays*. (From Raffaele *et al*., 2007)

Other findings (regarding group 1 remorins) such as differential phosphorylation upon treatment of Arabidopsis cells with the pathogen-associated molecular pattern (PAMP) flg22 (Benshop, 2007) and its dependency on the presence of the resistance

protein RPM1 (Widjaja *et al*., 2009) suggest roles of these proteins during plant-pathogen interactions (reviewed in Jarsch and Ott, 2011). Moreover, another member of group 1 remorins (AtREM1.2) was found to be interacting with RIN4, a protein involved in plant immunity (Liu *et al*., 2009).

Raffaele and colleagues (2009) suggest that remorins are possible membrane raft markers. Plasma membrane microdomains consist of sterols, sphingolipids and proteins that serve as a platforms acting in membrane signalling and trafficking (Bessueille et al., 2009; Lingwood and Simons, 2010; Mongrand *et al*., 2010; Jarsch and Ott, 2011). They were found and were highly enriched in detergent insoluble membrane (DIM) fractions (Raffaele *et al*., 2009; Lefebvre *et al*., 2007, 2010). It was shown not only biochemically but also Raffaele and colleagues (2009) showed that another member of group 1 remorins, NtREM1.2 accumulates in purified DIM. Furthermore, when the protein was fused to the green fluorescent protein (GFP) and was expressed in tobacco leaves, it was found to be localized to distinct PM domains (Raffaele *et al*., 2009). It was also hypothesised in Lefebvre *et al.* (2010) and summarized in Jarsch and Ott (2011) that some of the remorins (e.g. MtSYMREM1) might function as scaffold protein, since they share common features with protein described as scaffold in mammalian field, and might recruit other proteins involved in signalling and membrane modification to the membrane rafts.

1.5.1. MtSYMREM1, a remorin involved in root-nodule symbiosis

Group 2 remorins have been found only in legumes and Poplar so far (Raffaele *et al*., 2007, Lefebvre *et al*., 2010). A group 2 remorin protein was found in organ-specific expression profiling qPCR experiment performed in *L. japonicus* (Colebatch *et al*., 2004). Lefebvre and co-workers (2010) analyzed all remorins found in *M. truncatula* during the symbiosis and only the remorin belonging to the group 2 remorins (MtREM2.2 in Raffaele *et al*., 2007), named MtSYMREM1 was identified as root nodule symbiosis specific. MtSYMREM1 was induced in a nodulation-specific manner and 24 hours post application of isolated Nod factors from *Sinorhizobium meliloti* (Lefebvre *et al*., 2010). Using different rhizobial strains that cause altered infection at different stages of infection, revealed MtSYMREM1 expression to be dependent on infection and bacterial release rather than symbiotic nitrogen fixation. These data suggest a possible role of the protein in preinfection steps, IT formation and throughout the nodule life (Lefebvre *et al*., 2010).

Furthermore, *Mtsymrem1* mutants were found to compose about 25% less and stunted nodules and aborted ITs (formation of sac-like structures and branching ITs) that also proves that MtSYMREM1 is required for bacterial infection and nodule development.

MtSYMREM1 localizes to the PM of leaf epidermal cells when it was tested as a fusion protein with a cyan fluorescent protein (CFP) in *N. benthamiana*. When fractionation was performed on inoculated (with *S. meliloti*) *M. truncatula* roots, the protein was detected in the DIM fractions, a further evidence for PM and membrane raft localization, respectively. The localization of the endogenous protein in *M. truncatula* was examined using in situ immunofluorescence when localization at the PM of ITs in zone II (infection zone) and at the symbiosome membrane in zone III (nitrogen fixing) and at the nodular infection thread as well, using immunogold labeling and transmission electron microscopy (Lefebvre *et al*., 2010). Furthermore, it was found that the protein interacts with the symbiotic RLKs NFP, LYK3 and DMI2 and homo-oligomerizes with itself as well in bimolecular fluorescent complementation and split-ubiquitin yeast assay, respectively (Lefebvre *et al*., 2010).

1.6. Aim of this study

A tightly regulated signalling cascade regulates RNS in legumes. Perception of the respective host-specific rhizobial symbionts by the plant is mediated by a set of receptor-like kinases. In *M. truncatula*, a legume that develops indeterminate nodules, these RLKs interact with the remorin protein MtSYMREM1. While almost all signalling components are highly conserved between *M. truncatula* and the second model legume *L. japonicus*, an exceptionally high sequence divergence was observed for the SYMREM1 proteins. These data suggest possible functional differentiation that may correlate with differences in nodule organogenesis and maturation between both legumes. The aim of this study was to functionally characterize the *SYMREM1* gene from *L. japonicus*, to unravel its transcriptional regulation and to identify new interaction partners of the LjSYMREM1 protein.

2. Material and Methods

2.1. Material

Chemicals

α-DsRed primary antibody	Clontech (Takar Bio Europe), France
α-GFP primary antibody	Rockland Immunochemicals, Gilbertsville, USA
α-HA-HRP antibody	Roche, Penzberg, Germany
α-LexA primary antibody	Dualsystems Biotech, Schlieren, Switzerland
α-Mouse-HRP secondary antibody	Biomol, Hamburg, Germany
α-Rabbit-HRP secondary antibody	GE Healthcare UK, Little Chalfont, UK
α-VP16 primary antibody	BD Bioscience, Heidelberg, Germany
β-Mercaptoethanol	Sigma-Aldrich, Taufkirchen, Germany
3,5 Dimethoxy-4-hydroxyacetophenone (DMSO)	Finnzymes, Espoo, Finland
Acetic acid 100% p.a.	Merck, Darmstadt, Germany
Acetone 99%	Merck, Darmstadt, Germany
Acetosyringone	Fluka, Buchs, Switzerland
Acrylamide (Rotiphorese Gel 30)	Roth, Karlsruhe, Germany
Agar HP696	Kalys S.A, Bernin, France
APS (Ammonium Persulfate)	Merck, Darmstadt, Germany
Bacto agar	Becton Dickinson, Heidelberg, Germany
Bacto peptone	Becton Dickinson, Heidelberg, Germany
Bacto yeast extract	Becton Dickinson, Heidelberg, Germany
Bromphenol blue	Roth, Karlsruhe, Germany
Calcium chloride ($CaCl_{2)}$	Mallinckrodt Baker, Griesheim, Germany
Chloroform/Isoamyl alcohol (24/1)	Roth, Karlsruhe, Germany
Coomassie brilliant blue R250	Serva Electrophoresis, Heidelberg, Germany
Dithiothreitol (DTT)	Roche, Penzberg, Germany
DNA MG Standard ladders	New England Biolabs, Frankfurt a. Main
dNTP mix	New England Biolabs, Frankfurt a. Main
DUALmembrane kit2 (P01001)	Dualsystems, Schlieren, Switzerland
Ethanol (technical) 99.9%	Merck, Darmstadt, Germany
Ethidium bromide solution (1%)	Fluka, Sigma-Aldrich, Taufkirchen, Germany
Ethylenediaminetetraacetate (Na_2EDTA)	Merck, Darmstadt, Germany
Gamborg B5 medium (Basal Salt Mixture)	Duchefa, Haarlem, The Netherlands
Gamborg B5 vitamin mixture	Duchefa, Haarlem, The Netherlands
Gateway LR Clonase enzyme mix	Invitrogen, Karlsruhe, Germany
Glucose	Applichem, Darmstadt, Germany
Glycerine, 99.5 % p.a	Roth, Karlsruhe, Germany

Glycine p.a	Applichem, Darmstadt, Germany
Isopropanol 99.9%	Mallinckrodt Baker, Griesheim, Germany
LE Agarose	Biozym, Oldendorf, Germany
Lithium acetate	Roth, Karlsruhe, Germany
Loading dye 6x	New England Biolabs, Frankfurt a. Main
Luminogen™ TMA-6	GE Healthcare UK, Little Chalfont, Buckinghamshire, UK
Lyticase (L2524-10KU)	Sigma-Aldrich, Taufkirchen, Germany
Magnesium chloride ($MgCl_2$) p.a.	Merck, Darmstadt, Germany
Milk powder	Roth, Karlsruhe, Germany
Nitrocellulose membrane Hybond N+	Amersham Biosciences, Freiburg, Germany
NucleoBond® PC 500	Macherey-Nagel, Düren, Germany
NucleoSpin ExtractII®	Macherey-Nagel, Düren, Germany
NucleoSpin Plasmid®	Macherey-Nagel, Düren, Germany
pENTR/D-TOPO kit	Invitrogen, Karlsruhe, Germany
pGEM-T cloning system	Promega, Mannheim, Germany
Phusion DNA Polymerase	Finnzymes, Espoo, Finnland
Phenol/Chloroform/Isoamyl alcohol (25/24/1)	Roth, Karlsruhe, Germany
Phenylmethylsulfonylflurid (PMSF)	Roth, Karlsruhe, Germany
Polyethylenglycol (PEG 3350)	Sigma-Aldrich, Taufkirchen, Germany
Polyethylenglycol (PEG 8000)	Sigma-Aldrich, Taufkirchen, Germany
Potassium dihydrogen phosphate (KH_2PO_4) p.a.	Merck, Darmstadt, Germany
Potassium hydroxide (KOH) >85%, p.a	Mallinckrodt Baker, Griesheim, Germany
Potassium ferrocyanide ($K_4[Fe(CN)_6].3H_2O$)	Fluka, Sigma-Aldrich, Taufkirchen, Germany
Potassium ferricyanide ($K_3[Fe(CN)_6]$)	Fluka, Sigma-Aldrich, Taufkirchen, Germany
Protease inhibitor cocktail	Sigma-Aldrich, Taufkirchen, Germany
Proteinase K	Invitrogen, Karlsruhe, Germany
Proteinmarker prestained, broad range (7-175 kDa)	New England Biolabs, Frankfurt a. Main, Germany
Restrictionendonucleases	New England Biolabs, Frankfurt a. Main
Single stranded carrier DNA (P06001)	Dualsystems Biotech, Schlieren, Switzerland
Sodium acetate (NaAcetate), p.a	Merck, Darmstadt, Germany
Sodium chloride (NaCl) p.a.	Mallinckrodt Baker, Griesheim, Germany
Sodium dodecyl sulfate (SDS)	Roth, Karlsruhe, Germany
Sucrose	Applichem, Darmstadt, Germany
Taq DNA Polymerase	New England Biolabs, Frankfurt a. Main
T4 DNA Ligase	New England Biolabs, Frankfurt a. Main
TEMED (Tetramethylethylenediamine)	Roth, Karlsruhe, Germany
Trichloroacetic acid (TCA) p.a.	Roth, Karlsruhe, Germany
TrisHCl p.a.	Applichem, Darmstadt, Germany
Triton-X 100	Roth, Karlsruhe, Germany
Tween 20	Roth, Karlsruhe, Germany

X-Gluc	Roth, Karlsruhe, Germany
Yeast nitrogen base w/o amino acids	(Difco) BD, Sparks, MD, USA
Yeast protease inhibitor cocktail	Sigma-Aldrich, Taufkirchen, Germany

Equipment and Devices

ABI 3730 48 capillary sequencer	Applied Biosystems, Darmstadt, Germany
Allegra 64R Centrifuge	Beckman, Munich, Germany
Centrifuge, Eppendorf 5424	Eppendorf, Hamburg, Germany
Confocal laser scanning microscope, (Leica TCS SP5)	Leica Mikrosysteme, Wetzlar, Germany
DNA Engine Tetrad 2 Peltier Thermal Cycler	Bio-Rad, Munich, Germany
Electroporator	Bio-Rad, Munich, Germany
Fusion SL detection system	Peqlab, Erlangen, Germany
Galaxy Ministar Microcentrifuge	VWR, Darmstadt, Germany
Gene Pulser System (Gene Pulser, Capacitance Extender, Pulse Controller)	Bio-Rad, Munich, Germany
HeraSafe biological safety cabinet	Thermo Fisher Scientific, Schwerte, Germany
Incubator, Binder WTB	BINDER GmbH, Tuttlingen, Germany
Infors HAT Multitron incubator/shaker	INFORS AG, Bottmingen, Germany
Inverted (epifluorescence) microscope (Leica DMI 6000B)	Leica Mikrosysteme, Wetzlar, Germany
Microcentrifuge 5418R	Eppendorf, Hamburg, Germany
Nanodrop ND-1000 Spectrophotometer	Labtech International, Burkhardtsdorf, Germany
Pipetman (P10, P20, P200, P1000)	Gilson, Middleton, USA
Plant growth chamber, SANYO, MLR-350H	SANYO Europe Ltd, Watford UK
PowerPac Basic Power Supply	Bio-Rad, Munich, Germany
Protein Blotting Cell	Bio-Rad, Munich, Germany
Rocker Shaker, UNITWIST	UniEquip, Planegg, Germany
Sorvall RC 5C Plus	DuPont Sorvall, Bad Homburg, Germany
Stereo microscope (Leica MZ 16FA)	Leica Mikrosysteme, Wetzlar, Germany
Thermomixer comfort/compact	Eppendorf, Hamburg
Tissue lyser	Qiagen, Hilden, Germany
TProfessional Thermocycler	Biometra, Göttingen, Germany
Ultra Clear UV Plus water system	Millipore, Schwalbach, Germany
Ultrospecc 3000pro (UV spectrophotometer)	Amersham Biosciences, Freiburg, Germany
UV Stratalinker 2400 (UV crosslinker)	Stratagene,Heidelberg, Germany
Varifuge 3.0R (centrifuge)	Heraeus Sepatech GmbH, Osterode, Germany
Varioklav 135 S steam sterilizer	Thermo Scientific, Schwerte, Germany
Vertical Electrophoresis Cell	Bio-Rad, Munich, Germany
Vortex Genie 2	Bender & Hobein AG, Zurich, Switzerland

Water bath	GFL, Großburgwedel, Germany

Other implements

Amicon Ultra-4 centrifugal devices	MILLIPORE Corp.; Carrigtwohill, Ireland
Films Amersham Hyperfilm^{TM} ECL	GE Healthcare UK, Little Chalfont, UK
Filter (Celluloseacetat; 0.22µm)	Whatman; GE Healthcare UK
Glass beads	B. Braun Melsungen, Germany
Glass jars	J. WECK GmbH, Wehr-Öflingen, Germany
Parafilm (Laboratory Film)	Pechiney Plastic Packaging, Menasha, USA
PVDF membrane	GE Healthcare UK, Little Chalfont, UK
Steritop filter 0.22µm	Millipore GmbH, Schwalbach, Germany
Tungsten beads	BioRad, Munich, Germany

2.1.1. Bacterial and yeast media and solutions

LB medium

Bacto trypton	10 g	
Bacto yeast extract	5 g	
NaCl	5 g	
adjust pH to ~7.5 with 1 M NaOH		
MQ-H_2O	up to 1 l	

SOB medium

Bacto tryptone	20 g	
Bacto yeast extract	5 g	
NaCl	0.584 g	
KCl	0.186 g	
MQ-H_2O	up to 1 l	

TY medium

Bacto tryptone	5 g	
Yeast extract	3 g	
$CaCl_2.H_2O$	0.81 g	
MQ-H_2O	up to 1 l	
Bacto agar	15 g	1.5% final

YPAD medium

Bacto yeast extract	10 g	1% final
Bacto peptone	20 g	2% final
Glucose monohydrate	20 g	2% final
Adenine sulphate	40 mg	0.004% final
MQ-H_2O	up to 1 l	
Bacto agar	20 g	2% final

10x YNB (Yeast Nitrogen Base w/o amino acids)

67 g	1 l MQ-H_2O

40% Glucose

400 g	1 l MQ-H_2O

AA-stock solutions (amino acid solution w/o certain amino acids)

10x AA-LW (w/o Leucine and Tryptophan)

6.4 g	1 l MQ-H_2O

10x AA-LWH (w/o Leucine, Tryptophan and Histidine)

6.2 g	1 l MQ-H_2O

10x AA-LWHAde (w/o Leu, Trp, His and Adenine)

6.2 g	1 l MQ-H_2O

500xHis (500x Histidine stock)	10 g/l
500xTrp (500x Tryptophane stock)	10 g/l
100xLeu (100x Leucine stock)	10 g/l

SD (synthetic, minimal) medium, liquid

10x YNB	0.1 l	0.67 g final
10x AA-stock solution	0.1 l	
40% Glucose	0.05 l	2% final
MQ-H_2O/	0.75 l	

SD (synthetic, minimal) medium, solid

10x YNB	0.1 l	0.67 g final
10x AA-stock solution	0.1 l	
40% Glucose	0.05 l	2% final
Bacto agar	0.75 l	2% final

Antibiotics

Ampicillin	100 mg/ml
Carbenicillin	50 mg/ml
Cefotaxim	300 mg/ml
Gentamicin	25 mg/ml
Hygromicin	50 mg/ml
Kanamycin	50 mg/ml
Rifampicin	25 mg/ml
Spectinomycin	50 mg/ml
Streptomycin	50 mg/ml

Rifampicin was dissolved in methanol. All other antibiotics were dissolved in H_2O. Stock solutions were 1000x diluted or as it is indicated in respective chapters.

All solutions for yeast media were autoclaved for 15 min at 115°C, with exception of amino acid solutions and YNB. They were sterile filtrated via 0.22 µm or 0.45 µm filters. Bacterial media were autoclaved for 20 min at 120°C. Antibiotics were sterile filtrated.

2.1.2. Plant media and solutions

Fahräeus medium

$MgSO_4.7H_2O$	0.5 mM
KH_2PO_4	0.7 mM
$Na_2HPO_4.2H_2O$	0.8 mM
Fe-EDTA	50 µM
$MnSO_4$	0.1 µg/l
$CuSO_4$	0.1 µg/l
$ZnSO_4$	0.1 µg/l
H_3BO_3	0.1 µg/l
Na_2MoO_4	0.1 µg/l
H_2O	up to 1 l
adjust pH~6.5	

add after autoclaving	
$CaCl_2$	1 mM

Gamborg´s medium

Gamborg B5 Basal Salt	3.3 g
Sucrose	20 g
Bacto agar	10 g
H_2O	up to 1 l
pH~5.5 with NaOH	

1% Water-agar

Bacto Agar	1 g
ddH_2O	0.1 l

GUS staining solution

Na_2HPO_4 (pH~7.0)	0.1 M
Na_2EDTA	10 mM
$K_3Fe(CN)_6$	1 mM
$K_4Fe(CN)_6$	1 mM
Triton-X 100	0.1 %
X-Gluc	1 mM

100mM X-Gluc

1 mg X-Gluc	dissolved in 2 ml DMSO

Media were autoclaved for 20 min at 120°C.

2.2. Methods

2.2.1. Bacterial and yeast growth and transformation

2.2.1.1. Bacterial growth and transformation

Escherichia coli

E. coli DH5α, TOP10, XL1-Blue and DB3.1 strains (from Invitrogen, Germany; Appendix, Table A1) were used for plasmid propagation. *E. coli* strains were grown in LB liquid medium supplemented with appropriate antibiotic at 37°C over-night. Transformed bacterial strains were stored as glycerol stocks at - 80°C.

Electro-competent cells were transformed using Bio-Rad electroporator with the following settings:

Capacitance: 25 μF

Capacitance extender: 125 μF

Resistance: 400 Ω

Set volt: 2.0 kV

Time constant: 0.0

Time-constant after transformation: 8-9

After electroporation cells were grown in SOB medium at 37°C for a maximum of 1 h with a gentle shaking (300 rpm, Eppendorf thermomixer) before being plated onto LB solid medium containing the appropriate antibiotic and grew in 37°C incubator over-night.

Chemo-competent cells (prepared as described in Sambrook and Russell, 2001) were incubated for 15 min on ice together with the respective plasmid, then heat-shocked at 42°C for 1 min. After heat-shock, cells were incubated on ice for 5 min before addition of liquid LB medium. Cells were pre-grown at 37°C for a maximum of 1 h with gentle shaking (300 rpm; Eppendorf thermomixer) before being plated onto LB medium containing the appropriate antibiotic.

Agrobacterium tumefaciens* and *Agrobacterium rhizogenes

A. tumefaciens GV3101 (C58:pMP90RK, Koncz and Schell, 1986), AGL1 (Lazo *et al*., 1991) and *A. rhizogenes* AR1193 (Stougaard *et al*., 1987) strains (Appendix, Table A1)

were used for transient and/or stable plant transformations. All strains were transformed via electroporation using Bio-Rad instrument and settings as follow:

Capacitance: 25 µF

Capacitance extender: 125 µF

Resistance: 400 Ω

Set volt: 1.25 kV

Time constant: 0.0

Time-constant after transformation: 8-9

After electro-shock LB medium was added to the cells, they were incubated at 28°C with gentle shaking (300rpm, Eppendorf Thermomixer) for at least 2 h then plated onto LB supplemented with antibiotic for both the respective plasmid and strain. Plates were incubated at 28°C for 2-3 days.

Mesorhizobium loti

Mesorhizobium loti (strain MAFF 303099 expressing DsRed fluorophore; Gherbi *et al*., 2008; Appendix, Table A1) was used for *L. japonicus* infection. Rhizobia were grown on TY solid and/or liquid medium containing 15µg/ml Gentamicin, at 28°C for 3-4 days. Rhizobia liquid culture were harvested, washed and resuspended in Fåhraeus medium (Fåhraeus, 1957; see above) then diluted to a particular OD_{546} (specified in the respective chapter).

2.2.1.2. Yeast growth

For *Saccharomyces cerevisiae* (Appendix, Table A1) transformation a single yeast colony was picked from YPAD (full yeast medium) plates (no older than 3 weeks), inoculated in YPAD liquid medium and grown as a pre-culture overnight at 28/30°C in a shaking incubator (200 rpm). Transformed yeast cells were plated onto synthetic drop-out yeast medium (SD) supplemented with amino acid mixture lacking particular amino acids that served as auxotrophic markers (bait vector carrying Leu; prey vector carries Trp selection marker). Plates were sealed with parafilm and incubated at 28°C for 3 days.

For yeast protein extraction and plasmid preparation from yeast, single colonies were picked from synthetic drop-out (SD) plates, inoculated in liquid SD medium lacking the appropriate auxotrophic markers and grown at 28°C at 200 rpm for 1 or 2 nights.

2.2.2. Molecular Biology DNA Techniques

2.2.2.1. PCR application

To amplify a DNA fragment for cloning Phusion Polymerase was used setting up the following reaction and conditions:

Forward primer (10 pmol/µl)		1 µl
Reverse primer (10 pmol/µl)		1 µl
Phusion DNA Polymerase (2 U/µl)		0.2 µl
10x Phusion buffer		3 µl
dNTPs (10 mmol/each)		1 µl
$MgCl_2$ (50 mM)		0.3 µl
st. MQ-H_2O	up to	30 µl

Initial denaturation	98°C	30 s	1 cycle
Denaturation	98°C	10 s	30-35 cycles
Annealing	55°C-60°C*	10 s	30-35 cycles
Extension	72°C	15 s-1 min**	30-35 cycles
Final extension	72°C	1 min	1 cycle

For colony PCR performed on *E. coli* as well as on Agrobacteria a single colony was picked and placed into the PCR-tube using the following set ups:

Forward primer (10 pmol/µl)		0.4 µl
Reverse primer (10 pmol/µl)		0.4 µl
Taq DNA Polymerase (5 U/µl)		0.2 µl
10x Taq buffer		2 µl
dNTPs (10 mmol/each)		0.4 µl
$MgCl_2$ (50 mM)		0.2 µl
st. MQ-H_2O	up to	20 µl

Initial denaturation	95°C	1 min	1 cycle
Denaturation	95°C	30 s	30-35 cycles
Annealing	55°C-60°C*	30 s	30-35 cycles

Extension	72°C	30 s-3 min**	30-35 cycles
Final extension	72°C	1 min	1 cycle

* depends on the annealing temperature of the given primer pair

** depends on the length of the given amplicon

2.2.2.2. Cloning

Constructs used for plant work were generated using Gateway technology. For this purpose *LjSYMREM1* (cDNA), *pLjSYMREM1:gLjSYMREM1* (genomic DNA) were amplified (as described above) using forward primers containing 5´-CACC overhangs and gene specific blunt-end reverse primers (see Appendix, Table A5), creating the following entry clones in pENTR/D-TOPO® vector (Invitrogen): TOPO:*LjSYMREM1* and TOPO: *pLjSYMREM1:gLjSYMREM1* (see Appendix, Table A3). Entry clones were used for subcloning into binary vectors (see Table A3) via LR Clonase reaction according to manufacturer (Invitrogen). Entry clones of NFR1 and NFR5 were kindly provided by J. Stougaard (University of Aarhus, Denmark). For interaction studies and protein localization in the heterologous *N. benthamiana* system pAM-PAT binary vectors were used carrying fluorophore tags. A binary vector pH7YWG2.0 without 35S (modified from Karimi *et al*., 2005) promoter was used in order to create *L. japonicus* stable transgenic lines for localization of LjSYMREM1 fused to YFP and expressed under its native promoter (*pLjSYMREM1:gLjSYMREM1:YFP*). All vectors created for interactions studies or protein localization *in planta* are summarized in Appendix, Table A3.

A binary vector pUb-gwy containing a hygromycin selection marker for plants (Maekawa *et al*., 2008) was modified in this study. A vector named as pUb:gwy:mOrange was created. The gateway cassette (attR1-ccdB gene – Cm resistance-attR2) of the original vector (pUb:gwy) was excised. A fragment including gateway (attR1-ccdB gene – Cm resistance-attR2) mOrange cassette was amplified from p35S-GW-mOrange-nos binary vector (Bayle *et al.*, 2008) using primers containing XbaI and PmeI restriction sites (Table A5) and classical cloning was performed. Ligation was performed as described below. Ligation reaction was transformed into *E. coli* DB3.1 cells for plasmid propagation.

Constructs for yeast split-ubiquitin system were created via classical cloning strategy, restriction-ligation. PCR fragment including SfiI restriction sites of their 5´and 3´termini were subjected to digestion via SfiI restriction enzyme (see below), gel

electrophoresis and subsequent gel extraction. Restricted and cleaned DNA fragments were set up for ligation with the respective digested plasmids as follows:

Plasmid DNA	40-50 ng
DNA fragment	10-50 ng
10x T4-DNA ligase buffer	2 µl
T4-DNA ligase	0.75 µl
st. MQ-H_2O	up to 20µl

Ligation reactions were incubated at RT for 1 h or at 17°C ON and subsequently transformed into *E. coli* for plasmid propagation as described in chapter 2.2.1.1.

2.2.2.3. DNA extraction

Plasmid DNA extraction

E. coli propagated plasmids were isolated using NucleoSpin® Plasmid QuickPure according to the manual provided by the manufacturer.

Plasmid DNA from yeast was isolated from 4 ml of ON culture and was spun at 13000 rpm for 1 min. Harvested cells were washed in STE buffer (see below) and spin again before resuspending the pellet in 50U/ml Lyticase. After incubation at 37°C for at least 30 min with shaking at 600 rpm, the enzyme was heat-inactivated at 95°C that also serves for opening the cells. After cooling down the suspension to RT, further procedure was performed using NucleoSpin® Plasmid QuickPure and as described by the manufacturer including an optional washing step with buffer AW. Plasmids were eluated in 30 µl H_2O.

1x STE buffer

NaCl	0.1 M
Tris-HCl, pH~8.0	10 mM
Na_2-EDTA	1 mM

Genomic DNA extraction

For genomic DNA extraction frozen *L. japonicus* leaves were grinded using tungsten beads and tissue lyser. Homogenized tissue were resuspended in extraction buffer (see below) and incubated at 65°C for 30 min. After centrifugation (13 000 rpm for 5 min)

of the samples, the supernatants were transferred to a new tube and phenol:chloroform:isoamyl alcohol (25:24:1) purification was performed twice consecutively. Precipitation of the upper aqueous phase after phenol treatment was achieved by addition of isopropanol for at least 1 h at -20°C. The pellet was washed twice with 70% EtOH, dried and resuspended in 50 µl sterile water.

Extraction buffer

Tris (pH~7.5)	200 mM
NaCl	250 mM
Na_2EDTA	25 mM
SDS	0.5 %

DNA concentration was determined using Nanodrop spectrophotometer.

2.2.2.4. DNA analysis

Restriction via endonucleases

Restriction of DNA via endonucleases was not only used in cloning processes, but also for control digestions of vectors. For this reason, the following reaction was set up:

DNA	400-800 ng
10x buffer (appropriate for the given enzyme)	2 µl
Restriction endonuclease	0.3 µl
100x BSA (if required for the given enzyme)	0.2 µl
sterile MQ-H_2O	set up 20 µl

The reaction was incubated at 37 or 50°C as required for the enzyme activity for at least 30 min.

Sequencing

Sequencing of DNA molecules in form of PCR fragment or plasmid was done by the Sequencing Service of the Genomic Service Unit (Genetics, LMU Munich) on ABI 3730 48 capillary sequencer. For this purpose reaction containing 1µl 10pmol/µl of primer, 150-300 ng of DNA filled up to total volume of 7µl with Tris-HCl buffer (pH~8.0) was prepared.

2.2.3. Plant growth, transformation and genotyping

2.2.3.1. *Lotus* growth, transient and stable transformation

Lotus japonicus wild-type (ecotype Gifu B-129; Appendix, Table A2) was used for *Agrobacterium rhizogenes* – mediated hairy root transformations. Dried seeds were treated with sulphuric acid (95-98 %) for 5-10 min. Afterwards they were washed three times with water before being incubated in 2 % NaClO and washed three times with sterile water. Soaked seeds were germinated on 1% water-agar plates for 3 days in dark and 3 days in light under controlled conditions (24°C, 8h dark/ 16h light, 60 % humidity; plant growth chamber). Roots of seedlings were removed from the shoot and hypocotyls were dipped into *A. rhizogenes* (AR1193) suspension – carrying the respective construct. Transformed plants were placed onto Gamborg B5 medium (Gamborg *et al* 1968; see chapter 2.1.2.) supplemented with 100 µg/ml B5 vitamin mixture, incubated in dark for 2 days and then placed into a growth chamber with conditions described above. To remove Agrobacteria, composite plants were transferred 5 days after transformation onto Gamborg B5 medium containing 300 µg/ml Cefotaxim. The transfer was repeated several times. Further processing of composite plants is described in respective chapters.

L. japonicus wild-type (ecotype Miyakojima MG-20; Table A2) was used for generation of stable transgenic lines. The T-DNA, used for generation of transgenic plants expressing *pLjSYMREM1:gLjSYMREM1:YFP*, contains a Hygromycin selection marker. *A. tumefaciens* (AGL1) – mediated *in vitro* transformation and plant regeneration procedures were performed by Lotus Transformation Service (LTS, Institute of Genetics LMU; coordinated by Griet Den Herder) as described in Lombari *et al* 2005 with slight modifications. Further work with plants received from LTS is described in respective chapters.

L. japonicus TILLING (EMS mutagenized Gifu B-129, M3 generation; Table A2), Gifu wt, MG-20 transgenic (T2 generation) and MG-20 wt seeds that were set up for plant growth were surface sterilized using sandpaper. After 5-10 min (pro ~50 seeds) scarifying seeds were incubated in 2 % Sodium hypochlorite (NaClO) solution for 7 min and washed three times with sterile water. Soaked seeds (few hours incubation in sterile H_2O by rotation) were germinated for 3 days in dark and 3 days in light under controlled conditions described above.

2.2.3.2. Genotyping and selection of *Lotus japonicus* transgenic and mutant lines

All transgenic or EMS-mutagenized (TILLING) plants that were set up for further growth and seed production in the greenhouse, received Plant Number (Plant No.) registered in the Lotus Plant and Seeds Database (Parniske Lab Plant and Seed Database; [4]; restricted access) at the ZopRA (Zope Research Architecture; [5]) Portal.

Transgenic *L. japonicus* plants (generated by LTService, see chapter 2.2.3.1 and Table A2) carrying the *pLjSYMREM1:gLjSYMREM1:YFP* construct were tested for presence of the transgene performing PCR (using *LjSYMREM1* forward and *YFP* reverse primers; primer list Table A1) on the genomic DNA prepared from leaves of the transformed plants (T1 generation) received from the Transformation Service. Seeds of confirmed transgenic T1 generation plants were set up for further examination. When seedlings were grown on B5 medium containing 40 µg/ml hygromicin selecting for the presence of the T-DNA. Seedlings carrying the construct were resistant and grew better on the selective medium. T2 offspring that segregated in the expected 3:1 (transgenic:wt) phenotypic ratio that represents a 1:2:1 (homozygous:hemizygous:wt) genotyp, were selected for further analysis like Confocal Laser Scanning Microscopy (CLSM) and/or western blot.

Genotyping of *L. japonicus* TILLING lines was performed via sequencing analysis of PCR fragments that were amplified using *LjSYMREM1* specific primers (Table A1) from genomic DNA of TILLING plants.

2.2.3.3. Transient transformation of *Nicotiana benthamiana* leaves

For *in planta* protein localization and protein-protein interaction studies, *Agrobacterium tumefaciens* – mediated transient transformation of *N. benthamiana* leaves was performed. Leaves of six weeks old *N. benthamiana* (provided by the Greenhouse of the Biocenter LMU) were co-infiltrated with *A. tumefaciens* GV3101 C58 carrying the respective construct for protein localization or BiFC assay (Appendix, Table A3) and an *A.tumefaciens* GV3101 C58 strain mediating expression of the silencing inhibitor P19 to reduce transgene-silencing (Koncz and Schell, 1986; Voinnet *et al*., 2003). For infiltration of tobacco leaves, Agrobacteria grown in liquid LB medium (supplemented with appropriate antibiotics) were harvested and resuspended in a Agro-Mix solution containing

10 mM $MgCl_2$, 10 mM MES/KOH and 150 mM Acetosyringone, with final OD_{600} 0.05 of each suspension. Leaves were infiltrated using a 2ml syringe. For visualization of localization or interactions, leave discs at 2 dpi were excised, infiltrated with water and placed on glass slides in a drop of water. Imaging of fluorophore signal was conducted under Inverted epifluorescence microscope (Leica DMI 6000B) or Confocal Laser Scanning Microscope (SP5, Leica).

2.2.4. Promoter analysis and histochemical ß-glucuronidase assay

For promoter analysis of *LjSYMREM1*, a 2kb and a 975bp long sequence upstream of the start codon were amplified using primers named LjsymREMprom2k_1F (for 2kb amplicon); LjsymREMprom1k_1F (for 975bp amplicon) and a common reverse primer, LjsymREMprom_1R (Appendix, Table A5). Initial cloning was performed using the pGEM-T cloning system (Promega). Both putative promoter regions were fused to the *uidA* reporter gene encoding ß-Glucuronidase by sub-cloning into the binary vector pBI101 (Jefferson *et al*., 1987; Table A3).

Composite plants carrying the respective promoter constructs (generated via *A. rhizogenes*-mediated gene transfer, described in chapter 2.2.3.1.) were grown for 4 weeks on vertical squared Petri dishes. To induce *LjSYMREM1* promoter activity plants were inoculated with *M. loti* (MAFF expressing DsRed fluorophore) for a maximum of four weeks or with purified NFs (isolated from *M. loti*) at 10^{-8} M for 24 h by placing droplets 2-4 cm above the root tips, susceptible zone for rhizobial recognition (Heidstra *et al*., 1994). As a control, composite plants carrying the promoter construct were treated with medium lacking rhizobia or NF. Plants were planted into sand-vermiculite mixture (1:1) supplied with Fåhraeus medium in glass jars, mini-greenhouse or seeding tray before inoculation with *M. loti*. Rhizobia (3 days old liquid culture) were harvested then washed and resuspended in Fåhraeus medium (Fahraeus, 1957) and diluted to an OD_{600} 0.01. For each experiment composite plants carrying the promoter construct as well as the empty binary vector (as negative control) were generated.

In order to determine promoter activity in early stages of nodulation, composite plants were transferred onto plates with sterile Whatman filter paper that was placed on the top of Fåhraeus medium. The medium was supplemented with 0.1 µM AVG (aminoethoxyvinylglycine ([S]-*trans*-2-amino-4-(2-aminoethoxy)-3-butenoic acid

hydrochloride) – an inhibitor of endogenous ethylene production that might suppress infection process (Groth, 2010) – one day prior to rhizobial infection. Plants were infected with rhizobial suspension of OD_{600} 0.001 and grown under controlled conditions in growth chamber (24°C 8h dark/16h light).

ß-glucuronidase assay

For histochemical ß-glucuronidase staining, roots of infected and non-infected composite plants were cut and were placed into Falcon tubes containing 5-10 ml of GUS staining solution (Chapter 2.1.2.). Vacuum was applied three times for 3 min, and then roots were incubated at 37°C in the dark. Roots were checked for blue staining after 4-5 hours under a stereomicroscope. If no blue staining was found, roots were incubated in the staining solution overnight. Evaluation and documentation of roots was performed using stereomicroscope Leica MZ16FA and Leica DFC300FX camera.

2.2.5. Interaction methods

2.2.5.1. Split-ubiquitin yeast system

The split-ubiquitin system is a yeast-based assay for protein-protein interaction studies. By the help of this assay one can investigate interactions between membrane proteins, membrane-associated proteins and soluble proteins, if one of the proteins of interest is membrane-associated. The system is based on the small ubiquitin molecule that labels proteins for proteasomal degradation (ubiquitin-proteasome system). The molecule was split into an N-terminal (Nub) and a C-terminal half (Cub). The two halves can refold and form a native-like ubiquitin molecule (Johnsson and Varshavsky, 1994). An artificial transcription factor (TF) is fused to the Cub domain, which is cleaved off when the two domains are rebuilt and recognized by ubiquitin specific proteases (UBPs). The released TF (LexA-VP16) diffuses into the nucleus and starts the transcription of the reporter genes serving as readout of the system (Stagljar *et al*, 1998). Here the DUALmembrane split-ubiquitin system from the Dualsystems Biotech Company was used. The system consists of the *S. cerevisiae* NMY32 strain (MATa his3Δ200 trp1-901 leu2-3,112 ade2 LYS2::$(lexAop)_4$-HIS3 URA3::$(lexAop)_8$-lacZ ade2::$(lexAop)_8$ ADE2 GAL4), prey vectors for creation of NubG fused proteins with Trp auxotrophic marker, bait vectors

carrying Cub domain fusion with a LexA-VP16 TF and Leu selection marker. Furthermore, positive and negative control vectors carrying Alg5 yeast resident membrane protein for testing the localization and right folding the protein of interest in this system. Vectors and clones created for interaction studies in yeast are summarized in Appendix, Table A3.

Split-ubiquitin based yeast assays were performed to test protein-protein interactions of membrane-associated proteins. Small-scale transformation was performed in order to test interactions on 1 to 1 basis. Yeast strain *S. cerevisiae* NMY32 was transformed via LiAc/PEG method as described by the manufacturer (Dualsystems, P01001). For small-scale transformation, homemade solutions (50% PEG 3350; 1M LiAc) and homemade, shared herring sperm DNA (ss-DNA, 2mg/ml), ~150 ng/µl of prey and ~200ng/µl of bait vector were used. Large-scale transformation was performed for library screening. A modified large-scale transformation protocol was established and described below.

Screening procedure

The pDL2-Nx prey vector was used to clone cDNAs deriving from nodulated and mycorrhized roots and fused N-terminally to the NubG domain (NubG:cDNA library; kindly provided by M. Parniske, LMU Munich). The cDNA-library prepared from *E. coli* using DNA-extraction kit was re-transformed into *E. coli* cells. Colony PCR was performed on 96 colonies (using 96-well plate) using vector-specific primers (Table A1) to check the diversity of the library. Amplicons of different sizes (from 200bp-1800bp) were detected on 1% agarose gels.

After performing two pilot screen experiments (following the protocol provided by the manufacturer DUALmembrane, P01001-B03) in order to establish an optimized screening procedure, a third large-scale transformation experiment was performed. A sequential transformation (NMY32::Cub:LjSYMREM1 was over-transformed with NubG:library) and a simultaneous co-transformation (yeast strain NMY32 was co-transformed with the bait and the prey at the same time) procedure were done in parallel. As a control, co-transformations of Cub:LjSYMREM1 and Alg5:NubG were performed to assess the specificity and stringency of the experiment. The sequential transformation procedure was performed as described by the manufacturer (Dualsystems). The simultaneous co-transformation was performed as described in manual (Yeast Protocols

Handbook, PT3024-1) provided by Clontech with the following minor modifications. Co-transformant yeast cells were resuspended in 0.1% in 1.5 ml NaCl, when 400 µl were plated onto big round plates with SD-LW, SD-LWH + 15 mM and 30 mM 3-AT, SD-LWHAde medium, respectively. To determine the transformation efficiency 100 µl were plated onto small SD-LW plates in dilution series (non-diluted, 10^{-1} to 10^{-5}). This experiment was considered as a successful screen therefore it is summarized in chapter 3. Results.

Yeast clones grown on the SD-LWH + 30 mM 3-AT master plate were picked and they were grown in SD-LW liquid culture for recovery of the plasmid carrying the putative interaction partner. Plasmids purified from yeast (see chapter 2.2.2.3.) were re-transformed into bacteria since the amount of the DNA and the purity of the plasmid preparations is unsatisfactory for further analysis. *E. coli* XL1-Blue cells were used for re-transformation. When re-transformation was unsuccessful, plasmid preps were dialysed and re-transformation into bacterial cells was repeated. Colony PCR was performed, one strip per each re-transformed *E. coli* plate to check the diversity of plasmids carried by independent bacterial colonies. Yeast cells are able to take up more plasmids, whereas *E. coli* only one that is why more colonies were tested using vector specific primers. Plasmids (NubG: putative interactors) isolated from *E.coli* were re-co-transformed with Cub:LjSYMREM1 into yeast strain NMY32 as well as with the negative control construct Alg5:Cub. Yeast colonies were picked and inoculated into 100 µl SD-LW medium and they were grown ON at 28°C with shaking at 200 rpm. On the next day dilution series (non-diluted, 10^{-1} to 10^{-5}) were set up in sterile water from the ON-culture and stamped (using a 48 or 96-teeth metal pin replicator) onto SD-LW, SD-LWH + 15 mM 3-AT and SD-LWH + 30 mM 3-AT selective plates. Via these drop-tests, positive putative interactors could be selected and the negative ones filtered out. Putative positive interaction partners were sequenced and sequences analyzed *in silico*.

2.2.5.2. Bimolecular Fluorescence Complementation Assay

Bimolecular Fluorescence Complementation Assay (BiFC) is an *in planta* method for investigating protein-protein interactions, based on a similar principal as split-ubiquitin system. A fluorophore (YFP or GFP) is divided into N-terminal (YFP_N) and C-terminal (YFP_C) sub-domains that are not able of spontaneous re-assembly. However, when each

half is fused to proteins that interact, the two halves are brought into a physical connection and they are able to form *de novo* fluorescence (Hu *et al*., 2002; Bhat *et al*., 2006). In this study, proteins of interest were fused (listed in Appendix, Table A2) to the N-terminal half (YFP_N or Y_N) as well as to the C-terminal half (YFP_C or Y_C) of the YFP fluorophore. *N. benthamiana* leaves were infiltrated with the respective constructs using *A. tumefaciens* mediated gene transfer (see chapter 2.2.3.3.). Leaves co-expressing the respective constructs were inspected to microscopical analysis 2 dpi.

2.2.6. Protein extraction and Western blot analysis

2.2.6.1. Protein extraction from *Saccharomyces cerevisiae* and *Lotus japonicus* roots

Total protein extraction from yeast

For both, total protein extraction and fractionation 10 ml of ON yeast culture was harvested and cells were washed with 1 mM EDTA. Cells for total protein extraction were incubated in 2 M NaOH for 10 min on ice before 1 volume 50% TCA was added and further incubated on ice for at least 1 hour. The pellet was washed with ice-cold acetone and spun again at 14000 rpm for 20 min at 4°C. The pellet was resuspended in 5% SDS and the same volume of SDS-sample buffer for yeast (described below) was added and samples were incubated at 37°C for 15 min. Samples were spun down, supernatants were transferred into a new tube and stored at -20°C or used for further analysis.

Fractionation of yeast proteins

For protein fractionation, yeast cells were resuspended in 700 µl Protein Extract Lysis Buffer (PELB, see below) and grinded with glass beads via vortexing, in between the samples were chilled on ice for 1 min. This was repeated for at least seven times. Samples were spin down at 4°C for 20 min at 700x g and transferred to a new tube and centrifugation was repeated. Samples were subsequently subjected to ultracentrifugation for 1h at 100 000xg at 4°C. Supernatants containing the soluble proteins were transferred to a fresh tube and stored at -20°C or used for Western blot analysis. Pellets were resuspended in SDS-sample buffer for yeast, incubated at 37°C for 15 min before samples were sedimented at 4°C, 100 000x g for 1 h. Supernatants containing the membrane fractions (or insoluble proteins) were used for further investigation.

SDS-sample buffer for yeast

Tris-HCl, pH 6.8	25 mM
Urea	9 M
EDTA	1 mM
SDS	1 %
β-mercaptoethanol	0.7 M
Glycerol	10 %

"**PELB**" (Protein Extract Lysis Buffer)

50mM Tris-HCl, pH~7.5

Yeast Protease Inhibitor Cocktail (for fungal and yeast extracts, Sigma P8215)

Total protein extraction from Lotus japonicus roots

Roots of *L. japonicus* were grinded in liquid nitrogen using a mortar and and pestle. Proteins were solubilised by addition of homogenization buffer (100 µl buffer for 100 mg of plant material) and incubation at 37°C for 45 min.

Homogenization buffer

HEPES, pH 7.5	240 mM
EDTA, pH8.0	10 mM
Sucrose	10% (w/v)
NaCl	150 mM
SDS	1%
Urea	5 M
Thiourea	2 M
DTT	2 mM

Protease Inhibitor Coctail

2.2.6.2. Western blot analysis

SDS-PAGE

Before performing SDS gel electrophoresis, protein samples were incubated together with loading buffer (125 mM Tris-HCl; 50 % Glycerol; 4 % SDS; Bromophenol

blue) for 10 min at 70°C. Samples were loaded on 10% SDS-Polyacrylamide gel (described below) and subjected for separation via vertical electrophoresis at 150V for 1 h in 1x SDS-running buffer (see below). SDS-Polyacrylamide gels were prepared as described below.

1x SDS running buffer

Tris	25 mM
Glycine	192 mM
SDS	0.1 %

Separation gel

Polyacrylamide solution	10 %
(30 % Acrylamide/ 0.8 % Bisacrylamide)	
Tris-HCl, pH~8.8	0.36 M
SDS	0.1 %
APS	0.1 %
TEMED	0.04 %

Stacking gel

Polyacrylamide solution	5 %
(30 % Acrylamide/ 0.8 % Bisacrylamide)	
Tris-HCl, pH~6.8	0.18 M
SDS	0.1 %
APS	0.1 %
TEMED	0.1 %

Immunoblot

After the separation procedure, proteins were transferred onto PVDF (polyvinylidene fluoride) membrane using 1x transfer buffer (see below) for 1h-2h at RT and 100V or ON at 4°C and 30V. Before incubation with antibody, the membranes were treated with blocking solution (5% Milk in1x$TBS_{0,1\%Tween}$) at RT for 1h.

Yeast NubG-HA tagged proteins were incubated with α-HA-HRP antibody (applied at a 1:2000 dilution), the Cub-LexA-VP16 tagged proteins with primary α-LexA (1:5000) or α-

VP16 (1:1000), following a treatment with secondary α-Mouse-HRP (1:10000) or α-Rabbit-HRP antibodies (1:20000). YFP-tagged proteins were incubated with α-GFP primary antibody (1:5000), following a treatment with secondary α-Mouse-HRP (1:10000) and mOrange-tagged proteins were detected using primary α-DsRED antibody and a subsequent incubation with α-Rabbit-HRP (1:20000) secondary antibody. Antibody treatment was performed in 5% Milk (in TBS-T) solution in the case of HRP-conjugated antibody at RT for 1 h and incubation with non-conjugated antibody was performed ON at 4°C, following a 10 min washing step in1x$TBS_{0,1\%Tween}$ (TBS-T) three times repeated. Between primary antibody and secondary antibody application, membranes were washed three times for 10 min in 1x TBS-T buffer. Proteins were detected using chemiluminescent reagent (Luminogen, GE Healthcare or PIERCE) and subsequent radiographical record using Amersham Hyperfilm ECL film or camera (Fusion detection system) detecting for chemiluminescent.

Solutions

1x TBS buffer

Tris	20 mM
NaCl	140 mM
Adjust pH~7.6 with HCl	

1x Transfer buffer

Tris	25 mM
Glycine	192 mM
Adjust pH~8.3 with HCl	

3. Results

3.1. LjSYMREM1, ortholog of MtSYMREM1

MtSYMREM1 is a plasma membrane-associated signalling component involved in the nodulation process of *Medicago truncatula*, a legume that forms indeterminate nodules. Mutant *Mtsymrem1* plants showed alterations in IT formation and nodule morphology, indicating a role during rhizobial infection and its regulation. The protein is localized on nodular infection thread and symbiosome membranes and it interacts with at least three symbiotic receptor-like kinases NFP, LYK3 and DMI2 (Lefebvre *et al*., 2010). MtSYMREM1 is a member of the group 2 remorin protein family that is legume-specific.

3.1.1. Identification of *Lotus japonicus SYMREM1*

Using MtSYMREM1 as a template we identified *L. japonicus* chr4.CM0004.60.r2.d (*Lotus* database, [1]) as the most closely related sequence on nucleotide and amino acid level. Investigating the expression profile of this gene *in silico* revealed a nodulation-specific expression pattern (Hogslund *et al*., 2009) as previously described for MtSYMREM1 (Colebatch *et al*., 2004; Lefebvre *et al*., 2010). To test whether Ljchr4.CM0004.60.r2.d share the same common ancestor with MtSYMREM1 we retrieved all putative group 2 remorin sequences from soybean, common bean and poplar in addition to *L. japonicus* and *M. truncatula*. Phylogenetic analysis based on sequence comparisons in 172 independent positions revealed that both genes indeed originate from a common ancestor (Figure 3.1). We thus named the gene '*LjSYMREM1*'.

LjSYMREM1 (chr4.CM0004.60.r2.d; *Lotus* database, [1]) is located on the chromosome IV of the diploid *L. japonicus*. The gene represents a 1282bp long genomic sequence that consists of five exon and four intron regions as *MtSYMREM1*, with a difference in length of the first and the second intron regions (Figure 3.2; Tóth *et al*., accepted). The exon regions encompass a 624bp long CDS encoding LjSYMREM1 protein consisting of 207 aa.

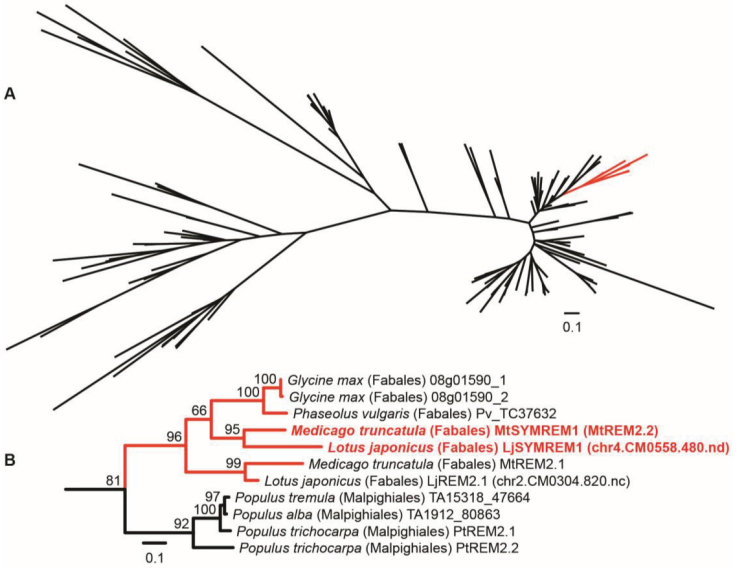

Figure 3.1 Phylogenetic analysis shows orthology between LjSYMREM1 and MtSYMREM1
LjSYMREM1 sequence is similar to the published one of MtSYMREM1, a group 2 remorin protein. (A) Phylogenetic analysis based on 147 amino acid remorin sequences using 101 unambiguously aligned residues in the conserved C-terminal region identified the group 2 of the plant specific remorin protein family (marked in red). (B) Amino acid sequences of 11 group 2 remorins from legumes and poplar were aligned and analyzed in 172 positions. MtSYMREM1 and LjSYMREM1 cluster together that indicates orthology of these two remorin proteins. True branch lengths were inferred by maximum-likelihood analysis; scale represents a probability of 0.1 amino acid changes per site (analysis performed by Dr. Arthur Schüßler, LMU; modified from Tóth *et al*., accepted).

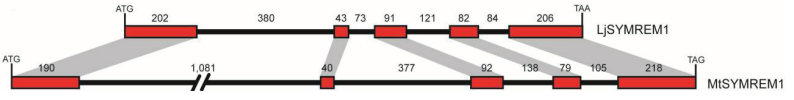

Figure 3.2 Exon-intron structure comparison of LjSYMREM1 and MtSYMREM1
Both remorins comprise of 5 exon regions (red boxes) and 4 intron regions (interspaces, black line). Numbers demonstrate the length of the respective region in base pairs (Modified from Tóth *et al*., accepted).

Both SYMREM1 proteins are composed of a highly variable, unstructured N-terminal region and a conserved C-terminal region encompassing a coiled-coil domain (COILS probability > 90%; Tóth *et al*., accepted). Figure 3.3 shows sequence alignment of

LjSYMREM1 and MtSYMREM1 on amino acid level. There is an overall 55.5 % identity between the two proteins meanwhile their conserved C-terminal regions share 72.9 % identity. However their N-terminal regions exhibit only 27.2 % identity (Table 3.1).

Figure 3.3 Sequence alignment of MtSYMREM1 and LjSYMREM1
Overall identity of the two SYMREM1 proteins is 55.5 %. Identity of N-terminal regions 27.2 % (1-80 aa; marked with bright red), identity of C-terminal regions is 72.9 % (81-207aa; marked in gray). Red boxes show the identical amino acid residues.

Because of the low conservation found between the two SYMREM1 proteins, we performed sequence comparison analysis of other member proteins of the group 2 remorins. Using MtSYMREM1 as a template we compared SYMREM1 remorins and their homologs from legumes soybean (*G. max*) and common bean (*P. vulgaris*) and non-legumes poplar (*P. trichocarpa*) and grape wine (*V. vinifera*). Interestingly, a similarly high difference between the N-terminal regions (sequence similarity of the N-terminal regions were around 40 %) of the involved proteins was found (Table 3.1). While their C-terminal parts show the characteristic high conservation (Table 3.1).

Identity/Similarity values in % for putative SYMREM1 homologs (based on MtSYMREM1)						
Domain	***Medicago***	***Lotus***	**Soybean**	**Poplar**	**Common bean**	**Grape wine**
Full-length	100	55.5/67.1	53.1/65.1	49.8/62.9	52.4/65.0	42.9/59.0
C-term	100	72.9/85.3	67.4/79.1	63.6/76.0	67.4/79.1	58.9/76.0
N-term	100	27.2/38.3	30.0/42.5	26.3/40.8	27.3/41.6	15.8/30.3

Table 3.1 Sequence comparison of several remorins within the group 2
Sequences of LjSYMREM1 and MtSYMREM1 were compared with other putative homologs (sequences derived from the best hit against the genome sequences) of the group 2 remorins, based on MtSYMREM1 sequence. N-terminal regions of the compared proteins were found to exhibit a high variability (showed identity/ similarity). While their C-terminal region showed a high sequence identity/ similarity (%) characteristic for the conserved C-terminal region of the remorin proteins (from Tóth *et al*., accepted).

This relatively low conservation between SYMREM1s gave rise to perform sequence analysis of a few known players of the symbiotic signalling pathway from *L. japonicus* and *M. truncatula*. We compared orthologous symbiotic proteins (NFR5/ NFP; SYMRK/ DMI2; POLLUX/ DMI1; CCaMK/ DMI3; CYCLOPS/ IPD3; NIN/ NIN; NSP2/ NSP2; Leghemoglobin 1b/ Leghemoglobin 1) from *L. japonicus* and *M. truncatula* to define their sequence identity and similarity (Table 3.2). All of these proteins exhibit a higher conservation among each other than SYMREM1s. The found high divergence between the two remorin proteins prompted us to gain a deeper insight into the function of LjSYMREM1 in the nodulation process of a legume with determinate nodules.

Medicago	***Lotus***	**identity**	**similarity**
NFP	NFR5	72.0%	82.8%
DMI2	SYMRK	81.6%	87.6%
DMI1	POLLUX	80.8%	85.3%
DMI3	CCAMK	85.7%	92.2%
IPD3	CYCLOPS	78.2%	87.1%
NIN	NIN	57.4%	67.5%
NSP2	NSP2	73.9%	83.4%
Leghemoglobin 1	Leghemoglobin 1b	70.3%	80.4%

Table 3.2 Sequence analysis of symbiotic proteins from *L. japonicus* and *M. truncatula*
Sequence analysis of proteins involved in symbiotic signalling pathway of *L. japonicus* (a legume developing determinate nodules) and *M. truncatula* (developing indeterminate nodules). All of them show higher identity/similarity with its orthologs than LjSYMREM1 and MtSYMREM1. With exception of the two NIN orthologs that exhibit only 57.4% identity (from Tóth *et al*., accepted).

3.2. Spatio-temporal expression analysis of *LjSYMREM1*

Remorins of the group 2 were found to be highly induced during nodulation in both model legume *L. japonicus* and *M. truncatula* (Colebatch *et al*., 2004; Høgslund *et al*., 2009; Lefebvre *et al*., 2010). Nevertheless, an approach to resolve spatial expression of *SYMREM1s* during the entire process has not been performed so far. To reveal the spatial expression pattern of *LjSYMREM1*, promoter activity analysis using GUS (β-glucuronidase-activity) -histochemical assay (Jefferson *et al*., 1987) was carried out.

3.2.1. Identification and functional analysis of *LjSYMREM1* promoter region

In order to identify a functional promoter, 2kb and 975bp long sequence upstream of the ATG initiation codon of *LjSYMREM1* were amplified and fused to the *ß-Glucuronidase* (*GUS*) reporter gene (*pLjSYMREM1:GUS*). Composite plants expressing the *pLjSYMREM1:GUS* reporter constructs were inoculated with *M. loti* and analyzed 15 dpi for the functionality of the putative promoter regions. Both putative promoter regions showed strongest GUS activity in nodules at 15 dpi. Promoter activity was detected in inner cortical cells of root nodules while no staining was found in out cortical cells (Figure 3.4).

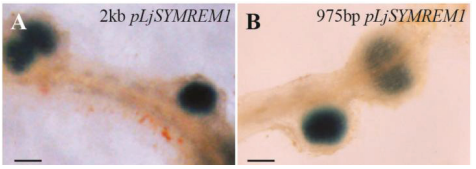

Figure 3.4 *LjSYMREM1* promoter activity.
To identify a functional promoter region of *LjSYMREM1*, a 2kb (A) and 975bp (B) region upstream of the start codon of the gene were fused to the *β-glucuronidase* reporter gene to follow the functionality of the promoter regions by the help of the histochemical GUS staining. Both promoter regions showed the same pattern: activity in inner cells of the nodule (blue staining) but no staining in the outer cortical cell layer 15dpi with *M. loti*, after 5 hours GUS staining. Scale bars indicate 250µm.

3.2.2. Spatio-temporal analysis of *LjSYMREM1* using its 975bp promoter region

Since both promoter regions tested in GUS-activity assay exhibited the same spatial pattern, the shorter 975bp *LjSYMREM1* promoter (*975pLjSYMREM1:GUS*) was used for further analysis.

In order to test whether *pLjSYMREM1* can also be activated upon application of isolated NFs, 10^{-8} M NFs were locally applied to transgenic *L. japonicus* roots carrying *975pLjSYMREM1:GUS* construct as well as empty vector as negative control (Figure 3.5A) to recognize possible background staining. Promoter activity was detected in epidermal and cortical cells above the root tip (Figure 3.5B, Figure 3.6A).

To follow the dynamics of *LjSYMREM1* gene activity, composite plants were inoculated with *M. loti* and roots were harvested every 24 hours post infection and

subjected to histochemical GUS staining. First blue staining was observed at 2 dpi indicating promoter activation in root epidermal and cortical cells above the root tip along a 2-3cm zone (Figure 3.5C) showing a similar pattern to that observed upon NF application. Rarely, blue staining could be observed in vascular tissue or in root tip, but there were never observed completely blue stained roots or nodules in negative control plants transformed with empty vector (Figure 3.5A).

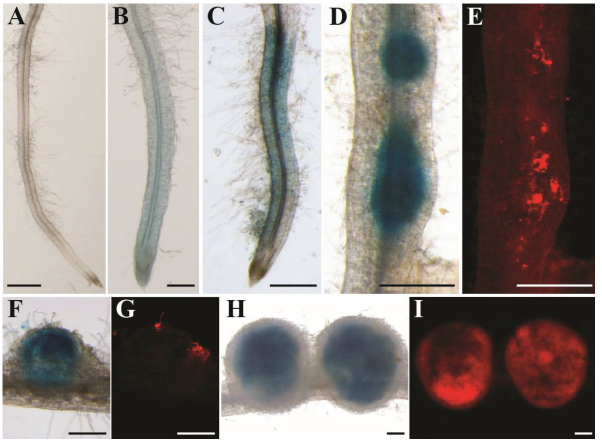

Figure 3.5 *LjSYMREM1* expression pattern through the entire nodulation process
In order to follow *LjSYMREM1* expression during the symbiosis, 975bp long sequence upstream of the ATG start codon of *LjSYMREM1* was fused to the *GUS* reporter gene. Transgenic *L. japonicus* roots carrying the reporter construct (*975pLjSYMREM1:GUS*) were investigated and subjected to histochemical GUS staining 24h after NF (10^{-8}M) treatment (B); 2dpi with *M. loti* (expressing DsRed) (C). In both cases promoter activity can be observed in epidermal and cortical cells above the root tip, in a susceptible zone for rhizobial infection. While no GUS staining was observed in transgenic roots transformed with the empty vector control and treated with NF (A). Four days after rhizobial inoculation, the promoter activity disappeared from the epidermal cells and it was detected in dividing cortical cells (nodule primordia) coinciding with rhizobial infection that could be detected via DsRed fluorescence produced by bacteria (D-E). In later stages as in young nodules (6dpi with *M. loti*) the expression of *LjSYMREM1* can be observed in nodule cortex underneath rhizobial infection (F-G). In old nodules (3wpi with *M. loti*) *LjSYMREM1* promoter activity was detected in infected cells of the nodule as it can be followed by DsRed fluorescence derived from bacteria expressing DsRed (H-I). Scale bars indicate 500 µm.

A stronger promoter activity was observed 4 dpi with *M. loti* in nodule primordia at the site of successful rhizobial infections where bacteria were detectable via DsRed fluorescence (Figure 3.5D-E). Promoter activity of similar staining intensity was observed in young nodules at 6 dpi coinciding with bacterial release into the nodule cortex (Figure 3.5F-G).

Furthermore, in mature nodules (3 wpi) also a very intensive accumulation of β-glucuronidase activity was detected together with presence of rhizobia in the fixation zone and in nodule parenchyma, but not in nodule outer cortical cells (Figure 3.5H-I, 3.6B).

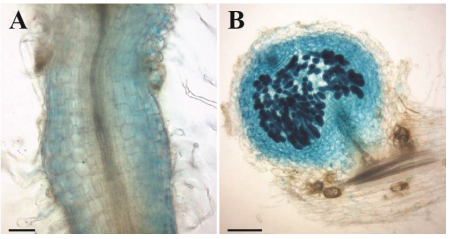

Figure 3.6 Root and nodule section showing *LjSYMREM1* expression pattern
(A) Longitudinal section of a GUS-stained root carrying *975pLjSYMREM1:GUS* reporter construct. Promoter activity detected in epidermal and cortical cells of roots 24 hpi with 10^{-8}M NF. (B) In order to detect in which cell layers of the nodule *LjSYMREM1* is expressed, a mature nodule (3wpi with *M. loti*) carrying the *975pLjSYMREM1:GUS* reporter construct was subjected to sectioning. *LjSYMREM1* promoter showed activity in the infected cells and in nodule parenchyma as well. No GUS staining was detected in nodule cortex. Material was embedded in 5% low melt agarose and sections (100µm-150µm) were prepared. Scale bar indicates 50 µm (A) and 250 µm (B).

3.3. Localization of LjSYMREM1

3.3.1. LjSYMREM1 protein localization expressed under its native promoter

In order to study localization of the protein under native expression conditions, stable transgenic lines carrying the *pLjSYMREM1:gLjSYMREM1:YFP* construct were created. Generation of stable transgenic *L. japonicus* (MG20 ecotype) lines via *A.tumefaciens* mediated gene transfer carrying the fusion construct was initiated by the help of the Lotus Transformation Service (LTS) at the Institute of Genetics LMU. Six independent stable transgenic lines were obtained and were subjected for genotyping via PCR to isolate plants carrying the transgene. These plants (T1 generation) were selected for further growth and seed production (Table 3.3). In order to define presence or absence of the insertion cassette that includes a hygromycin selectable marker gene, seeds from all six T1 lines (Table 3.3) were germinated on water-agar plates containing 40 µg/ml hygromycin. Progeny plants carrying the T-DNA are resistant and thus selectable on

growth performance. Individuals of T2 generation that segregated in a 3:1 (transgenic:wt) phenotypic ratio – standing for a 1:2:1 (wt:hemizygous:homozygous) genotype – and showed the strongest resistance towards the antibiotic were selected for further analysis.

Plant No. (T1 generation)	**Seed bag No.**	**Phenotypic segregation of T2 generation** transgenic:wt	**Protein expression**
L9713	87138	3:1	No further analysis
L9714	87139	1:3	No further analysis
L9716	87140	1:3	No further analysis
L9717	86645	3:1	CLSM, Western blot
L9720	87142	1:1	No further analysis
L9723	87141	1:3	CLSM, not detected

Table 3.3 Summary of stable *pLjSYMREM1:gLjSYMREM1:YFP* transgenic *L. japonicus* lines
All putative transgenic plants were genotyped for presence of the transgene, entered into the database (Plant Number) and set up for seed production. Seeds originating from the T1 generation were harvested and independently collected in a seed bag (Seed bag No.). Seedlings of segregating T2 generation were grown on W/A plates supplemented with 40µg/ml hygromycin selecting for the presence of the T-DNA. Plants exhibiting 3:1 (transgenic: wt) phenotypic segregation ratio – that represents a 1:2:1 (wt: hemizygous: homozygous) genotype – were selected for further analysis.

T2 offsprings of the lines L9717 and L9723, segregated in the expected 3:1 ratio, were selected and inoculated with *M. loti*. First CLSM analysis searching for YFP fluorescent signal deriving from the LjSYMREM1:YFP fusion protein was performed at 8 dpi. To discriminate YFP from background auto-fluorescence λ-scans for emission fingerprinting were performed in the range of 500-600nm. Fluorescence that was detected by microscopy and/or by laser scanning was a false positive signal arising from auto-fluorescence of *L. japonicus* roots.

YFP fluorescence could be detected in nodules (of T2 plants of the line L9717) at 3 wpi with *M. loti*, when they were sectioned. YFP signal of the LjSYMREM1:YFP fusion protein coincided with DsRed signal deriving from cells harbouring rhizobia (Figure A-D, E-H).

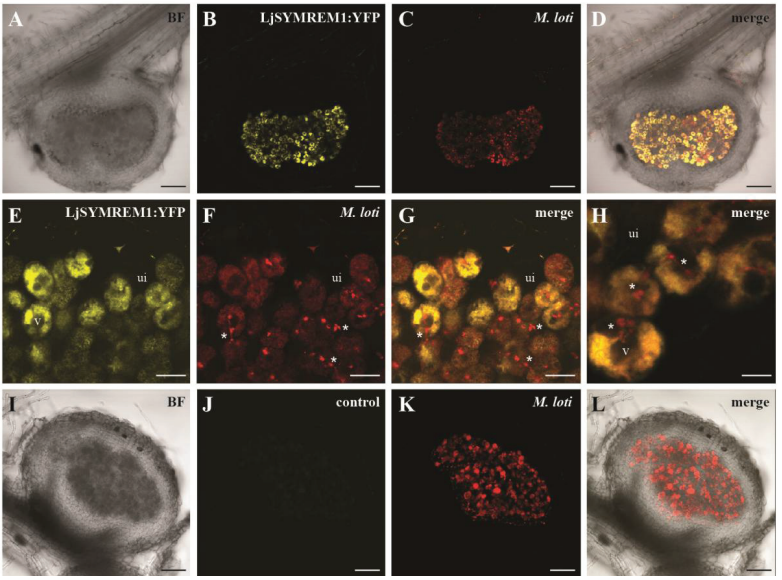

Figure 3.8 LjSYMREM1 localizes to the infected cells in nodule
Stable transgenic *L. japonicus* lines were generated in order to investigate LjSYMREM1 localization fused to YFP fluorophore and expressed under its endogenous promoter (*pLjSYMREM1:gLjSYMREM1:YFP*). Sections of nodules 21 dpi with *M. loti* (expressing DsRed) were made to inspect the localization using CLSM. The YFP-tagged LjSYMREM1 localizes to the infected cells in the central zone of the nodule (B). Presence of bacteria could be observed by the help of DsRed fluorophore expressed by the symbiont *M. loti* (C). Overlay (of B and C) demonstrates that localization of LjSYMREM1:YFP coinciding with infected cells (D). Closer look at the infected cells (E-H). Cells that were not infected (ui) did express neither DsRed nor YFP fluorescence. V-vacuole located in the centre of infected cells. Sign "*" indicates nodular infection threads. YFP signal of the fusion protein coinciding with bacterial DsRed signal (merge, G-H). Non-transgenic wild type nodule was investigated to exclude unspecific auto-fluorescence background of *L. japonicus* roots (I-L). Nodules were embedded in 5% low-melt agarose and 150µm sections were made. Scale bars indicate 100 µm (A-D, I-L), 20 µm (E-G) and 10 µm (H). BF-bright field.

No YFP fluorescence was observed in non-infected cells indicated by the lack of rhizobial DsRed signal (Figure 3.8A-D, E-H). Since analysis of λ-scan spectra did not allow fully reliable discrimination of the signals, nodules of non-transgenic MG-20 wt plants were sectioned and analyzed via CLSM. In these control nodules, no fluorescence in the emission spectrum of YFP fluorophore could be detected (Figure 3.8 I-L). Western blot analysis (using α-GFP antibody against the YFP-tag) of proteins extracted from nodules also confirmed the presence of LjSYMREM1:YFP fusion protein (Figure 3.10B).

To test whether the signal indeed resulted from symbiosome membranes, individual bacteroids were isolated by application of mechanical force. Indeed the LjSYMREM1:YFP signal co-localized with the bacteria indicating localization of the protein on the symbiosome membrane (Figure 3.9A-C). Furthermore, a closer look at the infected cells of a sectioned nodule (3 wpi with *M. loti*) showed that the LjSYMREM1 localizes to the nodular infection threads as well (3.9D-F).

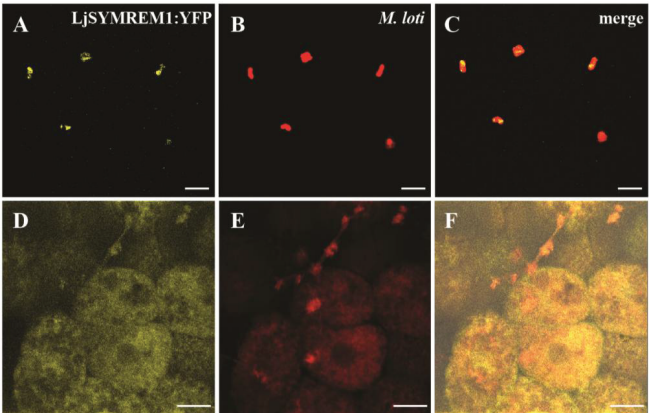

Figure 3.9 LjSYMREM1 localizes at the symbiosome membrane and to nodular infection threads
Nodules expressing *pLjSYMREM1:gLjSYMREM1:YFP* were mechanically destroyed to observe the exact localization of the protein. LjSYMREM1:YFP co-localizes with DsRed signal expressed by rhizobia on the symbiosome (peribacteroid) membrane (A-C). Closer look at the nodular infection threads (in nodules 3 wpi with *M. loti* expressing DsRed) showed that LjSYMREM1 localizes to the nodular infection thread followed by DsRed fluorophore (D-F). Nodule was embedded in 5% low-melt agarose, 150 µm sections were made and inspected using CLSM. Scale bars indicate 5 µm (A-C) and 10 µm (D-F).

3.3.2. Plasma Membrane localization in *Lotus japonicus* roots

Localization of natively expressed LjSYMREM1 (*pLjSYMREM1:gLjSYMREM1:YFP*) could not be detected in root epidermal and cortical cells as it was shown in *LjSYMREM1* expression experiments using *pLjSYMREM1:GUS* construct (chapter 3.2.2.). In order to ascertain localization of LjSYMREM1 protein within root epidermal cells where *LjSYMREM1* promoter activity was shown, transgenic *L. japonicus* roots expressing LjSYMREM1:mOrange fusion protein under control of the constitutive *Lotus* polyubiquitin promoter (*pUb:LjSYMREM1:mOrange*) were generated. Expression of the

polyubiquitin promoter in all root and nodule cell types was described previously (Maekawa *et al*., 2008). Since we experienced a high level auto-fluorescence of *L. japonicus* roots in emission spectrum of the YFP fluorophore (maximal excitation at 514 nm; maximal emission at 527 nm), we decided to use mOrange fluorophore with another emission spectrum (maximal excitation at 548 nm; maximal emission at 562 nm) and a brighter fluorescence signal. A clear mOrange fluorescence signal was detected at the periphery of root epidermal cells, indicating a PM-associated localization of LjSYMREM1 protein (Figure 3.11A).

Protein expression in *pLjSYMREM1:gLjSYMREM1:YFP* stable line (described in chapter 3.3.1.) and in transgenic roots expressing the *pUb:LjSYMREM1:mOrange* construct was verified and presence of the fusion proteins was detected at different time points. LjSYMREM1:mOrange expressed constitutively was detected at each time-point tested (Figure 3.10A). In contrast LjSYMREM1:YFP driven by its native promoter could only be detected 15 dpi with *M. loti* (Figure 3.10 B), indicating over-expression of LjSYMREM1 when expressed under control of the polyubiquitin promoter.

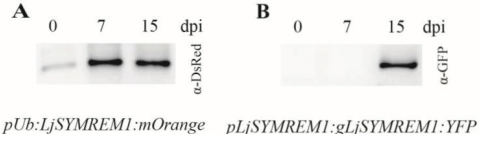

Figure 3.10 Detection of LjSYMREM1 protein expressed under control of different promoters
To verify the proteins detected via CLSM, total protein extraction was performed on *L. japonicus* transgenic roots expressing LjSYMREM1:mOrange under control of the constitutive pUb promoter (*pUb:LjSYMREM1:mOrange*) and on transgenic roots expressing LjSYMREM1:YFP fusion protein driven by its native promoter (*pLjSYMREM1:gLjSYMREM1:YFP*). Expression of the fusion proteins were detected at 0, 7 and 15 dpi with *M. loti*. (A) LjSYMREM1 expressed constitutively could be detected at each time-point using α-DsRed antibody against the mOrange fluorophore (~ 43 kDa). (B) LjSYMREM1: YFP expressed under its native promoter could be detected 15 dpi (using α-GFP antibody against the YFP fluorophore, ~ 50 kDa).

3.3.2.1. The C-terminal region of LjSYMREM1 is responsible for its PM localization of the protein

In order to ascertain whether the unstructured N-terminal region or the highly conserved C-terminal region directs the protein to the PM, both regions were cloned independently as a 78 aa long stretch (LjSYMREM1$_N$; 1-78 aa) defining the N-terminal

and 129 aa for the C-terminal part of the protein (LjSYMREM1$_C$; 79-207 aa). Both regions were tagged with mOrange fluorophore (LjSYMREM1$_C$: mOrange, LjSYMREM1$_N$: mOrange) and they were expressed under control of the constitutive polyubiquitin promoter in transgenic roots. Roots were subjected to CLSM analysis to detect the localization of the individual halves. The C-terminal region localized to the periphery of epidermal cells indicating and showing the same PM localization (Figure 3.11B) pattern as the full-length protein (Figure 3.11A). While LjSYMREM1$_N$ localized in the cytosol and in the nucleus (Figure 3.11C) of root epidermal cells.

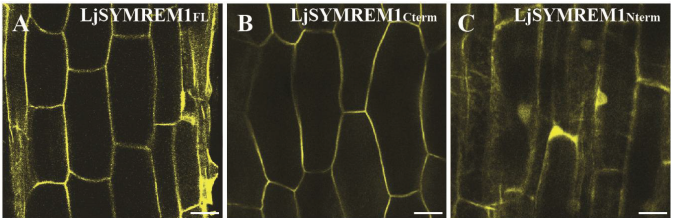

3.11 LjSYMREM1 and its C-terminal region localizes to the plasma membrane while the N-terminal region is cytoplasmic
LjSYMREM1 and its N-terminal and C-terminal part were fused to mOrange fluorophore and they were expressed under control of the constitutive *Lotus* polyubiquitin promoter in *L. japonicus* transgenic roots. LjSYMREM1 full-length (A) as well as LjSYMREM1 C-terminal region (B) yielded in fluorescence located at the periphery of root epidermal cells. In contrast, N-terminal region of LjSYMREM1 (C) showed a cytosolic and nuclear localization. Scale bars indicate 200µm.

As a conclusion, the C-terminal part or a hidden pattern for PM-anchoring harboured in this region is responsible for the PM-associated localization of the LjSYMREM1 protein. The lonely N-terminal region has not only a cytosolic localization but also a nuclear one that might be explained with its small size that allows the tagged-protein to enter the nucleus.

3.4. Assessing LjSYMREM1 phenotype

3.4.1. Phenotype caused by over-expression of *LjSYMREM1*

In order to assess a role of LjSYMREM1 in RNS, nodulation phenotype was followed up upon *LjSYMREM1* over-expression. Moreover, the individual remorin halves, LjSYMREM1$_N$ and LjSYMREM1$_C$ were also over-expressed. Plants carrying the full-length (FL) protein, the C-terminal and the N-terminal region fused to mOrange and expressed under control of the *Lotus* polyubiquitin promoter as well as plants carrying empty vector control were inoculated with *M. loti* and nodulated for eight weeks.

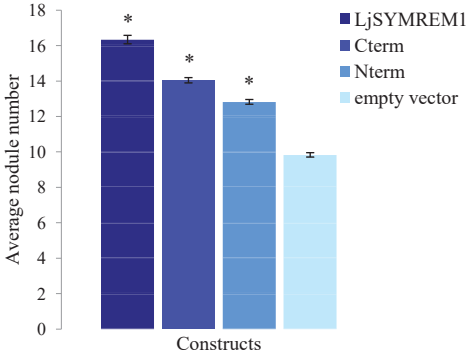

Figure 3.12 Over-expressing *LjSYMREM1*, its N-terminal and C-terminal regions caused increased nodule number
Increased nodule number was observed on the roots of composite plants over-expressing LjSYMREM1 full-length protein (about 40 % more nodules), LjSYMREM1 N- (about 23.4 % more nodules) and C-terminal regions (about 30 % more nodules) under control of the *Lotus* polyubiquitin promoter in comparison with transgenic roots carrying the empty binary vector. Plants were analyzed 8 wpi with *M. loti* (* t-test $p < 0.01$; plants expressing FL LjSYMREM1= 21; expressing Cterm= 27; expressing Nterm= 33; expressing empty vector control= 29). Error bars indicate standard errors.

Transgenic root systems were investigated for presence of the fluorophore-tagged proteins prior to phenotypic analysis of nodulated roots. Composite plants expressing LjSYMREM1$_{FL}$ exhibited significantly ($p < 0.01$) about 40 % more nodules in comparison with plants carrying the empty vector construct (Figure 3.12). Interestingly, over-expression of the individual remorin regions resulted in significantly increased nodule number ($p < 0.01$) as well. Over-expressing LjSYMREM1$_C$ resulted in about 30 % more while LjSYMREM1$_N$ over-expression caused about 23.4 % more nodules (Figure 3.12).

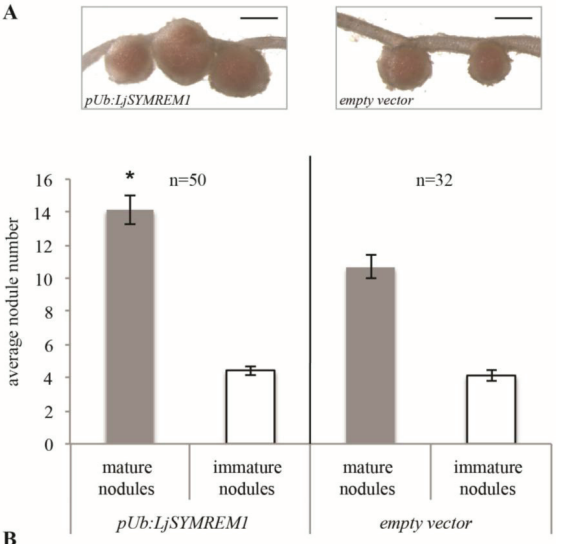

Figure 3.13 Increased nodulation phenotype caused by *LjSYMREM1* over-expression
In order to determine the putative function of LjSYMREM1 protein in nodulation process, the protein was overexpressed in *L. japonicus*. (A) Composite plants carrying LjSYMREM1 fused to mOrange fluorophore and expressed under control of the constitutive polyubiquitin promoter exhibit significantly more (* t-test p< 0.01) in comparison with empty vector control. (B) Morphologically non-altered nodules were observed on transgenic roots carrying the *pUb:LjSYMREM1* and on roots carrying the empty vector control, as well. Plants were analyzed 4 wpi with *M. loti*. Nodules were morphologically analyzed using stereomicroscope. Scale bars indicate 1 mm.

Experiment was repeated once, when composite plants carrying the over-expression construct of the FL protein were inoculated and analyzed 4 wpi with *M. loti*. Root systems were subjected to microscopical analysis to define the transgenic ones. The increased nodulation phenotype could be confirmed, composite plants possessed about 25% more nodules (p> 0.01) than roots carrying the empty vector control (Figure 3.13B). Nodules were microscopically analyzed and they were found morphologically non-altered and fixing (Figure 3.13 A). In this experiment, bumps and infection threads were also evaluated. No significant changes were observed in terms of number of bumps (Figure 3.13B). Aborted and non-aborted ITs also showed a similar number to that of those observed on control roots (data not shown).

The fact that over-expressing LjSYMREM1 and its N-terminal and C-terminal regions caused increased nodule number indicates an important role of the protein involved in

nodulation process and that both LjSYMREM1 regions are important for the biological function of the protein.

3.4.2. EMS mutagenized *LjSYMREM1* lines

To identify potential knock-out mutants and assess a *Ljsymrem1* phenotype, we screened for mutant lines in an EMS mutagenized population (*L. japonicus* Gifu background) taking the advantage of the TILLING (Targeting Induced Local Lesions IN Genomes) platform at John Innes Centre (RevGen UK, Norwich Research Park, Norwich, UK; Perry *et al*., 2003). The PCR-based screen (performed by the TILLING facility) identified three independent mutant lines of which seeds from the M3 progeny were obtained. One (SL0061-N) of these lines carries a premature stop codon, one (SL4207-1) of them possess a missense point mutation in coding region and the third one (SL6600-1) carries a point mutation on the first exon-intron junction (Figure 3.14). All plants were genotyped via sequencing to identify homozygous mutant lines. Among M3 plants of the lines carrying the missense point mutation and the mutation on the first exon-intron border homozygous one were isolated, while homozygous M3 plant carrying the premature stop codon could not be identified. Table 3.4 summarizes the lines, their genotype and the current state of analysis.

Seeds of the homozygous line carrying a missense mutation (SL4207; 165D>N), a wt homozygous line for the given mutation in the *LjSYMREM1* locus and *L. japonicus* Gifu wt from the seed storage of Institute of Genetics (LMU) were grown in parallel for nodulation experiments at two different temperatures 18°C and 26°C. Such permissive temperatures have been found to pronounce weak phenotypes in several lines (Jens Stougaard, University of Aarhus, Denmark; personal communication). Plants were preceded for phenotypical analysis 4 wpi with *M. loti*, when shoot and root length were measured and nodule numbers were counted. This mutation did not cause a phenotype neither on the plants grown at 18°C nor on the plants grown at 26°C (data not shown).

Homozygous plants of the line carrying the splice-site mutation (SL6600-1) were investigated. The experiment was repeated three times in order to find out the authenticity of the increased nodulation phenotype caused by the point mutation on the first exon-intron border. All three experiments were evaluated 4 wpi with *M. loti*.

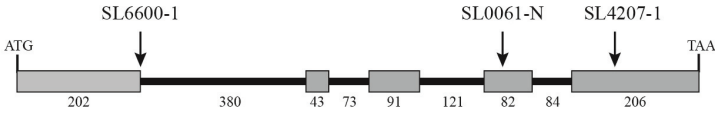

Figure 3.14 Point mutations in *LjSYMREM1* locus
In order to assess a phenotype caused by knockdown or knockout of *LjSYMREM1*, an EMS mutagenized population of *L. japonicus* was screened for mutations in *LjSYMREM1* locus. Among a few lines that were found via TILLING analysis (RevGen UK, Norwich Research Park, Norwich, UK; Perry *et al*., 2003), three lines: SL6600-1 carrying a point mutation at the first exon-intron border, the line SL0061-N carrying a mutation causing a premature stop codon and a missense mutation causing an amino acid change in the line SL4207-1. Grey boxes represent exons and the black lines in between illustrate introns of *LjSYMREM1* gene. Numbers demonstrate the length of exons and introns in bp. Arrows indicate the mutation sites.

Line	Mutation	Change caused	Genotype/Phenotype
SL0061-N* received as M3	stop-codon mutation	W123X	heterozygous, tested, no phenotype
SL4207-1 received as M3	missense in coding region	D165N	homozygous, tested, no phenotype
SL6600-1 received as M3	mutation at the first exon-intron site	no	homozygous, tested, nodulation phenotype

Table 3.4 *LjSYMREM1* EMS mutagenized lines
Summary of three *LjSYMREM1* EMS mutagenized lines received from TILLING analysis (RevGen UK, Norwich Research Park, Norwich, UK; Perry *et al*., 2003). All lines exhibit G >A point mutation. The point mutation in line SL0061-N (* seeds originating from different mother plants) causes a premature stop codon (W changed to X) and homozygous plants were used for phenotyping. An amino acid substitution (D changed to N) in line SL4207-1 and analysis of homozygous mutant plants did not show a nodulation phenotype. Line SL6600-1 possesses a point mutation at the first exon-intron junction resulting in a significantly increased nodulation phenotype.

Plants developed significantly more nodules (about 20%, $p < 0.01$) in comparison with wild type plants (Figure 3.15). Plants carrying the mutation also developed significantly longer shoots ($p < 0.01$) compared to wild type plants (Figure 3.15). A detailed transcript analysis remains to be performed in order to determine whether the phenotype is caused by altered transcript variants.

Seeds (offsprings of generation M3) of three heterozygous plants carrying the point mutation causing premature stop codon (SL0061-N) were set up for phenotypical analysis 4 wpi with *M. loti*. About 300 plants of a segregating population were analyzed with respect to shoot length, root length and nodulation.

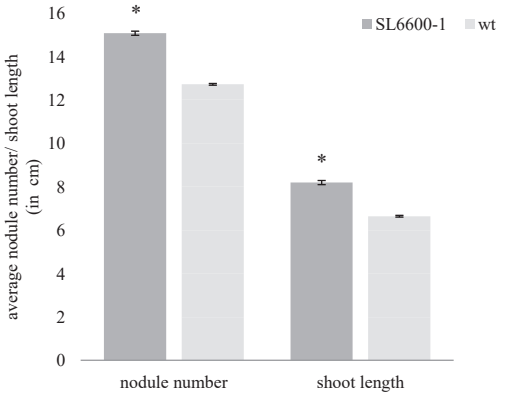

Figure 3.15: Nodulation phenotype caused by a point mutation on the first exon-intron junction of *LjSYMREM1*
The TILLING line carrying a point mutation on the first exon-intron junction in *LjSYMREM1* locus exhibits an increased nodulation phenotype in comparison with wild type *Lotus* Gifu plants (columns left; average nodule number). Plants were subjected to phenotypic analysis 4 wpi with *M. loti*. As a consequence of the significantly higher nodule number (* t-test $p < 0.01$), the shoot length of the mutant plants (n=42) is also significantly longer (* t-test $p < 0.01$) than those of the wild type plants (n=46). Error bars indicate standard errors.

Genotypes of 36 randomly chosen individuals were determined by sequencing *LjSYMREM1*. 23 sequences could be analyzed resulting in identification of 11 wild-type plants, 11 heterozygous and only one homozygous mutant plant. Unfortunately, the expected 1:2:1 (wt: heterozygous: homozygous) segregation ratio was not obtained not only in genotyping, but the plants also did not exhibit a remarkable phenotype (data not shown). The experiment was carried out once. Therefore, it has to be repeated to gain a rational conclusion.

3.5. LjSYMREM1 interacts with symbiotic receptor-like kinases

It was shown that MtSYMREM1 interacts with upstream elements of the symbiotic signalling pathway, such as the symbiotic receptor-like kinases NFP, LYK3 and DMI2 (Lefebvre *et al*., 2010). Here we tested whether LjSYMREM1 exhibits the same interaction pattern as MtSYMREM1.

3.5.1. Interactions and oligomerization of LjSYMREM1 in Bimolecular Fluorescence Complementation assay

Bimolecular Fluorescence Complementation (BiFC) studies were performed in order to investigate interactions assumed between LjSYMREM1 and *L. japonicus* RLKs NFR1, NFR5 and SYMRK. *Nicotiana benthamiana* leaves were used to perform BiFC assay, a tool for investigating protein-protein interactions *in planta* (Bhat *et al*., 2006).
Since these experiments required expression of proteins investigated in heterologous system, the proteins were tagged with a fluorophore and they were expressed under control of the constitutively active CaMV 35S promoter. A C-terminal fusion of LjSYMREM1 to Cyan Fluorescent Protein (CFP; LjSYMREM1:CFP) fluorophore was created and leaves were transformed with this construct using *A. tumefaciens* mediated gene-transfer. *N. benthamiana* leaves transiently expressing the fusion-proteins were analyzed 2 dpi. Strong fluorescent CFP signal was exclusively detected at the periphery of the cells indicating PM localization (Figure 3.16A). Before investigating the putative interactions, localizations of NFR1 and NFR5 fused C-terminally to YFP fluorophore were also tested in *N. benthamiana* leaves. They also showed PM-associated localization of leaf epidermal cells (Figure 3.16B-C).

In order to examine interactions assumed between LjSYMREM1 and *Lotus* RLKs NFR1 and NFR5, we created C-terminal fusion proteins to N-terminal (YFP_N=Y_N) and C-terminal (YFP_C=Y_C) halves of the YFP fluorophore (split YFP) for BiFC assay.

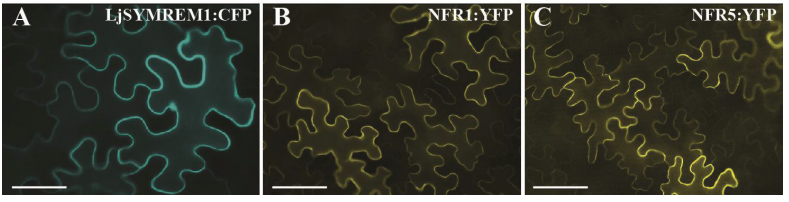

Figure 3.16 Plasma membrane localization of LjSYMREM1 and the symbiotic RLKs NFR1 and NFR5
LjSYMREM1 fused to CFP (A), NFR1 and NFR5 fused to YFP (B and C) were tested for localization in *N. benthamiana* leaf epidermal cells prior to work with the proteins in Bimolecular Fluorescence Complementation assay. The fluorescence signal of the fusion proteins localized at the periphery of the leaf epidermal cells demonstrating a plasma membrane-associated localization of each protein tested. Leaves were inspected under epifluorescent microscope 2dpi. Scale bars indicate 50µm.

Interactions of LjSYMREM1 with NFR5, NFR1 and SYMRK (SYMRK constructs were kindly provided by M. Antolín-Llovera, LMU Munich) were investigated in *N. benthamiana* leaves co-expressing the respective constructs 2 dpi (Table 3.5). All combinations tested, resulted in YFP fluorescence (as a consequence of re-assembly of the split YFP halves when they fused to proteins that interact) observed at the periphery of leaf epidermal cells that indicates interactions occurring in the PM region (Figure 3.17A-C). Interestingly, co-expression of LjSYMREM1 with NFR1 and NFR5 showed fluorescence not only at the PM but also fluorescent foci could be observed (Figure 3.17A-B). In order to test authenticity of these results, co-expression of MtSYMREM1 with *Lotus* symbiotic RLKs was performed (Table 3.5). Co-expressing Y_N/Y_C:MtSYMREM1 and NFR5/NFR1/SYMRK:Y_C/Y_N did not result in interactions (Figure 3.17D-F), although these MtSYMREM1 constructs showed interactions with *Medicago* symbiotic RLKs fused also C-terminally to YFP halves (Lefebvre *et al*., 2010). In contrast co-expression of the proteins owning the same fusion direction with split YFP halves (RLKs:Y_C/Y_N and MtSYMREM1:Y_C/Y_N; Table 3.5) surprisingly yielded a fluorescent signal at the PM (Figure 3.17G-I; Table 3.5). This fact might be a consequence of the strong coiled-coil domain encompassed in the conserved C-terminal region of both remorins and/or an influence of the fluorophore fusion direction on the proteins. Probably, it can be excluded that the detected interactions are a consequence of an over-expression artefact (originating from the constitutive CaMV 35S promoter), since Y_N/Y_C:MtSYMREM1 did not show interactions with LjRLKs:Y_C/Y_N. Interestingly, co-expression of MtSYMREM1 with NFR5 and NFR1 also showed a "dotted" pattern (Figure 3.17G-H).

Furthermore, homo-oligomerization of LjSYMREM1 was tested as it is known that MtSYMREM1 oligomerizes with itself in BiFC experiments (Lefebvre *et al*., 2010). Co-expression of LjSYMREM1:Y_N and LjSYMREM1:Y_C resulted in reconstitution of the two split YFP halves and in fluorescence located at the periphery of *N. benthamiana* leaf epidermal cells (Figure 3.18A), suggesting homo-oligomerization of the protein. Since both SYMREM1 proteins are able to undergo homo-oligomerization, the question arose whether they might be able to hetero-oligomerize with each other. Co-expression of LjSYMREM1 C-terminally fused to split YFP moieties (LjSYMREM1:Y_N/Y_C) with MtSYMREM1 N-terminally fused split YFP fusion protein (Y_N/Y_C:MtSYMREM1) did not lead to a YFP fluorescence (Figure 3.18B). While co-expressing SYMREM1s, both C-terminally tagged with the fluorophore halves (LjSYMREM1:Y_N/Y_C and

MtSYMREM1:Y_C/Y_N), yielded a YFP signal in the PM (Figure 3.18C; Table 3.5), indicating interaction (hetero-oligomerization) of the two remorin proteins derived from relative species.

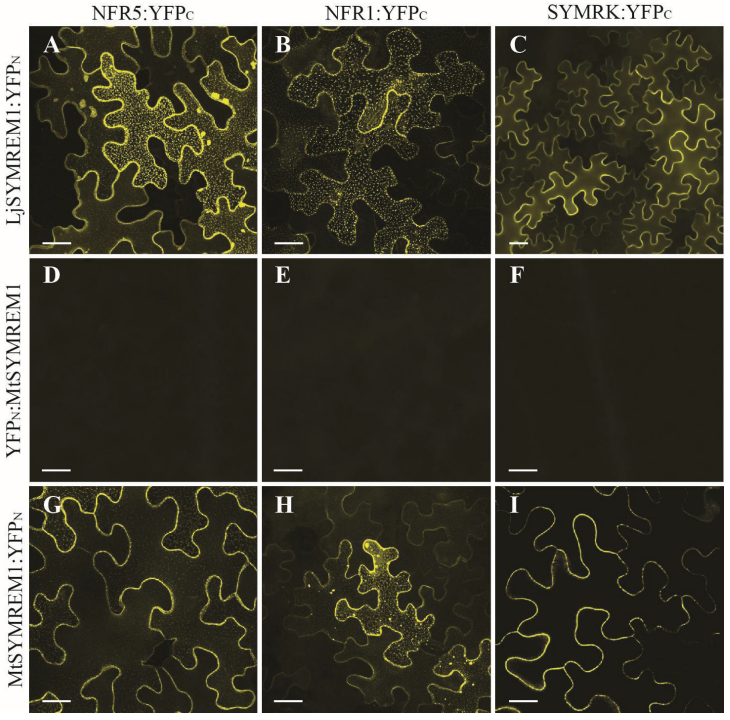

Figure 3.17 Interactions of SYMREM1s with *L. japonicus* symbiotic RLKs
In BiFC assay interactions of LjSYMREM1 with symbiotic RLKs NFR1, NFR5 and SYMRK were tested. Fluorescence at the periphery of the leaf epidermal cells was detected when LjSYMREM1 was co-expressed with NFR5 (A), NFR1 (B) and SYMRK (C), as a result of reassembly of the split YFP halves when the proteins fused to them interact. Upon co-expression of LjSYMREM1 with NFR1 and NFR5 fluorescent foci could be also observed (A-B). Co-expressing N-terminally fused MtSYMREM1 to split YFP halves with the *Lotus* RLKs (as a control experiment) NFR5, NFR1, SYMRK did not result in interactions (D-F). While co-expression of C-terminally tagged MtSYMREM1 with the same RLKs resulted in YFP fluorescence at the periphery of the transformed epidermal cells (G-I). Fluorescent foci could be observed as well (G-H). When co-expressing N-terminally fused MtSYMREM1 and C-terminally fused RLKs, re-assembled YFP fluorescence could not be observed, because of a putative sterical hindering or physical distance of the split YFP halves. *N. benthamiana* leaves expressing the respective constructs were inspected 2 dpi using CLSM. Scale bars indicate 30µm.

These data indicate that the polymorphisms between both SYMREM1 proteins are not essential for oligomerization of the protein. Since re-assembly of the YFP halves could happen only when both SYMREM1s were tagged C-terminally, it might be concluded that the possible interaction surface is their conserved C-terminal region. To highlight this issue in more details, an experiment was performed when C-terminally fused MtSYMREM1 (MtSYMREM1:Y_C/Y_N) was co-expressed with N-terminally tagged MtSYMREM1 (Y_N/Y_C:MtSYMREM1), however the trial failed and the experiment has to be repeated.

	LjSYMREM1:YFP_N	MtSYMREM1:YFP_N	YFP_N:MtSYMREM1
NFR1:YFP_C	+	+	–
NFR5:YFP_C	+	+	–
SYMRK:YFP_C	+	+	–
LjSYMREM1:YFP_C	+	+	–
MtSYMREM1:YFP_C	+	——	——
YFP_C:MtSYMREM1	–	——	+

Table 3.5 Interactions tested in BiFC assay
To determine interactions of LjSYMREM1 BiFC studies were performed. LjSYMREM1 was co-expressed with *L. japonicus* symbiotic RLKs NFR1, NFR5 and SYMRK. In order to test authenticity of the results obtained, we co-expressed MtSYMREM1 with *L. japonicus* RLKs. When we co-expressed proteins having the same fusion direction to split YFP halves, they resulted in fluorescence (+). N-terminal fused constructs of MtSYMREM1 did not display YFP signal in any combinations (-) except co-infiltration with itself. "——" results of these combinations could not be obtained, since the experiment failed.

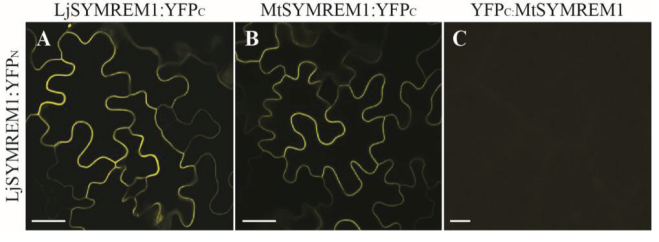

Figure 3.18 LjSYMREM1 forms homo- and heterooligomers
In order to determine whether LjSYMREM1 is able to interact with itself and to answer the question whether the conserved coiled-coil containing C-termini of the two SYMREM1s (from related species) are able to oligomerize, C-terminally tagged LjSYMREM1 was co-expressed with itself, with C-terminally tagged MtSYMREM1 and with N-terminally tagged MtSYMREM1. (A) Co-expression of LjSYMREM1:YFP_N with LjSYMREM1:YFP_C resulted in YFP fluorescence at the periphery of the leaf epidermal cells. (B) Co-expression of LjSYMREM1:YFP_N with MtSYMREM1:YFP_C resulted in fluorescence as well, while (C)

LjSYMREM1:YFP_N with YFP_C:MtSYMREM1. *N. benthamiana* leaves carrying the respective constructs were investigated 2 dpi using CLSM. Scale bars indicate 50 µm (A, B) and 30µm (C).

3.5.2. Interactions of LjSYMREM1 in split-ubiquitin yeast assay

In order to verify interactions between LjSYMREM1 and NFR5, NFR1 and SYMRK detected in BiFC studies, the yeast split-ubiquitin system (SUS) was used as an independent assay. SUS was optimised for detection of interactions between PM resident proteins. The facts, that LjSYMREM1 is a PM-associated protein and previous reports on the successful use of this system when investigating interactions of MtSYMREM1 with *Medicago* symbiotic RLKs (Lefebvre *et al*., 2010), support this system to be suitable for this approach. Proteins tested were expressed as bait (Cub construct, protein of interest is fused to the C-terminal part of ubiquitin) as well as a prey (NubG construct, protein of interest is fused to the mutated N-terminal ubiquitin) in the yeast strain (NMY32) used for interaction studies. Before investigating interactions, expression and localization of LjSYMREM1 was verified in yeast cells. Membrane protein extraction and immunoblot analysis demonstrated membrane-associated localization of LjSYMREM1 (Figure 3.19). To assay whether all constructs (Cub/NubG:LjSYMREM1; NFR5:Cub/NubG; NFR1:Cub/NubG; SYMRK:Cub/NubG; RLK constructs were kindly provided by M. Antolín-Llovera, LMU) used for interaction studies are correctly expressed and functional in this system, co-transformations of bait constructs (Cub) with positive control Alg5:NubI (a yeast resident membrane protein fused to native N-terminal ubiquitin moiety) were performed. Conceptually, the Cub domain will form a native-like Ubiquitin molecule with the wild-type Nub(I) domain. Recognition of this molecule by ubiquitin-binding proteins (UBPs) will lead to cleavage of the artificial transcription factor (LexA-VP16) that is fused to the Cub domain and subsequent activation of the reporter genes *ADE2* and *HIS3*. Expression of these genes will result in complementation of the histidine and adenine auxotrophy of the yeast strain.

To verify that neither the bait nor the prey constructs form unspecific (false positive) interactions, we co-transformed the bait constructs with Alg5:NubG, the preys with Alg5:Cub negative control constructs (see chapter 2.2.5.1). All co-transformants were grown on synthetic yeast medium (SD) lacking the amino acids leucine (L) and tryptophan (W) (SD-LW) to select for presence of both plasmids. Colonies were then stamped onto medium depleted in LWH (SD-LWH) and supplemented by 15mM 3-amino-1,2,4-triazole

(3-AT), a competitive inhibitor of the *HIS3* gene product, to check for unspecific interactions or autoactivation of the system. Co-transformants of Cub:LjSYMREM1 and RLKs:Cub with Alg5:NubG did not show any growth of yeast on the triple selective medium supplemented with 15mM 3-AT (Figure 3.20, right panel). While all bait constructs co-tramsformed with the positive control Alg5:NubI leaded to yeast growth indicating the functionality of the proteins in the system (Table 3.6)

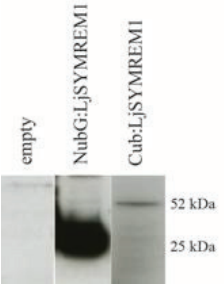

Figure 3.19 Detection of LjSYMREM1 protein expression in yeast
LjSYMREM1 fused N-terminally to the split ubiquitin moieties was detected in microsomal fraction demonstrating membrane-associated localization of the protein. Cub:LjSYMREM1 (52 kDa) was detected using α-LexA antibody against the LexA-VP16 transcriptional factor fused to the Cub half. NubG:LjSYMREM1 (25 kDa) was detected via α-HA antibody against the HA epitop placed between the NubG half and the protein. Non-transformed yeast culture was used as a negative control using both antibodies, the lane "empty" represents control for α-HA antibody.

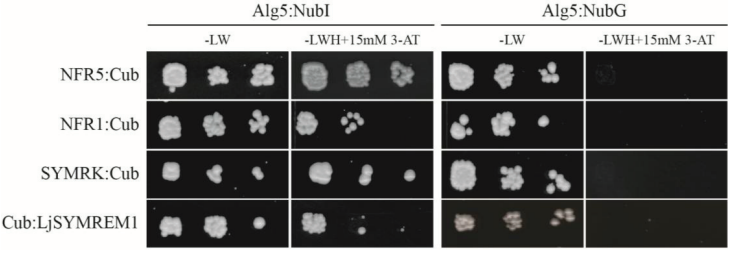

Figure 3.20 Functionality of the constructs used in split-ubiquitin yeast assay
Before testing interactions between LjSYMREM1 and the symbiotic RLKs, proteins were tested for their functionality in the split-ubiquitin yeast system. All proteins were co-expressed with the positive control construct Alg5:NubI (the native N-terminal ubiquitin moiety) to test whether they localize to the plasma membrane. Furthermore, they were co-expressed with the negative control construct Alg5:NubG, to check that the proteins in question do not from false positive interactions with the yeast resident PM-localized Alg5 control protein. Yeast colonies were grown on the SD-LW auxotrophic medium to control the yeast growth and on the selective SD-LWH medium supplemented with 15mM 3-AT (an inhibitor of the endogenous histidine metabolism) to establish stringent selection conditions for the protein interaction study. Drop-tests were performed on both media, where the yeast suspensions were applied as a drop in dilution series (non-diluted, 10^{-1}, 10^{-2}; from left to the right).

Next, interactions of LjSYMREM1 with the RLKs NFR5, NFR1 and SYMRK (Table 3.7) were examined and they were confirmed in this yeast assay (Figure 3.21). Colonies of co-transformants were subjected to drop-test. They were dropped as dilution series (non-diluted, 10^{-1} to 10^{-3}) onto SD-LWH + 15mM 3-AT (as well as onto SD-LW as control for yeast growth) to determine positive interactions.

	Alg5:Cub	Alg5:NubG	Alg5:NubI
Cub:LjSYMREM1	——	–	+
NubG:LjSYMREM1	–	——	——
NFR5:Cub	——	–	+
NFR5:NubG	–	——	——
NFR1:Cub	——	–	+
NFR1:NubG	–	——	——
SYMRK:Cub	——	–	–
SYMRK:NubG	–	——	——

Table 3.6 Testing functionality of the constructs used in yeast split-ubiquitin assay
Functionality of the constructs in the split-ubiquitin yeast system was tested, using the yeast resident membrane protein Alg5:NubI, the construct serves as positive control because the native NubI half is able of reassembly with the Cub domain if they get into close physical proximity via the proteisn fused to them. All co-transformations showed a functional assay (+). No interaction with the negative controls Alg5:Cub and Alg5:NubG (-) was detected indicating specificity of the proteins in this assay. ”——“combination not tested.

In a next set of experiments oligomerization patterns of the LjSYMREM1 protein was tested. Due to the high degree of sequence diversification in the N-terminal regions between LjSYMREM1 and MtSYMREM1, this pair provides an interesting opportunity to study the impact of this domain on remorin oligomerization. Thus Cub:LjSYMREM1 was independently co-expressed with NubG:LjSYMREM1 and NubG:MtSYMREM1, to test whether it displays the same oligomerization pattern as in the BiFC assay. Co-expression of LjSYMREM1 with itself resulted in yeast growth on triple selective medium (SD-LWH + 15mM 3-AT), confirming homo-oligomerization as also shown by BiFC above (Figure 3.22). In contrast, hetero-oligomerization of the two remorins found in BiFC, could not be confirmed in yeast (Figure 3.22). These data support the results obtained in BiFC, since only the C-terminal fusion proteins (LjSYMREM1:Y_N/Y_C and MtSYMREM1:Y_C/Y_N) were able to hetero-oligomerize. In contrast, co-expression of N-terminally fused MtSYMREM1 proteins (Y_C/Y_N:MtSYMREM1) with C-terminally fused LjSYMREM1

(LjSYMREM1:Y_N/Y_C) did not yield fluorescence (Figure 3.18). However, LjSYMREM1 was able to form homo-oligomers (Cub:LjSYMREM1 with NubG:LjSYMREM1; Figure 3.22) using the same fusion direction as in hetero-oligomerization experiments with MtSYMREM1.

	Cub:LjSYMREM1	NubG:LjSYMREM1
NFR5:Cub	——	+
NFR1:Cub	——	+
SYMRK:Cub	——	+
NFR5:NubG	+	——
NFR1:NubG	+	——
SYMRK:NubG	+	——

Table 3.7 LjSYMREM1 interacts with symbiotic RLKs in SUS
Co-expression of Cub:LjSYMREM1 with NFR5:NubG, NFR1:NubG, SYMRK:NubG as well as co-expression of NubG:LjSYMREM1 with RLKs fused to the Cub resulted in interaction (+). ”—— “combinations not tested.

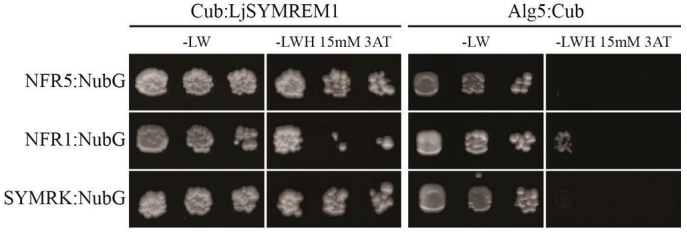

Figure 3.21 LjSYMREM1 interacts with symbiotic RLKs in yeast assay
LjSYMREM1 interacts with symbiotic RLKs NFR5, NFR1 and SYMRK (left panel). The RLKs were also co-expressed with the negative control Alg5:Cub, in order to check authenticity of the interactions. Yeast were grown in dilution series (non-diluted, 10^{-1} to 10^{-2}) on SD-LW auxotrophic medium as control of yeast growth and on SD-LWH supplemented with 15mM 3-AT to detect interactions. Yeast growth on the triple selective medium indicates interaction due to activation of the reporter gene (*HIS3*) system.

These results suggest that SYMREM1 proteins oligomerize via their C-terminal part. N-terminally fused LjSYMREM1 (Cub:LjSYMREM1/NubG:LjSYMREM1) homo-oligomerizes. However, co-expression of Cub:LjSYMREM1 with NubG:MtSYMREM1 resulted in slight yeast growth that was considered as no interaction (Figure 3.22). This

suggests a possible impact of the variable N-terminal region of both remorins on oligomerization or interaction event.

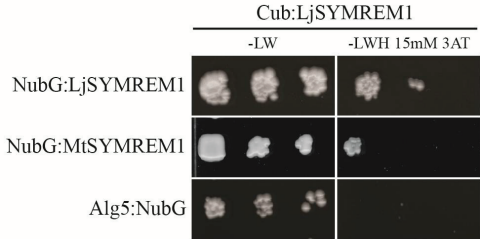

Figure 3.22 Homo- and hetero-oligomerization of LjSYMREM1 in yeast assay
Homo-oligomerization of LjSYMREM1 shown in BiFC assay could be confirmed in yeast.
Hetero-oligomerization of LjSYMREM1 with MtSYMREM1 only resulted in slight, presumably unspecific yeast growth. Yeast grew on SD-LW indicating the presence of both plasmids. Growth on SD-LWH supplemented with 15mM 3-AT in three dilution series (non-diluted; 10^{-1}; 10^{-2}) indicated interaction between the proteins.

3.6. Identification of new putative interactors using the yeast split-ubiquitin system

In order to gain more insights into the role of the LjSYMREM1 protein, novel putative interaction partners were identified using yeast split-ubiquitin system (SUS). The availability of a cDNA-library derived from nodulated and mycorrhized roots and cloned into prey vector (kindly provided by Martin Parniske, LMU) favoured this approach.

3.6.1. Preparation for large-scale cDNA-library screen and screen performance

For large-scale screening, library was created as prey (NubG) and the protein targeted as bait (LjSYMREM1:Cub). As described above (chapter 3.5.2.) expression and PM associated localization of LjSYMREM1:Cub construct was verified in Western blot analysis (Figure 3.19). Transformation efficiency and conditions of the experiment considered as a successful library screen are summarized in Table 3.8 and 3.9. In this experiment, two large-scale transformations (a “sequential transformation” and a “simultaneous co-transformation”) were carried out in parallel using two different protocols. In both transformation events Cub:LjSYMREM1 was co-transformed not only

with NubG:library to screen for interaction partners, but it was also co-transformed with Alg5:NubG to follow specificity and authenticity of the screening procedure.

	Sequential Transformation (DUALsystems protocol)		**Co-transformation** (Clontech protocol with modifications)	
Co-transformants	NMY32 carrying Cub:LjSYMREM1 + NubG:Library	NMY32 carrying Cub:LjSYMREM1 + Alg5:NubG	Cub:LjSYMREM1 + NubG:Library	Cub:LjSYMREM1 + Alg5:NubG
10^{-2}, SD-LW	>1000	>1000	302	262
10^{-3}; SD-LW	257	215	38	26
10^{-4}; SD-LW	34	32	2	5
Total number of transformants *	$3.85x10^6$	$3.225x10^6$	$5.7x10^5$	$3.9x10^5$
Transformation efficiency	$5.5x10^5$	$4.6x10^5$	$5.7x10^4$	$3.9x10^4$

Table 3.8 Transformation efficiency of the library screen considred as successful
Applying a sequential and a co-transformation procedure conducted two rounds of initial screening. Transformed cells were plated in dilution serried onto SD-LW selective plates to determine transformation efficiency. *Counted from number of colonies on 10^{-3} SD-LW plates.

Transformed yeast cells were plated onto SD-LW, SD-LWH + 15mM and 30mM 3-AT and SD-LWHAde selective plates to apply appropriate selection stringency. In addition cells were plated onto small SD-LW plates in dilutions 10^{-2}, 10^{-3}, 10^{-4} as readout of the transformation efficiency (Table 3.8). The screen done by "sequential transformation" achieved a higher transformation efficiency ($5.5x10^5$, Table 3.8), while the number of colonies growing on the most stringent selective medium (SD-LWH + 30mM 3-AT) was also higher than colony number on the plates from the "co-transformation" procedure (Table 3.9). Furthermore, no difference was observed with respect to colony number of LjSYMREM1-library co-transformants and LjSYMREM1-Alg5:NubG co-transformants (Table 3.9). This fact reflects high numbers of false positive clones. Thus the yeast colonies obtained in screening procedure performed by "co-transformation protocol" were further investigated.

Finally 160 yeast colonies were selected from the SD-LWH + 30mM 3-AT selective screen master plate (from the "co-transformation" procedure). Plasmids were extracted from all colonies and re-transformed into *E. coli.* A total number of 166 plasmids

were obtained due to the fact that yeast cells are able to carry more than one plasmid at the time. In order to verify interactions between LjSYMREM1 and its putative interactors, plasmids isolated from *E. coli* were re-transformed into yeast as small-scale co-transformations independently with the Cub:LjSYMREM1 construct and with Alg5:Cub negative control to test specificity of these interactions. Colonies of co-transformants were subjected to drop-test analysis, where they were grown as dilution series (non-diluted, 10^{-1} to 10^{-5}) on SD-LWH + 15mM and 30mM 3-AT (as well as on SD-LW as control for yeast growth) to define positive interactions. Clones that yielded in positive interactions with LjSYMREM1 and that were negative in co-transformation with Alg5:Cub were sequenced in order to identify the cDNA insert (Table 3.10). Sequences were subjected to BLAST analysis to ascertain the identity of clones isolated as putative interaction partners of LjSYMREM1. In case, when BLAST analysis against the *L. japonicus* genome using *Lotus* database (Kazusa DNA Research Institute; [1]) did not yield any significant hit, sequences were compared to those deposited at the National Center for Biotechnology Information (NCBI; [6]).

	Sequential Transformation (DUALsystems protocol)		**Co-transformation** (Clontech protocol with modifications)	
Co-transformants	NMY32 carrying Cub:LjSYM-REM1 + Library	NMY32 carrying Cub:LjSYM-REM1 + Alg5:NubG	Cub:LjSYM-REM1 + Library	Cub:LjSYM-REM1 + Alg5:NubG
SD-LW	uncountable	uncountable	uncountable	uncountable
SD-LWH + 15mM 3-AT	uncountable less than -LW	uncountable less than -LW	184	105
SD-LWH + 30mM 3-AT	1000	1100	160	4
SD-LWHAde	1440	1422	880	~470

Table 3.9 Summary of library screens performed using two transformation procedures
Co-transformants of both procedures were plated onto different selective media, where colonies were counted 5 days post transformation. Yeast suspension was plated onto SD-LW as control of yeast growth and onto triple selective media supplemented with 15mM and 30mM 3-AT respectively and onto SD-LWHAde (take advantage of the second reporter gene *Ade2*) to find out the most appropriate selection stringency.

From 85 clones found as putative positive interactors, about 40 clones were considered as false positive after sequencing. Such decision was based on their identities

where 29 clones encoding highly abundant ribosomal proteins were discarded from further analysis. Clones carrying empty vectors or inserts encoding histone proteins were also ignored during subsequent tests. Interestingly, the screen also identified a clone encoding LjSYMREM1, an interaction that was already shown independently before (Figure 3.22).

Among the identified putative interaction partners listed below (Table 3.10) can be found an MtN5-like protein, an ENOD40 peptide and a cell-wall associated hydrolase. The first two were already described involved in the nodulation process (Pii *et al*., 2009; Wan *et al*., 2007). The cell-wall associated hydrolase might be involved in hydrolysis of the root hair cell wall when entrapping bacteria in the root hair curl. Proteins such a copper transport protein ATOX1-like and ammonium transporter are interesting in terms of nutrition exchange between the symbiotic partners. Proteases involved in RNS have been already reported (Takeda *et al*., 2007), therefore the identified aspartic proteinase is also an interesting candidate for further investigations. The heat-shock protein 70 (Hsp70) might be interesting with respect to LjSYMREM1 structure. LjSYMREM1 N-terminal region exhibits a disordered structure (Tóth *et al*., accepted). Hsp70 is a chaperone that is known to be involved in protein folding (Sharma *et al*., 2009). Interactions of LjSYMREM1 with the above-mentioned putative interaction partners and further putative interaction partners listed below remain to be confirmed using other protein-protein interaction techniques and further investigation to unravel their roles within the symbiotic signalling pathway. Several proteins were selected for verification of the interaction with LjSYMREM1, those are described in the following chapter.

3.6.2. Verification of selected putative interaction partners identified in yeast screen

Sequencing of the putative interaction partners revealed possible frameshifts in the fusion protein that would lead to truncated variants. To test this aspect more specifically a selection of genes (Table 3.11) was re-cloned as full-length coding sequences into the respective vectors (NubG:gene of interest) and re-transformed into yeast cells. Genes were selected by aspects of their possible involvement in nodulation (like MtN5-like protein), in signalling and protein modification (Phosphatase, PeptidaseA1, AAA+ATPase domain containing protein) or by their putative localization to the PM or membrane rafts (like LTP or GPX).

Number of yeast colonies pick up	160
Isolated plasmids from *E.coli*	166
Confirmed as positive in Drop-test	85
Probably false positive	8 empty vectors 29 ribosomal proteins 2 *G. intraradices* RNA-binding protein 2-3 Histone proteins
Among the positive ones	LjSYMREM1; chr4.CM0004.60.r2.d
	NmrA-like protein; chr2.CM0249.1420.r2.m
	AAA+ATPase domain containing protein; BT052457
	UPF0497 membrane protein 7; LjSGA_029690.2
	MtN5-like protein; chr2.CM0667.240.r2.m
	Acid-phosphatase; chr2.CM0065.740.r2.d
	Epoxide hydrolase; chr3.CM0160.40.r2.m
	Aspartic proteinase; chr1.CM0982.580.r2.d
	GPX*; chr4.CM0042.1400.r2.m
	LTP**; chr3.CM0160.370.r2.m
	Oxoglutarate; chr2.CM0338.120.r2.m
	Cell wall-associated hydrolase; chr3.CM0396.440.r2.d
	Heat-shock protein 70; chr6.LjT47N10.130.r2.a
	Class-10 pathogenesis-related protein 1; LjSGA_063085.1
	Copper transport protein ATOX1-like; XM_003536270
	Pollen Ole e 1 allergen and extensin family protein; chr2.CM0002.600.r2.m
	ENOD40-2 protein; chr4.CM0161.400.r2.m
	Ammonium transporter 1; LjSGA_028202.1
	Aquaporin PIP2-7; chr3.CM0136.110.r2.m
	Glutaredoxin-like protein 4; chr1.CM1413.390.r2.m

Table 3.10 Summary of the identified and sequenced putative interactors
160 yeast colonies resulted in 166 plasmids isolated form *E.coli*, 85 plasmids were found as putative positive interactors in drop-test. About 45 (out of these 85) clones are considered as false positive. Among those that are considered as putative positive ones, LjSYMREM1 could be found as well.

Construct name	Protein expressed	Gene ID
NubG:Phosphatase	full-length	chr2.CM0065.740.r2.d
NubG:PeptidaseA1	full-length	chr1.CM0982.580.r2.d
NubG:MtN5-like	full-length	chr2.CM0667.240.r2.m
NubG:GPX*	full-length	chr4.CM0042.1400.r2.m
NubG:AAA-ATPase	AAA+ATPase domain#	not found in *Lotus* database
NubG:LTP**	full-length	chr3.CM0160.370.r2.m

Table 3.11 List of proteins selected for verification
Several putative interactions of LjSYMREM1 indentified in yeast screen were chosen for re-cloning and verification of the interactions. IDs of the genes encoding the proteins listed are from the *Lotus* database; [1]
*phospholipid hydroperoxide glutathione peroxidase; **plant lipid transfer protein
#protein prediction based on sequence homology with its putative *Medicago* ortholog found at NCBI

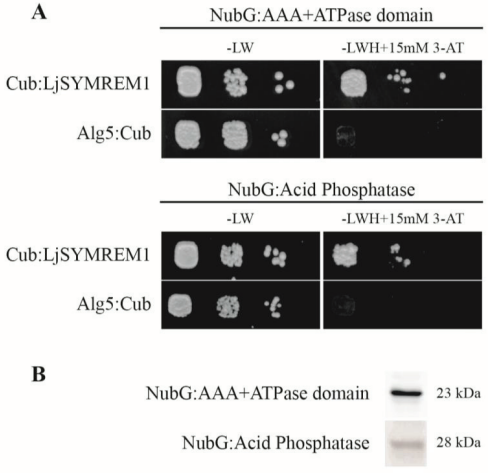

Figure 3.23 Identification of new interaction partners of LjSYMREM1
Co-expression of LjSYMREM1 with the newly identified and re-cloned putative interaction partner resulted in two clearly detected interactions. (A) Interaction with an AAA+ATPase core domain containing protein (upper panel) and with an Acid Phosphatase (bottom panel). Yeast was grown on SD-LW as control for yeast growth and on SD-LWH triple selective medium supplemented with 15mM 3-AT to detect the interactions. The putative interaction partners were co-expressed with the negative control construct Alg5:Cub to avoid false positive results. Yeast was dropped in dilutions series (non-diluted, 10^{-1}, 10^{-2}) on both types of medium. (B) Expression of the prey constructs was verified using α-HA antibody against the HA epitope build in between the NubG half and the protein investigated.

Coding sequences of the selected proteins were amplified from the original yeast clones that were identified during the screen. As an exception the single exon *PeptidaseA1* gene was directly cloned from genomic DNA. Furthermore, and due to availability of only the AAA+ATPase core domain this region was used for independent experiments.

A clear result was obtained only in the case of the Acid Phosphatase (Plant acid phosphatase; TIGR01675; [7]) and the AAA+ATPase core domain (SM00382; [8]) when the proteins showed positive interactions with LjSYMREM1 but no interactions with the negative control Alg5:Cub on the SD-LWH + 15mM 3-AT plates Figure 3.23A). Western blot analysis revealed integrity of the expressed proteins (Figure 3.23B). In all other cases, either the drop test resulted in slight yeast growth comparable to growth obtained with the negative controls or the protein could not be detected by Western blot analysis (data not shown). This indicates either unspecific interactions or auto-activation of the reporter genes by the particular protein. Thus, no conclusions could be drawn from these results. Further work is required to assess the interaction patterns in a reliable manner.

4. Discussion

4.1. LjSYMREM1 a putative functional homolog of MtSYMREM1

The plant-specific remorin protein family is comprised of six subgroups where members show remarkable high degrees of sequence divergence in their N-terminal regions (Raffaele *et al*., 2007). While remorins proteins of any of the subgroups can be found in all land plants, the presence of group 2 is restricted to legumes and closely related species such as *Populus trichocarpa* and *Vitis vinifera*. Latter two belong to the FaFaCuRo clade that shows a predisposition for nodulation (Kistner and Parniske 2002).

The aim of this thesis was to characterize the *SYMREM1* gene from *L. japonicus* and to unravel possible orthology between SYMREM1 genes and proteins from the model legumes *M. truncatula* and *L. japonicus*. Despite being evolutionary relatively closely related species these legumes exhibit major differences in the nodule type they develop. While *M. truncatula* builds indeterminate nodules that have a persistent meristem and are continuously infected by rhizobia, *L. japonicus* plants develop determinate nodules that have a defined life span and are not continuously colonized (Brewin, 1991; Popp and Ott, 2011).

Comparing remorin gene expression in *L. japonicus* with published data for the Medicago *MtSYMREM1* gene revealed only one gene to exhibit nodulation-specific expression (LjSYMREM1; chr4.CM0004.60.r2.d; Tóth *et al*., accepted). Surprisingly sequence alignments between the two corresponding proteins showed only very low degrees of overall sequence similarity (67.1%; Table 3.1) despite clear phylogenetic separation and clustering of the proteins (Figure 3.1; Tóth *et al*., accepted). In contrast full-length protein sequences of symbiotic receptor-like kinases and other components of the symbiotic signalling pathway show overall similarities between 75-90% when comparing these two legumes (Table 3.2; Tóth *et al*., accepted). Detailed phylogenetic analysis revealed that LjSYMREM1 and MtSYMREM1 indeed derive from a common ancestor strongly implying orthology between these two proteins (Figure 3.1). Due to the lack of homozygous knockout mutants for *LjSYMREM1* this question could not be assessed phenotypically. However, a line carrying a point mutation at the border of the first exon and intron exhibited an increased nodulation phenotype (Figure 3.15). The phenotype

could be confirmed in three independent experiments. The homozygous mutant plants exhibit not only about 20% more nodules, but they also have significantly longer shoots in comparison with wild type plants suggesting that this nodulation phenotype is caused by this point mutation in the *LjSYMREM1* gene. The nodules showed non-altered morphology and fixing phenotype, whether the longer shoots are a possible consequence of the higher nodule number requires further investigations. In order to explain, whether the mutation could have caused a splicing alteration and therefore a possible different protein product, transcript analysis has to be done. Further evidence for orthology of *LjSYMREM1* and *MtSYMREM1* was obtained in the group when an RNAi approach against another group 2 remorin protein (*LjMYCREM*) resulted in a nodulation phenotype similar to the one described for *MtSYMREM1* (Joana Bittencourt-Silvestre and Thomas Ott, unpublished data). While this construct potentially also targeted *LjSYMREM1*, the use of a *LjMYCREM*-specific RNAi construct did not result in a nodulation phenotype. However, efficient silencing with the above-mentioned construct remains to be proven experimentally.

High sequence divergence in the N-terminal region of the SYMREM1 proteins may suggest several evolutionary possibilities and may question functional requirement of these domains. Interestingly, not only the full-length LjSYMREM1 over-expression, but also its individual N-terminal and C-terminal regions also caused an increased nodulation phenotype (Figure 3.12). These results suggest that both regions contribute to the biological function of the protein involved in the nodulation process.

4.2. LjSYMREM1 accompanies nodulation process

A nodule-specific induction of the *LjSYMREM1* gene was found in transcriptomic analysis of *L. japonicus* (Colebatch *et al.,* 2004; Høgslund *et al.,* 2009). Quantitative real-time PCR approach revealed that *MtSYMREM1* is not only nodule-specifically expressed already at 4 dpi with *S. meliloti* but also 24 hours after application of 10^{-8} M isolated NFs (Lefebvre *et al*., 2010). To follow the spatio-temporal expression pattern of the *LjSYMREM1* gene, *LjSYMREM1* promoter activity was analyzed using a *pLjSYMREM1:GUS* reporter construct. This study unraveled *LjSYMREM1* to be induced 24 hours upon NF application in epidermal as well as cortical cells in a susceptible zone above the root tip (Figure 3.5B, 3.6A). GUS staining was not observed in non-treated roots

suggesting no promoter activity, however a basic level expression could have been observed in expression profiling studies (Høgslund *et al.,* 2009; Lefebvre *et al*., 2010).

Early nodulin promoters have been described that were activated earlier than 24h upon NF application in histochemical promoter:GUS studies, showing an expression pattern in root epidermis (Journet *et al*., 1994; Boisson-Dernier *et al*., 2005; Marsh *et al*., 2007). The *MtENOD12* promoter is activated in differentiating root epidermal cells of secondary roots 2-3 hours later upon NF application (Journet *et al*., 1994). The *pMtENOD11* exhibits the earliest activation 6 hours in the epidermis (Catoira *et al*., 2000; Charron *et al*., 2004; Marsh *et al*., 2007) while Boisson-Dernier *et al*. (2005) investigated the promoter activity 16 hours after NF treatment.

LjSYMREM1 promoter activity was observed on roots at 2 dpi with *M. loti* (Figure 3.5C). Such pattern was also reported for *pMtENOD12* expression monitored 20 h after *S. meliloti* inoculation (Pichon *et al*., 1992). However, GUS staining was restricted to epidermal cell layers. Additionally, Boisson-Dernier *et al*. (2005) described a specific activation of *pMtENOD11:GUS* construct in curled root hairs and in the adjacent outer cortical cells 3 dpi with *S. meliloti*. *LjSYMREM1* promoter activity was assessed in nodule primordia cells 4 dpi that coincided with rhizobial infection (Figure 3.5D-E). From this time-point no GUS-activity was observed in epidermal cells. Similar GUS staining pattern was monitored in dividing cortical cells of composite plants involving *pCYCLOPS:GUS* construct upon *M. loti* treatment (Yano *et al*., 2008). Furthermore, β-glucuronidase-activity co-localizing with DsRed signal deriving from rhizobia harboured by the infected cells was detected in young (6 dpi) and mature nodules (3wpi) (Figure 3.5F-G). Such pattern was also observed for the *CYCLOPS* promoter (Yano *et al*., 2008).

Since SYMREM1 has been shown to interact with the symbiotic receptors, it remains to be answered whether expression of the corresponding genes coincides with each other. So far localization data have only been presented for the *Medicago* RLKs *DMI2*, *NFP* and *LYK3*. These genes are expressed in the developing root hair zone above the root tip observed in non-inoculated transgenic roots carrying GUS reporter construct of the respective RLKs (Bersoult *et al*., 2005; Arrighi *et al*., 2006; Mbengue *et al*., 2010). GUS-activity could be observed 2 dpi with *S. meliloti* in inner and middle cortex (DMI2 and NFP) and in nodule primordium (LYK3). Their expression was also observed in nodules, in pre-infection and in infection zones (Bersoult *et al*., 2005; Arrighi *et al*., 2006; Mbengue *et al*., 2010).

In summary data presented here clearly show transcriptional patterns known for early nodulins. Expression of *LjSYMREM1* coincides with bacterial infection and nodule organogenesis. These processes have recently been dissected genetically (Madsen *et al*., 2010). Downstream of NF perception and root hair curling a set of proteins such as the GRAS-like transcription factors NSP1 and NSP2 (Kaló *et al*., 2005; Heckmann *et al*., 2006), proteins involved in actin re-arrangement (NAP1, PIR1; Yokota *et al*., 2009) and the E3 ubiquitin ligase CERBERUS (Yano *et al*., 2009) are required for infection thread formation. Signal transduction and organogenesis appears to be regulated by an independent pathway that is controlled by SYMRK and genetic components required for calcium spiking. Similarities to expression patterns of *CYCLOPS* and a recent finding that *MtSYMREM1* induction is specifically blocked in a *Medicago ipd3* mutant (the ortholog of CYCLOPS) suggest a close relationship of SYMREM1 and CYCLOPS and genetically places it immediately downstream of calcium-spiking (Ovchinnikova *et al*., 2011).

4.2.1. LjSYMREM1 localizes to symbiosome membranes and to nodular infection threads

In *M. tuncatula* MtSYMREM1 localized to nodular infection threads and symbiosome membranes (Lefebvre *et al*., 2010). Similar patterns were observed in stable transgenic Lotus plants expressing the *pLjSYMREM1:gLjSYMREM1:YFP* construct. The fusion protein was also detected on nodular infection threads interconnecting infected cells (Figure 3.9D-F). Such localization has not been observed for MtSYMREM1 while this protein localized to nodular IT membranes within the infection zone of the indeterminate nodule (Lefebvre *et al*., 2010). Full PM localization was also retained when over-expressing an LjSYMREM1:CFP construct heterologously in *N. benthamiana* leaves (Figure 3.16) and LjSYMREM1: mOrange homologously in *L. japonicus* roots (Figure 3.11). Furthermore, independent expression of the C- and N-terminal regions of LjSYMREM1 indicated the presence of a membrane-binding domain in the C-terminal region of the protein (Figure 3.11). The nature of this motif remains to be studied in detail. However, *in silico* prediction did not yield any known membrane-binding motif, suggesting that remorins anchor via a so far non-described mechanism to plasma membranes.

While no fluorescent signal could be observed in root hairs upon NF treatment, the abovementioned promoter:GUS data suggest *LjSYMREM1* transcription in these epidermal cells (Figure 3.5B, 3.6A). Interestingly, a LYK3:GFP fusion protein expressed under the native *LYK3* promoter was recently visualized in these cells (Haney et al., 2011). LYK3 was found to cluster in defined membrane micro-domains that co-localize with the flotillin protein FLOT4 upon inoculation of the plants with rhizobia (Haney et al., 2011). Such membrane domains had been previously shown for two flotillin proteins FLOT2 and FLOT4 independently of the presence of rhizobia and/or Nod Factors (Haney et al., 2010). Remorin proteins have been described to serve as marker proteins for membrane domains, called membrane rafts (reviewed in Jarsch and Ott, 2011). A group 1 remorin from potato (StREM1.3) was shown to localize to such domains when being expressed in tobacco leaves (Raffaele et al., 2009). While no such domains were observed when expressing C-terminally tagged LjSYMREM1 protein in the stable transgenic *L. japonicus* line nor in *N. benthamiana* leaves, unpublished data indicate membrane domain clustering of N-terminally tagged MtSYMREM1 protein (Popp and Ott, unpublished data). Such clusters were not observed when expressing C-terminally tagged versions of the LjSYMREM1 protein. Thus, it cannot be ruled out that C-terminal tagging of LjSYMREM1 prevents domain formation while association with the plasma membrane is not impaired.

Both, LjSYMREM1 protein and promoter activity were detected in infected cells (Figures 3.6B, 3.8A-D, E-H). However, clear GUS staining was observed in outer cortical cells of mature nodules, while no fluorescence of the LjSYMREM1:YFP fusion protein was detected in these cell layers. This may be due to low abundance of the protein and thus below detection limit. However, post-transcriptional regulation can also be assumed. Similarly, no protein fluorescence was detected during early stages of infection while promoter:GUS studies clearly showed promoter activity upon NF application and in nodule primordia (Figures 3.5). Indeed micro-RNA-mediated regulation of non-symbiotic remorin transcripts has been described in *Arabidopsis thaliana* (Fahlgren *et al*., 2007). Whether such mechanism also plays a role in regulation of *SYMREM1* genes remains to be studied. However, it should be noticed that *L. japonicus* roots also exhibit high levels of auto-fluorescence that hinder detection of YFP signals at low levels.

4.3. LjSYMREM1 interaction partners

Earlier work showed that MtSYMREM1 interacts with the *Medicago* receptor-like kinases LYK3, NFP and DMI2 (Lefebvre *et al*., 2010). To test whether LjSYMREM1 shows the same interaction patterns and to support putative orthology between the two proteins, interactions of LjSYMREM1 with the homologous *L. japonicus* RLKs was tested using BiFC and split-ubiquitin yeast assay. Interactions of LjSYMREM1 with NFR1, NFR5 and SYMRK were shown by the help of both protein-protein interaction methods (Figure 3.17 and Figure 3.21). Furthermore, interaction of LjSYMREM1 and NFR1 was confirmed with an independent, FLIM-FRET analysis (Tóth *et al*, accepted). By the help of this technique the interaction was quantified using Cerulean-mOrange FRET pair. Upon interaction of the investigated proteins tagged with the two fluorophores, it comes to fluorescence lifetime reduction because of energy transfer from the donor fluorophore (Cerulean) to the acceptor fluorophore (mOrange) that can be quantified. 8.8% FRET efficiency could be observed that clearly demonstrates physical interaction between LjSYMREM1 and NFR1 (Tóth *et al*., accepted). Data presented by Tóth and colleagues clearly show that a stable interaction between LjSYMREM1 and the kinase domains of the symbiotic RLKs is mediated by the remorin C-terminal region. This region harbours a coiled-coil domain. These motifs have been frequently reported to support protein-protein interactions (Strauss and Keller, 2008). However, data from in vitro phosphorylation assays identified phosphorylation sites in the N-terminal region of the protein (Tóth *et al*., accepted) suggesting transient interaction with this region. Interestingly, no fluorescence was observed in BiFC assays where N-terminally tagged MtSYMREM1 proteins were co-expressed with the Lotus RLKs (Figure 3.17) despite high sequence conservation of the SYMREM1 C-terminal region. It remains to be elucidated if such lack of fluorescence is caused by steric hindrance of the interaction.

It was shown that LjSYMREM1 is able to interact with itself (Figure 3.18, 3.22). Homo-oligomerization of LjSYMREM1 was found in BiFC as well as in split-ubiquitin yeast assay (Figure 3.18A, 3.22). Moreover, it was detected that SYMREM1s of the two model legumes can undergo a hetero-oligomerization with each other suggesting that the highly conserved C-terminal half might allow an interaction between the two remorins from related species (Figure 3.18). However, their interaction could not be confirmed when LjSYMREM1 is tagged C-terminally and MtSYMREM1 is tagged N-terminally with the

split YFP halves (Figure 3.18). In split-ubiquitin yeast assay their co-expression also did not result in interaction (Figure 3.22). These results suggest that oligomerization might happen via their evolutionary conserved coiled-coil domains.

4.3.1. Newly identified putative interaction partners of LjSYMREM1

It was suggested that remorins may act as molecular scaffold proteins (Lefebvre *et al*., 2010; Jarsch and Ott, 2011). Such scaffold proteins exhibit a variety of functions and mediate recruitment of signalling components to specialized membrane domains and/or facilitate signalling complex assembly (Lajoie *et al*., 2009). The molecular mechanism of signal transduction between the plasma membrane resident receptor-like kinases and downstream nuclear activation of calcium-spiking has not been resolved, yet. However a set of proteins interacting with the RLKs has been identified (Popp and Ott, 2011). Two putative interactors of *Lotus* SYMRK and *Medicago* NORK have recently been described. The ARID-type DNA binding protein (SIP1) interacts with SYMRK via its C-terminal domain, while the N-terminal helix-turn-helix domain (ARID) is required for DNA interaction (Zhu *et al*., 2008). No mechanism has been postulated that would explain the mechanism of interaction between the nuclear SIP1 protein with the PM-resident SYMRK. Furthermore a PM-resident 3-Hydroxy-3-Methylglutaryl Coenzyme A Reductase1 (HMGR1) was reported to interact with the SYMRK homolog NORK (Kevei *et al*., 2007). The authors suggested that HMGR1 that catalyzes a step in mevalonate biosynthesis is involved in flavonoid production that is triggered by the plant upon nitrogen-starvation. Indeed the strong phenotype where ITs were aborted in root hairs and outer cortical cells supports a function of HMGR1 during early steps of root nodule symbiosis.

Here a large-scale split-ubiquitin yeast library screen was performed to identify putative new interaction partners of LjSYMREM1. This approach aimed to identify novel components that act between PM signal perception and downstream nuclear responses.
In this yeast screen experiment a number of interesting putative interactors was identified (Table 3.10). The fact that LjSYMREM1 was identified as a putative interactor indicates a successful screening procedure, since oligomerization of the protein was also shown in independent assays (Figure 3.18, 3.22). Two other candidates, whose interactions with LjSYMREM1 could be confirmed after re-cloning them, are a Plant Acid Phosphatase and an AAA+ATPase core domain containing protein fragment (Figure 3.23). *In silico* analysis

of the expression of their putative *Medicago* orthologs using the *Medicago* expression atlas (Benedito *et al*., 2008), no characteristic nodulation specific expression patterns could be found neither for the Acid Phosphatase nor for the AAA+ATPase core domain containing protein. It is known that proteins with disordered structure are involved in protein-protein interactions, signalling events, forming protein complexes and they might get folded upon interaction occurrence or just prior to involvement in an interaction, the AAA+ATPase protein family is involved in such processes (Wright and Dyson, 1999; Dyson and Wright, 2005; Dunker *et al*., 2008). AAA+ATPases represent a large protein family which members are involved in many diverse processes of the cell. They might participate in membrane dynamics, protein folding, proteolysis, vesicle transport and in performing many other cellular functions (Ogura and Wilkinson, 2001; White and Lauring, 2007)
Identification of the AAA+ATPase core domain as a possible interactor of LjSYMREM1 supports the hypothesis that LjSYMREM1 might act as a scaffold protein recruiting other proteins implied in protein complex formation of the symbiotic receptor-like kinases. Since it is a predicted cytosolic protein, it might be recruited from the cytosol to the PM or membrane rafts via LjSYMREM1. The exact role of this AAA+ATPase core domain containing protein is an exciting task with respect to not only its role to LjSYMREM1 but also whether it can affect the receptor-like kinases or other component of the symbiotic signalling pathway.

The acid phosphatase might de-phosphorylate the protein, since LjSYMREM1 phosphorylation via NFR1 and SYMRK kinase domains could be detected (Tóth *et al*., accepted) indicating that LjSYMREM1 needs to be phosphorylated perhaps with regards to its biological function. DeLong (2006) reviewed possible roles of PP1, PP2, PP4, PP5, PP6 and nuclear phophatases that are involved in embryogenesis, defence, brassinosteroid, blue-light and abscisic acid signalling and also can modulate receptor-like kinases. The acid phosphatase found in the screen cannot be classified in more details because of the lack of further information. Whether it interacts and/or deposphorylates LjSYMREM1 remains a challenging topic of another study.

5. Summary

Remorins are plasma membrane-resident proteins that may serve functions of molecular scaffold proteins to facilitate assembly of signalling complexes in membrane rafts. The fact that the remorin protein MtSYMREM1 from *Medicago truncatula* interacts with a number of receptor-like kinases (RLKs) and controls bacterial infection support this hypothesis. In this study, its putative ortholog LjSYMREM1 from *Lotus japonicus* was identified and further characterized. As MtSYMREM1, LjSYMREM1 localizes to symbiosome membranes and nodular infection threads and follows the same interaction patterns with the orthologous symbiotic receptor-like kinases NFR1, NFR5 and SYMRK from *L. japonicus*.

The spatio-temporal expression pattern of *LjSYMREM1* was investigated using its promoter region fused to the *GUS* reporter gene. Promoter activity of *LjSYMREM1* was observed in epidermal and cortical cells in proximity of the root tip, a susceptible zone for perception of rhizobial signalling molecules at 24h after NF treatment and 2 dpi upon *M. loti* inoculation. While expression vanished in epidermal cells 4 days post inoculation with *M. loti*, strong promoter activity was detected in nodule primordial cells at the sites of bacterial infection. In young nodules (6 dpi) and mature nodules (3 wpi) promoter activity followed rhizobial infection and remained in the central zone of nodules and the nodule parenchyma while *LjSYMREM1* is not expressed in the nodule cortex. Whereas the LjSYMREM1 protein fused to YFP was localized to infected cells of nodules, at the symbiosome membrane and the nodular infection threads.

Interestingly over-expression of full-length LjSYMREM1 as well as the sole N-termimal and C-terminal regions resulted in nodulation phenotype where plants developed significantly more nodules demonstrating the importance of both domains of this oligomeric protein during root nodule symbiosis.

In large-scale split-ubiquitin yeast screen further interaction partners of LjSYMREM1 were identified. Beside others an interactions with an acid phophatase and AAA+ATPase core domain-containing protein were confirmed in independent yeast re-transformation experiments. Since LjSYMREM1 is phosphorylated by the NFR1 and SYMRK kinase domains (Tóth *et al*., accepted), it can be hypothesized that the acid phosphatase might play a role during dephosphorylation of LjSYMREM1. The cytoplasmatic AAA+ATPase core domain-containg protein might be recruited to the

plasma membrane via LjSYMREM1 to serve any of the various functions such as protein folding, membrane dynamics, proteolysis, vesicle transport have been described for this protein family.

Future Perspectives

This thesis provides the basis for further analysis of SYMREM1 function in legumes. Data presented here clearly show that SYMREM1 proteins from *L. japonicus* and *M. truncatula* share a common ancestor. However, their N-terminal regions have remarkably diverged during evolution. While functional complementation was not achieved by expression of a *pLjSYMREM1:gLjSYMREM1:YFP* construct a number of other approaches can be taken to assess this question. For this LjSYMREM1 may be expressed under the control of the *pMtSYMREM1* or the constitutively active *pUbiquitin* promoter in the *Mtsymrem1* mutant background. Furthermore, complementation analysis when expressing chimeric constructs which were created in frame of this PhD project (e.g. the N-terminal region LjSYMREM1 fused to the C-terminal region of MtSYMREM1) will give insights into functional divergence of these proteins.

In frame of this thesis a number of new putative interaction partners of SYMREM1 have been identified. While an acid phosphatase may be involved in SYMREM1 dephosphorylation, an AAA+-ATPase core domain containing protein might play roles in protein folding. Furthermore a number of proteins involved in lipid transfer and re-arrangement that were found to interact with SYMREM1 may possess functions during infection thread progression and/or bacterial release. Future experiments will have to independently verify interaction with SYMREM1 and demonstrate their indispensability for root nodule symbiosis by reverse genetic approaches. These studies will provide novel insights into SYMREM1 function and thus regulation of the symbiotic signalling pathway.

Összefoglalás

A plazmamembrán lokalizációval rendelkező növényi remorin fehérjék scaffold fehérjeként működhetnek, ezáltal elősegíthetik szignalizációs komplexumok összeszerelését. Az a tény, hogy az MtSYMREM1 remorin családba tartozó fehérje *Medicago truncatula*-ban kölcsönhat számos receptor-szerű kinázzal, ezáltal saját ellenőrzése alá vonva a Rhizobium és pillangósvirágú közötti bakteriális fertőzés folyamatát, szintén alátámasztja a fent említett gondolatot. Ebben a tanulmányban, azonosítottuk és jellemeztük az MtSYMREM1 fehérje ortológját *Lotus japonicus*-ban és elneveztük LjSYMREM1-nek. LjSYMREM1 az MtSYMREM1 fehérjéhez hasonlóan a szimbioszóma membránon és a gümőkben található infekciós fonalon helyezkedik el, valamint kölcsönhatásban működik a szimbiotikus receptor-szerű kinázokkal: az NFR1, az NFR5 és a SYMRK fehérjékkel..

Az *LjSYMREM1* gén promótere vizsgálatával kiderítettük, hogy a promóter 24 órával Nod Faktor alkalmazása és két nappal a rhizobiális fertőzés után az epidermális és kortikális gyökérsejtekben aktiválódik. Ez az aktivitás a 4. napon a bakteriális fertőzés után eltűnik az epidermális sejtekből, de jelen van az osztodó kortikális sejtekben (gyökérgümő kezdemények), valamint azokban a sejtekben amelyekben a bakteriális fertőzés folyamata megindult. Követve a bakteriális fertőzés helyét a promóter aktivitását regisztráltuk fiatal (6 nappal fertőzés után) illetve érett gümőkben (3 héttel fertőzés után) is. Az LjSYMREM1 fehérjét az epidermális sejtek plazma membránjában valamint a gyökérgümőn belül a szimbioszóma membránon, illetve a fertőzött sejteket összekötő infekciós fonalon lokalizáltuk.

Transzgénikus *L. japonicus* növényekben az LjSYMREM1 fehérjét valamint N- és C-terminális doménjeit túltermeltettük. Ezen fehérjék megnövekedett mennyisége megnövekedett számú gyökérgümő képződéshez vezetett, amely arra utal, hogy az LjSYMREM1 fehérje és mindkét terminális doménje jelentős szerepet játszik a biológiai funkcióban.

Élesztő két-hibrid eljárás segítségével, az LjSYMREM1 fehérje további interakciós partnereit fedeztük fel. Ezek közül az egyik egy növényi savas foszfatáz, amely valószínűleg az NFR1 és SYMRK által foszforilált LjSYMREM1 fehérjét defoszforilálja (Tóth *et al*., PloS ONE közlésre elfogadva). A másik kölcsönható fehérje egy AAA+ATPáz core domént hordozó fehérje, amely különböző sejtfunkciókban vesz részt

(mint például fehérjék harmadlagos szerkezetének kialakítása (folding/refolding), membrán dinamika, proteolízis, vezikuláris transzport.

Acknowledgements

I have the special circumstances to thank Professors and Colleagues for help, support and advice at two different universities in two different countries.

I thank you, Dr. Thomas Ott (LMU, Munich) for giving me the opportunity to perform research in your group and supervising me, a student with a stubborn character. I am thankful for the research topic you gave me. I liked the project that I worked on. I thank you for all the help, support, discussions, agreements, disagreements, constructive criticism and patience.

Thank you, Dr. Zsuzsanna Buzás for being my supervisor and sometimes strict but nice teacher at the ABC in Gödöllő. I am thankful for all the support and help that you continued to provide, even during the years spent in Munich.

I thank Prof. Dr. László Orosz for giving me the opportunity to work as a PhD student in his Classical and Molecular Genetics PhD Program at the ELTE in Budapest. I am thankful for the always opened door in case of any questions or requests for help.

I thank Prof. Dr. Martin Parniske for the opportunity to continue my PhD work at the Institute of Genetics (LMU, Munich) and for your help, advice and input.

I thank our whole Ott group, for the great time, for your help, support and patience. Special thanks go to my ex-diploma student, Thomas F. Stratil for being a great student and for your contribution to our first-author paper. Thank to Sebastian S. A. Konrad for being my nice and cheery “bench-mate” and later on “office-mate”. A thank you goes to Iris K. Jarsch, Claudia Popp and Joana Bittencourt-Silvestre for sharing with me the life of a “PhD” and for listening to me. Thank to you, Dr. Macarena Marín for your scientific and professional advice and for your understanding. Thanks to Jessica Folgmann and Karl-Heinz Braun for your great technical help. Thanks to the whole group for the fruitful discussions, critical questions and for bearing my “ups and downs”.

I am thankful to all Parniske group members, especially Dr. Meritxell Antolín-Llovera and Dr. Griet den Herder (a special thanks for generating my stable *Lotus* lines) for experienced help and providing several constructs, further thanks to Martin Groth, Sylvia Singh, Kristina Haage, Martina Ried, Simone Hardel, Andreas Binder and Matthias Ellerbeck for supporting me with materials, protocols and discussions.

Thanks to Dr. Arthur Schüßler for your contribution to my paper and Dr. Andreas Brachmann for discussions about yeast and sequencing issues.

A thank you goes to all colleagues at the “third floor Genetics” (LMU, Munich) for all the little smiles.

Last, but not least, I would like to thank you, former colleagues at the ABC in Gödöllő and colleagues at the ELTE in Budapest.

Finally, I would like to thank my family, my friends and my flatmates for supporting me and loving me as I am.

References

Allen, N. S., Bennett, M. N., Cox, D.N., Shipley, A., Ehrhardt, D. W., Long, S.R. (1994). Effects of Nod factors on alfalfa root hair Ca^{2+} and H^{+} currents and cytoskeleton behavior. In Advances in Molecular Genetics of Plant-Microbe Interactions. Eds Daniels MJ, Downie JA, Osbourn AE (Kluwer Academic Publishers, Dordrecht, The Netherlands), pp 107–114.

Amor, B. B., Shaw, S. L., Oldroyd, G. E., Maillet, F., Penmetsa, R. V., Cook, D., Long, S. R., Denarie, J. and Gough, C. (2003). The NFP locus of *Medicago truncatula* controls an early step of Nod factor signal transduction upstream of a rapid calcium flux and root hair deformation. Plant J 34(4): 495-506.

Ane, J. M., Kiss, G. B., Riely, B. K., Penmetsa, R. V., Oldroyd, G. E., Ayax, C., Levy, J., Debelle, F., Baek, J. M., Kalo, P., Rosenberg, C., Roe, B. A., Long, S. R., Denarie, J. and Cook, D. R. (2004). Medicago truncatula DMI1 required for bacterial and fungal symbioses in legumes. Science 303(5662): 1364-1367.

Appleby, C. A., Tjepkema, J. D. and Trinick, M. J. (1983). Hemoglobin in a nonleguminous plant, parasponia: possible genetic origin and function in nitrogen fixation. Science 220(4600): 951-953.

Arrighi, J. F., Barre, A., Ben Amor, B., Bersoult, A., Soriano, L. C., Mirabella, R., de Carvalho-Niebel, F., Journet, E. P., Gherardi, M., Huguet, T., Geurts, R., Denarie, J., Rouge, P. and Gough, C. (2006). The *Medicago truncatula* lysin motif-receptor-like kinase gene family includes NFP and new nodule-expressed genes. Plant Physiol 142(1): 265-279.

Bariola, P. A., Retelska, D., Stasiak, A., Kammerer, R. A., Fleming, A., Hijri, M., Frank, S. and Farmer, E. E. (2004). Remorins form a novel family of coiled coil-forming oligomeric and filamentous proteins associated with apical, vascular and embryonic tissues in plants. Plant Mol Biol 55(4): 579-594.

Bauer, W., D. (1981) Infection of Legumes by Rhizobia. Ann. Rev. Plant Physiol. 32:407-449.

Bayle, V., Nussaume, L. and Bhat, R. A. (2008). Combination of novel green fluorescent protein mutant TSapphire and DsRed variant mOrange to set up a versatile in planta FRET-FLIM assay. Plant Physiol 148(1): 51-60.

Benedito, V. A., Torres-Jerez, I., Murray, J. D., Andriankaja, A., Allen, S., Kakar, K., Wandrey, M., Verdier, J., Zuber, H., Ott, T., Moreau, S., Niebel, A., Frickey, T., Weiller, G., He, J., Dai, X., Zhao, P. X., Tang, Y. and Udvardi, M. K. (2008). A gene expression atlas of the model legume Medicago truncatula. Plant J 55(3): 504-513.

Benschop, J. J., Mohammed, S., O'Flaherty, M., Heck, A. J., Slijper, M. and Menke, F. L. (2007). Quantitative phosphoproteomics of early elicitor signaling in Arabidopsis. Mol Cell Proteomics 6(7): 1198-1214.

Benson, D. R. and Silvester, W. B. (1993). Biology of Frankia strains, actinomycete symbionts of actinorhizal plants. Microbiol Rev 57(2): 293-319.

Bergersen, F. J. (1955). The cytology of bacteroids from root nodules of subterranean clover (Trifolium subterraneum L.). J Gen Microbiol 13(3): 411-419.

Bersoult, A., Camut, S., Perhald, A., Kereszt, A., Kiss, G. B. and Cullimore, J. V. (2005). Expression of the *Medicago truncatula* DM12 gene suggests roles of the symbiotic nodulation receptor kinase in nodules and during early nodule development. Mol Plant Microbe Interact 18(8): 869-876.

Bessueille, L., Sindt, N., Guichardant, M., Djerbi, S., Teeri, T. T. and Bulone, V. (2009). Plasma membrane microdomains from hybrid aspen cells are involved in cell wall polysaccharide biosynthesis. Biochem J 420(1): 93-103.

Bhat, R. A., Lahaye, T. and Panstruga, R. (2006). The visible touch: in planta visualization of protein-protein interactions by fluorophore-based methods. Plant Methods 2: 12.

Boisson-Dernier, A., Andriankaja, A., Chabaud, M., Niebel, A., Journet, E. P., Barker, D. G. and de Carvalho-Niebel, F. (2005). MtENOD11 gene activation during rhizobial infection and mycorrhizal arbuscule development requires a common AT-rich-containing regulatory sequence. Mol Plant Microbe Interact 18(12): 1269-1276.

Brewin, N. J. (1991). Development of the legume root nodule. Annu Rev Cell Biol 7: 191-226.

Broughton, W. J., Jabbouri, S. and Perret, X. (2000). Keys to symbiotic harmony. J Bacteriol 182(20): 5641-5652.

Burnie, D. (1994) Dictionary of Nature. Dorling Kindersley, London. ISBN: 0751351253.

Callaham, D. A. and Torrey, J. G. (1981). The structural basis for infection of root hairs of *Trifolium repens* by *Rhizobium*. *Can. J. Bot.* 59, 1647-1664.

Catoira, R., Galera, C., de Billy, F., Penmetsa, R. V., Journet, E. P., Maillet, F., Rosenberg, C., Cook, D., Gough, C. and Denarie, J. (2000). Four genes of *Medicago truncatula* controlling components of a nod factor transduction pathway. Plant Cell 12(9): 1647-1666.

Catoira, R., Timmers, A. C., Maillet, F., Galera, C., Penmetsa, R. V., Cook, D., Denarie, J. and Gough, C. (2001). The HCL gene of *Medicago truncatula* controls Rhizobium-induced root hair curling. Development 128(9): 1507-1518.

Charpentier, M., Bredemeier, R., Wanner, G., Takeda, N., Schleiff, E. and Parniske, M. (2008). Lotus japonicus CASTOR and POLLUX are ion channels essential for perinuclear calcium spiking in legume root endosymbiosis. Plant Cell 20(12): 3467-3479.

Colebatch, G., Desbrosses, G., Ott, T., Krusell, L., Montanari, O., Kloska, S., Kopka, J. and Udvardi, M. K. (2004). Global changes in transcription orchestrate metabolic differentiation during symbiotic nitrogen fixation in *Lotus japonicus*. Plant J 39(4): 487-512.

Dalton, D. A., Joyner, S. L., Becana, M., Iturbe-Ormaetxe, I. and Chatfield, J. M. (1998). Antioxidant defenses in the peripheral cell layers of legume root nodules. Plant Physiol 116(1): 37-43.

Dazzo, F. B., Truchet, G. L., Hollingsworth, R. I., Hrabak, E. M., Pankratz, H. S., Philip-Hollingsworth, S., Salzwedel, J. L., Chapman, K., Appenzeller, L., Squartini, A., Gerhold D. and Orgambide G. (1991). Rhizobium lipopolysaccharide modulates infection thread development in white clover root hairs. J Bacteriol 173(17): 5371-5384.

DeLong, A. (2006). Switching the flip: protein phosphatase roles in signaling pathways. Curr Opin Plant Biol 9(5): 470-477.

D'Haeze, W. and Holsters, M. (2002). Nod factor structures, responses, and perception during initiation of nodule development. Glycobiology 12(6): 79R-105R.

Diaz, C. L., Logman, T., Stam, H. C. and Kijne, J. W. (1995). Sugar-Binding Activity of Pea Lectin Expressed in White Clover Hairy Roots. Plant Physiol 109(4): 1167-1177.

Dixon, R., O., D. (1964). The structure of infection threads, bacteria and bacteroids in pea and clover root nodules. Arch. Mikrobiol. 48, 166.

Downie, J. A. and Walker, S. A. (1999). Plant responses to nodulation factors. Curr Opin Plant Biol **2**(6): 483-489.

Dunker, A. K., Oldfield, C. J., Meng, J., Romero, P., Yang, J. Y., Chen, J. W., Vacic, V., Obradovic, Z. and Uversky, V. N. (2008). The unfoldomics decade: an update on intrinsically disordered proteins. BMC Genomics 9 Suppl 2: S1.

Dyson, H. J. and Wright, P. E. (2005). Intrinsically unstructured proteins and their functions. Nat Rev Mol Cell Biol 6(3): 197-208.

Ehrhardt, D. W., Atkinson, E. M. and Long, S. R. (1992). Depolarization of alfalfa root hair membrane potential by Rhizobium meliloti Nod factors. Science 256(5059): 998-1000.

Ehrhardt, D. W., Wais, R. and Long, S. R. (1996). Calcium spiking in plant root hairs responding to Rhizobium nodulation signals. Cell 85(5): 673-681.

Endre, G., Kereszt, A., Kevei, Z., Mihacea, S., Kalo, P. and Kiss, G. B. (2002). A receptor kinase gene regulating symbiotic nodule development. Nature 417(6892): 962-966.

Esseling, J. J., Lhuissier, F. G. and Emons, A. M. (2003). Nod factor-induced root hair curling: continuous polar growth towards the point of nod factor application. Plant Physiol 132(4): 1982-1988.

Fahlgren, N., Howell, M. D., Kasschau, K. D., Chapman, E. J., Sullivan, C. M., Cumbie, J. S., Givan, S. A., Law, T. F., Grant, S. R., Dangl, J. L. and Carrington, J. C. (2007). High-throughput sequencing of Arabidopsis microRNAs: evidence for frequent birth and death of MIRNA genes. PLoS One 2(2): e219.

Fahraeus, G. (1957). The infection of clover root hairs by nodule bacteria studied by a simple glass slide technique. J Gen Microbiol 16(2): 374-381.

Farmer, E. E., Pearce, G. and Ryan, C. A. (1989). In vitro phosphorylation of plant plasma membrane proteins in response to the proteinase inhibitor inducing factor. Proc Natl Acad Sci USA 86(5): 1539-1542.

Felle, H. H., Kondorosi, E., Kondorosi, A. and Schultze, M. (1996). Rapid alkalinization in alfalfa root hairs in response to rhizobial lipochitooligosaccharide signals. Plant Journal 10(2): 295-301.

Ferguson, B. J., Indrasumunar, A., Hayashi, S., Lin, M. H., Lin, Y. H., Reid, D. E. and Gresshoff, P. M. (2010). Molecular analysis of legume nodule development and autoregulation. J Integr Plant Biol 52(1): 61-76.

Fisher, R. F. and Long, S. R. (1992). Rhizobium-plant signal exchange. Nature 357(6380): 655-660.

Fisher, R. F., Egelhoff, T. T., Mulligan, J. T. and Long, S. R. (1988). Specific binding of proteins from Rhizobium meliloti cell-free extracts containing NodD to DNA sequences upstream of inducible nodulation genes. Genes Dev 2(3): 282-293.

Fitter, A. H. (2005). Darkness visible: reflections on underground ecology. J. Ecol. 93, 231–243.

Foucher, F. and Kondorosi, E. (2000). Cell cycle regulation in the course of nodule organogenesis in *Medicago*. Plant Mol Biol 43(5-6): 773-786.

Gage, D. J. (2004). Infection and invasion of roots by symbiotic, nitrogen-fixing rhizobia during nodulation of temperate legumes. Microbiol Mol Biol Rev 68(2): 280-300.

Gamborg, O. L., Miller, R. A. and Ojima, K. (1968). Nutrient requirements of suspension cultures of soybean root cells. Exp Cell Res 50(1): 151-158.

Gherbi, H., Markmann, K., Svistoonoff, S., Estevan, J., Autran, D., Giczey, G., Auguy, F., Peret, B., Laplaze, L., Franche, C., Parniske, M. and Bogusz, D. (2008). SymRK defines a common genetic basis for plant root endosymbioses with arbuscular mycorrhiza fungi, rhizobia, and Frankiabacteria. Proc Natl Acad Sci USA 105: 4928-4932.

Gleason, C., Chaudhuri, S., Yang, T., Munoz, A., Poovaiah, B. W. and Oldroyd, G. E. (2006). Nodulation independent of rhizobia induced by a calcium-activated kinase lacking autoinhibition. Nature 441(7097): 1149-1152.

Good, A. G., Shrawat, A. K. and Muench, D. G. (2004). Can less yield more? Is reducing nutrient input into the environment compatible with maintaining crop production? Trends Plant Sci 9(12): 597-605.

Graham, P. H. and Vance, C. P. (2003). Legumes: importance and constraints to greater use. Plant Physiol 131(3): 872-877.

Groth, M. (2010). Genetic Analysis of Arbuscular Mycorrhiza Development in *Lotus japonicus*. PhD thesis. Fakultät für Biologie der Ludwig-Maximilians-Universität Munich, Ludwig-Maximilians-Universität, Munich Germany

Groth, M., Takeda, N., Perry, J., Uchida, H., Draxl, S., Brachmann, A., Sato, S., Tabata, S., Kawaguchi, M., Wang, T. L. and Parniske, M. (2010). NENA, a *Lotus japonicus* homolog of Sec13, is required for rhizodermal infection by arbuscular mycorrhiza fungi and rhizobia but dispensable for cortical endosymbiotic development. Plant Cell 22(7): 2509-2526.

Gualtieri, G. and Bisseling, T. (2000). The evolution of nodulation. Plant Mol Biol 42(1): 181-194.

Haney, C. H. and Long, S. R. (2010). Plant flotillins are required for infection by nitrogen-fixing bacteria. Proc Natl Acad Sci USA 107(1): 478-483.

Haney, C. H., Riely, B. K., Tricoli, D. M., Cook, D. R., Ehrhardt, D. W. and Long, S. R. (2011). Symbiotic rhizobia bacteria trigger a change in localization and dynamics of the Medicago truncatula receptor kinase LYK3. Plant Cell 23(7): 2774-2787.

Hayashi, T., Banba, M., Shimoda, Y., Kouchi, H., Hayashi, M. and Imaizumi-Anraku, H. (2010). A dominant function of CCaMK in intracellular accommodation of bacterial and fungal endosymbionts. Plant J 63(1): 141-154.

Heckmann, A. B., Lombardo, F., Miwa, H., Perry, J. A., Bunnewell, S., Parniske, M., Wang, T. L. and Downie, J. A. (2006). *Lotus japonicus* nodulation requires two GRAS domain regulators, one of which is functionally conserved in a non-legume. Plant Physiol 142(4): 1739-1750.

Heidstra, R., Geurts, R., Franssen, H., Spaink, H. P., Van Kammen, A. and Bisseling, T. (1994). Root Hair Deformation Activity of Nodulation Factors and Their Fate on *Vicia sativa*. Plant Physiol 105(3): 787-797.

Hirsch, A. M. (1992). Developmental biology of legume nodulation. New Phytol 122:211-237.

Hogslund, N., Radutoiu, S., Krusell, L., Voroshilova, V., Hannah, M. A., Goffard, N., Sanchez, D. H., Lippold, F., Ott, T., Sato, S., Tabata, S., Liboriussen, P., Lohmann, G. V., Schauser, L., Weiller, G. F., Udvardi, M. K. and Stougaard, J. (2009). Dissection of symbiosis and organ development by integrated transcriptome analysis of *Lotus japonicus* mutant and wild-type plants. PLoS One 4(8): e6556.

Hu, C. D., Chinenov, Y. and Kerppola, T. K. (2002). Visualization of interactions among bZIP and Rel family proteins in living cells using bimolecular fluorescence complementation. Mol Cell 9(4): 789-798.

Jarsch, I. K. and Ott, T. (2011). Perspectives on remorin proteins, membrane rafts, and their role during plant-microbe interactions. Mol Plant Microbe Interact 24(1): 7-12.

Jefferson, R. A., Kavanagh, T. A. and Bevan, M. W. (1987). GUS fusions: beta-glucuronidase as a sensitive and versatile gene fusion marker in higher plants. EMBO J 6(13): 3901-3907.

Johnsson, N. and Varshavsky, A. (1994). Split ubiquitin as a sensor of protein interactions in vivo. Proc Natl Acad Sci USA 91(22): 10340-10344.

Jones, K. M., Kobayashi, H., Davies, B. W., Taga, M. E. and Walker, G. C. (2007). How rhizobial symbionts invade plants: the Sinorhizobium-Medicago model. Nat Rev Microbiol 5(8): 619-633.

Journet, E. P., Pichon, M., Dedieu, A., de Billy, F., Truchet, G. and Barker, D. G. (1994). Rhizobium meliloti Nod factors elicit cell-specific transcription of the ENOD12 gene in transgenic alfalfa. Plant J 6(2): 241-249.

Kalo, P., Gleason, C., Edwards, A., Marsh, J., Mitra, R. M., Hirsch, S., Jakab, J., Sims, S., Long, S. R., Rogers, J., Kiss, G. B., Downie, J. A. and Oldroyd, G. E.

(2005). Nodulation signaling in legumes requires NSP2, a member of the GRAS family of transcriptional regulators. Science 308(5729): 1786-1789.

Kanamori, N., Madsen, L. H., Radutoiu, S., Frantescu, M., Quistgaard, E. M., Miwa, H., Downie, J. A., James, E. K., Felle, H. H., Haaning, L. L., Jensen, T. H., Sato, S., Nakamura, Y., Tabata, S., Sandal, N. and Stougaard, J. (2006). A nucleoporin is required for induction of Ca2+ spiking in legume nodule development and essential for rhizobial and fungal symbiosis. Proc Natl Acad Sci USA 103(2): 359-364.

Karimi, M., De Meyer, B. and Hilson, P. (2005). Modular cloning in plant cells. Trends Plant Sci 10(3): 103-105.

Kevei, Z., Lougnon, G., Mergaert, P., Horvath, G. V., Kereszt, A., Jayaraman, D., Zaman, N., Marcel, F., Regulski, K., Kiss, G. B., Kondorosi, A., Endre, G., Kondorosi, E. and Ane, J. M. (2007). 3-hydroxy-3-methylglutaryl coenzyme a reductase 1 interacts with NORK and is crucial for nodulation in Medicago truncatula. Plant Cell 19(12): 3974-3989.

Kijne, J., W., Bauchrowitz, M., A. and Diaz C., L. (1997). Root Lectins and Rhizobia. Plant Physiol. 115(3): 869–873.

Kistner, C. and Parniske, M. (2002). Evolution of signal transduction in intracellular symbiosis. Trends Plant Sci **7**(11): 511-518.

Kistner, C., Winzer, T., Pitzschke, A., Mulder, L., Sato, S., Kaneko, T., Tabata, S., Sandal, N., Stougaard, J., Webb, K. J., Szczyglowski, K. and Parniske, M. (2005). Seven Lotus japonicus genes required for transcriptional reprogramming of the root during fungal and bacterial symbiosis. Plant Cell 17(8): 2217-2229.

Klaus-Heisen, D., Nurisso, A., Pietraszewska-Bogiel, A., Mbengue, M., Camut, S., Timmers, T., Pichereaux, C., Rossignol, M., Gadella, T. W., Imberty, A., Lefebvre, B. and Cullimore, J. V. (2011). Structure-function similarities between a plant receptor-like kinase and the human interleukin-1 receptor-associated kinase-4. J Biol Chem 286(13): 11202-11210.

Koncz, C. and Shell, J. (1986). The promoter of TL-DNA gene 5 controls the tissue-specific expression of chimaeric genes carried by a novel type of *Agrobacterium* binary vector. Mol. Gen. Genet. 204:383-396.

Kosuta, S., Held, M., Hossain, M. S., Morieri, G., Macgillivary, A., Johansen, C., Antolin-Llovera, M., Parniske, M., Oldroyd, G. E., Downie, A. J., Karas, B. and Szczyglowski, K. (2011). *Lotus japonicus* symRK-14 uncouples the cortical and epidermal symbiotic program. Plant J 67(5): 929-940.

Lajoie, P., Goetz J. G., Dennis, J. W., Nobi, I.R. (2009). Lattices, rafts and scaffolds: domain regulation of receptor signaling at the plasma membrane. J Cell Biol 185(3):381-385.

Lazo, G. R., Stein, P. A. and Ludwig, R. A. (1991). A DNA transformation-competent Arabidopsis genomic library in Agrobacterium. Biotechnology 9(10): 963-967.

Lefebvre, B., Timmers, T., Mbengue, M., Moreau, S., Herve, C., Toth, K., Bittencourt-Silvestre, J., Klaus, D., Deslandes, L., Godiard, L., Murray, J. D., Udvardi, M. K., Raffaele, S., Mongrand, S., Cullimore, J., Gamas, P., Niebel,

A. and Ott, T. (2010). A remorin protein interacts with symbiotic receptors and regulates bacterial infection. Proc Natl Acad Sci USA 107(5): 2343-2348.

Lerouge, P., Roche, P., Faucher, C., Maillet, F., Truchet, G., Prome, J. C. and Denarie, J. (1990). Symbiotic host-specificity of Rhizobium meliloti is determined by a sulphated and acylated glucosamine oligosaccharide signal. Nature 344(6268): 781-784.

Levy, J., Bres, C., Geurts, R., Chalhoub, B., Kulikova, O., Duc, G., Journet, E. P., Ane, J. M., Lauber, E., Bisseling, T., Denarie, J., Rosenberg, C. and Debelle, F. (2004). A putative Ca2+ and calmodulin-dependent protein kinase required for bacterial and fungal symbioses. Science 303(5662): 1361-1364.

Limpens, E., Franken, C., Smit, P., Willemse, J., Bisseling, T. and Geurts, R. (2003). LysM domain receptor kinases regulating rhizobial Nod factor-induced infection. Science 302(5645): 630-633.

Lingwood, D. and Simons, K. (2010). Lipid rafts as a membrane-organizing principle. Science 327(5961): 46-50.

Liu, J., Elmore, J. M., Fuglsang, A. T., Palmgren, M. G., Staskawicz, B. J. and Coaker, G. (2009). RIN4 functions with plasma membrane H+-ATPases to regulate stomatal apertures during pathogen attack. PLoS Biol 7(6): e1000139.

Long, S. R. (1996). Rhizobium symbiosis: nod factors in perspective. Plant Cell 8(10): 1885-1898.

Madsen, E. B., Antolin-Llovera, M., Grossmann, C., Ye, J., Vieweg, S., Broghammer, A., Krusell, L., Radutoiu, S., Jensen, O. N., Stougaard, J. and Parniske, M. (2011). Autophosphorylation is essential for the in vivo function of the Lotus japonicus Nod factor receptor 1 and receptor-mediated signalling in cooperation with Nod factor receptor 5. Plant J 65(3): 404-417.

Madsen, E. B., Madsen, L. H., Radutoiu, S., Olbryt, M., Rakwalska, M., Szczyglowski, K., Sato, S., Kaneko, T., Tabata, S., Sandal, N. and Stougaard, J. (2003). A receptor kinase gene of the LysM type is involved in legume perception of rhizobial signals. Nature 425(6958): 637-640.

Madsen, L. H., Tirichine, L., Jurkiewicz, A., Sullivan, J. T., Heckmann, A. B., Bek, A. S., Ronson, C. W., James, E. K. and Stougaard, J. (2010). The molecular network governing nodule organogenesis and infection in the model legume Lotus japonicus. Nat Commun 1: 10.

Maekawa, T., Kusakabe, M., Shimoda, Y., Sato, S., Tabata, S., Murooka, Y. and Hayashi, M. (2008). Polyubiquitin promoter-based binary vectors for over-expression and gene silencing in Lotus japonicus. Mol Plant Microbe Interact 21(4): 375-382.

Markmann, K., Giczey, G., Parniske, M. (2008) Functional adaptation of a plant receptor-kinase paved the way for the evolution of intracellular root symbioses with bacteria. PLoS Biol 6(3):e68.

Marsh, J. F., Rakocevic, A., Mitra, R. M., Brocard, L., Sun, J., Eschstruth, A., Long, S. R., Schultze, M., Ratet, P. and Oldroyd, G. E. (2007). Medicago truncatula NIN is essential for rhizobial-independent nodule organogenesis induced by

autoactive calcium/calmodulin-dependent protein kinase. Plant Physiol 144(1): 324-335.

Mbengue, M., Camut, S., de Carvalho-Niebel, F., Deslandes, L., Froidure, S., Klaus-Heisen, D., Moreau, S., Rivas, S., Timmers, T., Herve, C., Cullimore, J. and Lefebvre, B. (2010). The *Medicago truncatula* E3 ubiquitin ligase PUB1 interacts with the LYK3 symbiotic receptor and negatively regulates infection and nodulation. Plant Cell 22(10): 3474-3488.

Mergaert, P., Uchiumi, T., Alunni, B., Evanno, G., Cheron, A., Catrice, O., Mausset, A. E., Barloy-Hubler, F., Galibert, F., Kondorosi, A. and Kondorosi, E. (2006). Eukaryotic control on bacterial cell cycle and differentiation in the Rhizobium-legume symbiosis. Proc Natl Acad Sci USA 103(13): 5230-5235.

Messinese, E., Mun, J. H., Yeun, L. H., Jayaraman, D., Rougé, P., Barre, A., Lougnon, G., Schornack, S., Bono, J. J., Cook, D. R. and Ané J. M. (2007) A Novel Nuclear Protein Interacts With the Symbiotic DMI3 Calcium- and Calmodulin-Dependent Protein Kinase of *Medicago truncatula.* Mol Plant Microbe Interact 20(8):912-921.

Middleton, P. H., Jakab, J., Penmetsa, R. V., Starker, C. G., Doll, J., Kalo, P., Prabhu, R., Marsh, J. F., Mitra, R. M., Kereszt, A., Dudas, B., VandenBosch, K., Long, S. R., Cook, D. R., Kiss, G. B. and Oldroyd, G. E. (2007). An ERF transcription factor in Medicago truncatula that is essential for Nod factor signal transduction. Plant Cell 19(4): 1221-1234.

Mitra, R. M., Gleason, C. A., Edwards, A., Hadfield, J., Downie, J. A., Oldroyd, G. E. and Long, S. R. (2004). A Ca2+/calmodulin-dependent protein kinase required for symbiotic nodule development: Gene identification by transcript-based cloning. Proc Natl Acad Sci USA 101(13): 4701-4705.

Miwa, H., Sun, J., Oldroyd, G. E. and Downie, J. A. (2006). Analysis of Nod-factor-induced calcium signaling in root hairs of symbiotically defective mutants of *Lotus japonicus*. Mol Plant Microbe Interact 19(8): 914-923.

Mongrand, S., Stanislas, T., Bayer, E. M., Lherminier, J. and Simon-Plas, F. (2010). Membrane rafts in plant cells. Trends Plant Sci 15(12): 656-663.

Mulligan, J. T. and Long, S. R. (1985). Induction of Rhizobium meliloti nodC expression by plant exudate requires nodD. Proc Natl Acad Sci USA 82(19): 6609-6613.

Mulligan, J. T. and Long, S. R. (1989). A family of activator genes regulates expression of Rhizobium meliloti nodulation genes. Genetics 122(1): 7-18.

Murray, J. D., Muni, R. R., Torres-Jerez, I., Tang, Y., Allen, S., Andriankaja, M., Li, G., Laxmi, A., Cheng, X., Wen, J., Vaughan, D., Schultze, M., Sun, J., Charpentier, M., Oldroyd, G., Tadege, M., Ratet, P., Mysore, K. S., Chen, R. and Udvardi, M. K. (2011). Vapyrin, a gene essential for intracellular progression of arbuscular mycorrhizal symbiosis, is also essential for infection by rhizobia in the nodule symbiosis of *Medicago truncatula*. Plant J 65(2): 244-252.

Mylona, P., Pawlowski, K. and Bisseling, T. (1995). Symbiotic Nitrogen Fixation. Plant Cell 7(7): 869-885.

Nap, J. P. and Bisseling, T. (1990). Developmental biology of a plant-prokaryote symbiosis: the legume root nodule. Science 250(4983): 948-954.

Newcomb, W., Sippell, D., Peterson R. L. (1979). The early morphogenesis of *Glycine max* and *Pisum sativum* root nodules. Canadian Journal of Botany, 57:(23) 2603-2616.

Ogura, T. and Wilkinson, A. J. (2001). AAA+ superfamily ATPases: common structure--diverse function. Genes Cells 6(7): 575-597.

Oldroyd, G. E. and Downie, J. A. (2004). Calcium, kinases and nodulation signalling in legumes. Nat Rev Mol Cell Biol 5(7): 566-576.

Oldroyd, G. E. and Long, S. R. (2003). Identification and characterization of nodulation-signaling pathway 2, a gene of *Medicago truncatula* involved in Nod factor signaling. Plant Physiol 131(3): 1027-1032.

Oldroyd, G. E., Murray, J. D., Poole, P. S. and Downie, J. A. (2011). The rules of engagement in the legume-rhizobial symbiosis. Annu Rev Genet 45: 119-144.

Ott, T., van Dongen, J. T., Gunther, C., Krusell, L., Desbrosses, G., Vigeolas, H., Bock, V., Czechowski, T., Geigenberger, P. and Udvardi, M. K. (2005). Symbiotic leghemoglobins are crucial for nitrogen fixation in legume root nodules but not for general plant growth and development. Curr Biol 15(6): 531-535.

Ovchinnikova, E., Journet, E. P., Chabaud, M., Cosson, V., Ratet, P., Duc, G., Fedorova, E., Liu, W., den Camp, R. O., Zhukov, V., Tikhonovich, I., Borisov, A., Bisseling, T. and Limpens, E. (2011). IPD3 controls the formation of nitrogen-fixing symbiosomes in pea and *Medicago* Spp. Mol Plant Microbe Interact 24(11): 1333-1344.

Parniske, M. (2008). Arbuscular mycorrhiza: the mother of plant root endosymbioses. Nat Rev Microbiol 6(10): 763-775.

Perret, X., Staehelin, C. and Broughton, W. J. (2000). Molecular basis of symbiotic promiscuity. Microbiol Mol Biol Rev 64(1): 180-201.

Perry, J. A., Wang, T. L., Welham, T. J., Gardner, S., Pike, J. M., Yoshida, S. and Parniske, M. (2003). A TILLING reverse genetics tool and a web-accessible collection of mutants of the legume *Lotus japonicus*. Plant Physiol 131(3): 866-871.

Peters, N. K., Frost, J. W. and Long, S. R. (1986). A plant flavone, luteolin, induces expression of Rhizobium meliloti nodulation genes. Science 233(4767): 977-980.

Pichon, M., Journet, E. P., Dedieu, A., de Billy, F., Truchet, G. and Barker, D. G. (1992). Rhizobium meliloti elicits transient expression of the early nodulin gene ENOD12 in the differentiating root epidermis of transgenic alfalfa. Plant Cell 4(10): 1199-1211.

Pii, Y., Astegno, A., Peroni, E., Zaccardelli, M., Pandolfini, T. and Crimi, M. (2009). The Medicago truncatula N5 gene encoding a root-specific lipid transfer protein is required for the symbiotic interaction with Sinorhizobium meliloti. Mol Plant Microbe Interact 22(12): 1577-1587.

Popp, C. and Ott, T. (2011). Regulation of signal transduction and bacterial infection during root nodule symbiosis. Curr Opin Plant Biol.

Prell, J. and Poole, P. (2006) Metabolic changes of rhizobia in legume nodules. Trends Microbiol 14: 161–168

Radutoiu, S., Madsen, L. H., Madsen, E. B., Felle, H. H., Umehara, Y., Gronlund, M., Sato, S., Nakamura, Y., Tabata, S., Sandal, N. and Stougaard, J. (2003). Plant recognition of symbiotic bacteria requires two LysM receptor-like kinases. Nature 425(6958): 585-592.

Radutoiu, S., Madsen, L. H., Madsen, E. B., Jurkiewicz, A., Fukai, E., Quistgaard, E. M., Albrektsen, A. S., James, E. K., Thirup, S. and Stougaard, J. (2007). LysM domains mediate lipochitin-oligosaccharide recognition and Nfr genes extend the symbiotic host range. EMBO J 26(17): 3923-3935.

Raffaele, S., Bayer, E., Lafarge, D., Cluzet, S., German Retana, S., Boubekeur, T., Leborgne-Castel, N., Carde, J. P., Lherminier, J., Noirot, E., Satiat-Jeunemaitre, B., Laroche-Traineau, J., Moreau, P., Ott, T., Maule, A. J., Reymond, P., Simon-Plas, F., Farmer, E. E., Bessoule, J. J. and Mongrand, S. (2009). Remorin, a solanaceae protein resident in membrane rafts and plasmodesmata, impairs potato virus X movement. Plant Cell 21(5): 1541-1555.

Raffaele, S., Mongrand, S., Gamas, P., Niebel, A. and Ott, T. (2007). Genome-wide annotation of remorins, a plant-specific protein family: evolutionary and functional perspectives. Plant Physiol 145(3): 593-600.

Redmond J. W., Batley M., Djordjevic M. A., Innes R. W., Kuempel P. L. and Rolfe B. G. (1986). Flavones induce expression of nodulation genes in *Rhizobium.* Nature 323: 632-635.

Reymond, P., Kunz, B., Paul-Pletzer, K., Grimm, R., Eckerskorn, C. and Farmer, E. E. (1996). Cloning of a cDNA encoding a plasma membrane-associated, uronide binding phosphoprotein with physical properties similar to viral movement proteins. Plant Cell 8(12): 2265-2276.

Roche, P., Debelle, F., Maillet, F., Lerouge, P., Faucher, C., Truchet, G., Denarie, J. and Prome, J. C. (1991). Molecular basis of symbiotic host specificity in Rhizobium meliloti: nodH and nodPQ genes encode the sulfation of lipo-oligosaccharide signals. Cell 67(6): 1131-1143.

Roth, L. E., Jeon, K. and Stacey, G. (1988). Homology in endosymbiotic systems: The term "symbiosome". In Molecular Genetics of Plant Microbe Interactions. American Phytopathology Society Press, St. Paul. Pp. 220-225.

Saito, K., Yoshikawa, M., Yano, K., Miwa, H., Uchida, H., Asamizu, E., Sato, S., Tabata, S., Imaizumi-Anraku, H., Umehara, Y., Kouchi, H., Murooka, Y., Szczyglowski, K., Downie, J. A., Parniske, M., Hayashi, M. and Kawaguchi, M. (2007). NUCLEOPORIN85 is required for calcium spiking, fungal and bacterial symbioses, and seed production in Lotus japonicus. Plant Cell 19(2): 610-624.

Sambrook, J. and Russell, D.W. (2001). *Molecular cloning a laboratory manual,* 3rd edition. Cold Spring Harbor Laboratory Press. Cold Spring Harbor.

Schauser, L., Roussis, A., Stiller, J. and Stougaard, J. (1999). A plant regulator controlling development of symbiotic root nodules. Nature 402(6758): 191-195.

Schultze, M. and Kondorosi, A. (1998). Regulation of symbiotic root nodule development. Annu Rev Genet 32: 33-57.

Schüßler, A., Schwarzott, D. and Walker, C. (2001). A new fungal phylum, the *Glomeromycota*: phylogeny and evolution. Mycol. Res. 105, 1413–1421.

Sharma, S.K., Christen, P., Goloubinoff, P. (2009). Disaggregating chaperones: an unfolding story. Curr Protein Pept Sci 10(5)432-446.

Sieberer, B. J., Timmers, A. C. and Emons, A. M. (2005). Nod factors alter the microtubule cytoskeleton in *Medicago truncatula* root hairs to allow root hair reorientation. Mol Plant Microbe Interact 18(11): 1195-1204.

Stagljar, I., Korostensky, C., Johnsson, N. and te Heesen, S. (1998). A genetic system based on split-ubiquitin for the analysis of interactions between membrane proteins in vivo. Proc Natl Acad Sci USA 95(9): 5187-5192.

Stougaard, J., Petersen, T. E. and Marcker, K. A. (1987). Expression of a complete soybean leghemoglobin gene in root nodules of transgenic Lotus corniculatus. Proc Natl Acad Sci USA 84(16): 5754-5757.

Stracke, S., Kistner, C., Yoshida, S., Mulder, L., Sato, S., Kaneko, T., Tabata, S., Sandal, N., Stougaard, J., Szczyglowski, K. and Parniske, M. (2002). A plant receptor-like kinase required for both bacterial and fungal symbiosis. Nature 417(6892): 959-962.

Stratil, T. F. (2010). Functional characterization of LjSYMREM1 and its protein domains. Diploma thesis. Fakultät für Biologie der Ludwig-Maximilians-Universität Munich, Ludwig-Maximilians-Universität, Munich Germany

Strauss, H. M. and Keller, S. (2008). Pharmacological interference with protein-protein interactions mediated by coiled-coil motifs. Handb Exp Pharmacol(186): 461-482.

Studer, D., Gloudemans, T., Franssen, H. J., Fischer, H. M., Bisseling, T. and Hennecke, H. (1987). Involvement of the Bacterial Nitrogen-Fixation Regulatory Gene (Nifa) in Control of Nodule-Specific Host-Plant Gene-Expression. European Journal of Cell Biology 45(1): 177-184.

Takeda, N., Kistner, C., Kosuta, S., Winzer, T., Pitzschke, A., Groth, M., Sato, S., Kaneko, T., Tabata, S., Parniske, M. (2007). Protease in plant root symbiosis. Phytochemistry 68(1):111-121.

Thornton, H. G. (1930) The early development of the root nodule of lucerne (*Medicago sativa* L). Ann. Bot.44: 385-392.

Timmers, A. C., Auriac, M. C. and Truchet, G. (1999). Refined analysis of early symbiotic steps of the Rhizobium-Medicago interaction in relationship with microtubular cytoskeleton rearrangements. Development 126(16): 3617-3628.

Tirichine, L., Imaizumi-Anraku, H., Yoshida, S., Murakami, Y., Madsen, L. H., Miwa, H., Nakagawa, T., Sandal, N., Albrektsen, A. S., Kawaguchi, M., Downie, A., Sato, S., Tabata, S., Kouchi, H., Parniske, M., Kawasaki, S. and Stougaard, J. (2006). Deregulation of a Ca2+/calmodulin-dependent kinase leads to spontaneous nodule development. Nature 441(7097): 1153-1156.

Tóth, K., Stratil, T. F., Madsen, E. B., Ye, J., Popp, C., Antolín-Llovera, M., Grossmann, C., Jensen, O. N., Schüßler, A., Parniske, M. and Ott T. (2011)

Functional domain analysis of the Remorin protein LjSYMREM1 in *Lotus japonicus*. Accepted in PLoS ONE.

van Brussel, A. A., Bakhuizen, R., van Spronsen, P. C., Spaink, H. P., Tak, T., Lugtenberg, B. J. and Kijne, J. W. (1992). Induction of pre-infection thread structures in the leguminous host plant by mitogenic lipo-oligosaccharides of Rhizobium. Science 257(5066): 70-72.

van Spronsen, P. C., Gronlund, M., Pacios Bras, C., Spaink, H. P. and Kijne, J. W. (2001). Cell biological changes of outer cortical root cells in early determinate nodulation. Mol Plant Microbe Interact 14(7): 839-847.

Vance, C., P. (2001). Symbiotic nitrogen fixation and phosphorus acquisition. Plant nutrition in a world of declining renewable resources. Plant Physiol 127(2): 390-397.

Vasse, J., de Billy, F., Camut, S. and Truchet, G. (1990). Correlation between ultrastructural differentiation of bacteroids and nitrogen fixation in alfalfa nodules. J Bacteriol 172(8): 4295-4306.

Voinnet, O., Rivas, S., Mestre, P. and Baulcombe, D. (2003). An enhanced transient expression system in plants based on suppression of gene silencing by the p19 protein of tomato bushy stunt virus. Plant J 33(5): 949-956.

Wan, X., Hontelez, J., Lillo, A., Guarnerio, C., van de Peut, D., Fedorova, E., Bisseling, T. and Franssen, H. (2007). Medicago truncatula ENOD40-1 and ENOD40-2 are both involved in nodule initiation and bacteroid development. J Exp Bot 58(8): 2033-2041.

Ward, H. M. (1887). On the Tubercular Swellings on the Roots of *Vicia faba*. Phil. Trans. R. Soc. Lond. B 178:539-562.

White, P. J. and Brown, P. H. (2010). Plant nutrition for sustainable development and global health. Ann Bot 105(7): 1073-1080.

White, S. R. and Lauring, B. (2007). AAA+ ATPases: achieving diversity of function with conserved machinery. Traffic 8(12): 1657-1667.

Whitehead, L. F. and Day D. A. (1997). The peribacteroid membrane. Physiologia Plantarum 100:30-44.

Widjaja, I., Naumann, K., Roth, U., Wolf, N., Mackey, D., Dangl, J. L., Scheel, D. and Lee, J. (2009). Combining subproteome enrichment and Rubisco depletion enables identification of low abundance proteins differentially regulated during plant defense. Proteomics 9(1): 138-147.

Wright, P. E. and Dyson, H. J. (1999). Intrinsically unstructured proteins: re-assessing the protein structure-function paradigm. J Mol Biol 293(2): 321-331.

Yano, K., Shibata, S., Chen, W. L., Sato, S., Kaneko, T., Jurkiewicz, A., Sandal, N., Banba, M., Imaizumi-Anraku, H., Kojima, T., Ohtomo, R., Szczyglowski, K., Stougaard, J., Tabata, S., Hayashi, M., Kouchi, H. and Umehara, Y. (2009). CERBERUS, a novel U-box protein containing WD-40 repeats, is required for formation of the infection thread and nodule development in the legume-Rhizobium symbiosis. Plant J 60(1): 168-180.

Yano, K., Yoshida, S., Muller, J., Singh, S., Banba, M., Vickers, K., Markmann, K., White, C., Schuller, B., Sato, S., Asamizu, E., Tabata, S., Murooka, Y., Perry, J., Wang, T. L., Kawaguchi, M., Imaizumi-Anraku, H., Hayashi, M. and Parniske, M. (2008). CYCLOPS, a mediator of symbiotic intracellular accommodation. Proc Natl Acad Sci USA 105(51): 20540-20545.

Yokota, K., Fukai, E., Madsen, L. H., Jurkiewicz, A., Rueda, P., Radutoiu, S., Held, M., Hossain, M. S., Szczyglowski, K., Morieri, G., Oldroyd, G. E., Downie, J. A., Nielsen, M. W., Rusek, A. M., Sato, S., Tabata, S., James, E. K., Oyaizu, H., Sandal, N. and Stougaard, J. (2009). Rearrangement of actin cytoskeleton mediates invasion of *Lotus japonicus* roots by *Mesorhizobium loti*. Plant Cell 21(1): 267-284.

Yoshida, S. and Parniske, M. (2005). Regulation of plant symbiosis receptor kinase through serine and threonine phosphorylation. J Biol Chem 280(10): 9203-9209.

Zhang, J., Subramanian, S., Stacey, G. and Yu, O. (2009). Flavones and flavonols play distinct critical roles during nodulation of *Medicago truncatula* by *Sinorhizobium meliloti*. Plant J 57(1): 171-183.

Zheng, Z. L. (2009). Carbon and nitrogen nutrient balance signaling in plants. Plant Signal Behav 4(7): 584-591.

Zhu, H., Chen, T., Zhu, M., Fang, Q., Kang, H., Hong, Z. and Zhang, Z. (2008). A novel ARID DNA-binding protein interacts with SymRK and is expressed during early nodule development in Lotus japonicus. Plant Physiol 148(1): 337-347.

Web sources

[1] *Lotus* database at the Kazusa DNA Research Institute (2011); www.kazusa.or.jp/lotus

[2] The Lotus Transcript Profiling Resource (2010); http://cgi-www.cs.au.dk/cgi-compbio/Niels/index.cgi?affy_id=chr4.CM0558.48_at%0D%0A++++&page=pp

[3] The Samuel Roberts Noble Foundation (2010); www.noble.org

[4] Parniske Lab Plant and Seed Database (2010); www.gi.bio.lmu.de/psdb/lotus/lo_pm

[5] Zope Research Architecture (ZopRA) (2010); http://www.zopra.de/

[6] NCBI/BLAST Home at the NCBI (2011); (National Center for Biotechnology Information); http://blast.ncbi.nlm.nih.gov/Blast.cgi?CMD=Web&PAGE_TYPE=BlastHome

[7] InterProScan (2011); http://www.ebi.ac.uk/Tools/pfa/iprscan/

[8] SMART (a Simple Modular Architecture Research Tool) (2011); http://smart.embl-heidelberg.de/

Appendix

Table A1: Strains used in this study

Species	Strain	Resistance/Auxo-trophic marker	Growth conditions	Purpose of use
Bacteria				
Agrobacterium rhizogenes	AR1193	Rif, Carb	28°C	Hairy root induction
Agrobacterium tumefaciens	AGL1	Rif, Carb	28°C	Stable transfomation
Agrobacterium tumefaciens	GV3101	Rif, Gent, Kan	28°C	Transient tobacco leaves infiltration
Escherichia coli	DH5α	no	37°C	Plasmid multiplying and maintenance
Escherichia coli	TOP10	no	37°C	Plasmid multiplying and maintenance
Escherichia coli	DB3.1	no	37°C	Plasmid multiplying and maintenance
Escherichia coli	XL1-Blue	no	37°C	Plasmid multiplying and maintenance
Mesorhizobium loti	MAFF 303099, expressing DsRed	Gent	28°C	*L. japonicus* infection
Yeast				
Saccharomyces cerevisiae	NMY32	Leu, Trp	28-30°C	Interaction studies

Table A2: Plant species and lines used in this study

Species	Ecotype	Background	Selection marker	Purpose of use
Lotus japonicus	Gifu B-129	Wild-type	-	Hairy root experiments
Lotus japonicus	Gifu B-129	EMS population	-	Assessing phenotype
Lotus japonicus	MG-20	Wild-type	-	Stable transformation
Lotus japonicus	MG-20	*pLjSYMREM1gLjSYM REM1:YFP*	hyg	Protein localization
Nicotiana benthamiana	-	Wild-type	-	Interaction studies

Table A3: Constructs used in this study

Construct name	Vector backbone	Insert	Selection marker	Purpose of use	Origin
TOPO: LjSYMREM1	pENTR/D-TOPO	LjSYMREM1 cDNA	Kan^R	Entry clone for subcloning	This study
TOPO: pLjSYMREM1 gLjSYMREM1	pENTR/D-TOPO	975bp pLjSYMREM1 + genomic LjSYMREM1	Kan^R	Entry clone for subcloning	This study
pDONR207:NFR1	pDONR207	NFR1 cDNA	$Gent^R$	Entry clone for subcloning	Aarhus, Denmark
pDONR207:NFR5	pDONR207	NFR5 cDNA	$Gent^R$	Entry clone for subcloning	Aarhus, Denmark
pGEM-T:975bp pLjSYMREM1	pGEM-T easy	975 bp LjSYMREM1 promoter	$Carb^R$	Clone for subcloning	This study
pGEM-T:2kb pLjSYMREM1	pGEM-T easy	2 kb LjSYMREM1 promoter	$Carb^R$	Clone for subcloning	This study
LjSYMREM1: CFP	pAM-PAT binary vector*	LjSYMREM1 cDNA	$Carb^R$	Protein localization *in planta*	This study
LjSYMREM1: YFP_N	pAM-PAT binary vector*	LjSYMREM1 cDNA	$Carb^R$	BiFC studies *in planta*	This study
LjSYMREM1: YFP_C	pAM-PAT binary vector*	LjSYMREM1 cDNA	$Carb^R$	BiFC studies *in planta*	This study
YFP_N: MtSYMREM1	pAM-PAT binary vector*	MtSYMREM1 cDNA	$Carb^R$	BiFC studies *in planta*	T. Ott#
YFP_C: MtSYMREM1	pAM-PAT binary vector*	MtSYMREM1 cDNA	$Carb^R$	BiFC studies *in planta*	T. Ott#
MtSYMREM1: YFP_N	pAM-PAT binary vector*	MtSYMREM1 cDNA	$Carb^R$	BiFC studies *in planta*	Claudia Popp#
MtSYMREM1: YFP_C	pAM-PAT binary vector*	MtSYMREM1 cDNA	$Carb^R$	BiFC studies *in planta*	Claudia Popp#
NFR1: YFP	pAM-PAT binary vector*	NFR1 cDNA	$Carb^R$	Protein localization *in planta*	This study
NFR5: YFP	pAM-PAT binary vector*	NFR5 cDNA	$Carb^R$	Protein localization *in planta*	This study
NFR1: YFP_C	pAM-PAT binary vector*	NFR1 cDNA	$Carb^R$	BiFC studies *in planta*	This study
NFR1: YFP_N	pAM-PAT binary vector*	NFR1 cDNA	$Carb^R$	BiFC studies *in planta*	This study
NFR5: YFP_C	pAM-PAT binary vector*	NFR5 cDNA	Carb	BiFC studies *in planta*	This study
NFR5: YFP_N	pAM-PAT binary vector*	NFR5 cDNA	Carb	BiFC studies *in planta*	This study

Construct name	Vector backbone	Insert	Selection marker	Purpose of use	Origin
SYMRK: YFP_C	pAM-PAT binary vector*	SYMRK cDNA	Carb	BiFC studies *in planta*	M. Antolín-Llovera#
SYMRK: YFP_N	pAM-PAT binary vector*	SYMRK cDNA	Carb	BiFC studies *in planta*	M. Antolín-Llovera#
pLjSYMREM1 gLjSYMREM1: YFP	pH7YWG2.0 w/o 35S**	975bp pLjSYMREM1 + genomic LjSYMREM1	Spec/ Hyg	Protein localization in Lj roots	This study
pUb:gwy:mOrange	pUb:gwy***	Gwy:mOrange	Kan/Hyg	Binary vector for protein localization	Modified in this study
pUb:LjSYMREM1	pUb:gwy:mOrange	LjSYMREm1: mOrange	Kan/Hyg	Protein localization in Lj roots and OE studies	This study

*Lefebvre B, Timmers T, Mbengue M, Moreau S, Herve C, et al. (2010). A remorin protein interacts with symbiotic receptors and regulates bacterial infection. Proc Natl Acad Sci U S A 107: 2343-2348.

**Karimi M, De Meyer B, Hilson P (2005). Modular cloning in plant cells. Trends Plant Sci 10: 103-105.

***Maekawa T, Kusakabe M, Shimoda Y, Sato S, Tabata S, et al. (2008). Polyubiquitin promoter-based binary vectors for over-expression and gene silencing in *Lotus japonicus*. Mol Plant Microbe Interact 21: 375-382.

Institute of Genetics, LMU, Munich

OE – over-expression

Table A4: Plasmids used for interaction studies in yeast assay

Backbone vector	Insert	Auxotrophic marker	Antibiotic resistance	Origin
Baits				
pCCW-Alg5	Alg5:Cub:LexA-VP16	Leu2	Kan^R	Provided by the manufacturer
pCCW:LjSYMREM1	LjSYMREM1:Cub: LexA-VP16	Leu2	Kan^R	Created in this study
pBT3-N: LjSYMREM1	LexA-VP16: Cub:LjSYMREM1	Leu2	Kan^R	Created in this study
pBT3-C:NFR5	NFR5:Cub: LexA-VP16	Leu2	Kan^R	Provided by M. Antolín-Llovera
pTMBV4:NFR1	NFR1:Cub: LexA-VP16	Leu2	Kan^R	Provided by M. Parniske
pTMBV4:SYMRK	SYMRK:Cub: LexA-VP16	Leu2	Kan^R	Provided by M. Parniske
Preys				
pAI-Alg5	Alg5:NubI	Trp	Amp^R	Provided by the manufacturer
pDL2-Alg5	Alg5:NubG	Trp	Amp^R	Provided by the manufacturer
pDL2xN: LjSYMREM1	LjSYMREM1:NubG	Trp	Amp^R	Created in this study
pDSL-Nx: LjSYMREM1	NubG:LjSYMREM1	Trp	Amp^R	Created in this study
pDL2xN:NFR1	NFR1:NubG	Trp	Amp^R	Provided by M. Parniske
pDL2xN:NFR5	NFR5:NubG	Trp	Amp^R	Provided by M. Parniske
pDL2xN:SYMRK	SYMRK:NubG	Trp	Amp^R	Provided by M. Parniske
pDL2Nx: cDNA-library	NubG:cDNA	Trp	Amp^R	Provided by M. Parniske
pDSL-Nx	No insert	Trp	Amp^R	DualMEMBRANE

Table A5: Primers used in this study

Primer name	Sequence	Amplicon	Restriction site included	Cloned into vector
LjsymREM1prom2k_1F	5´AAGCTTCAGAAGCAGCCAAGGAGATG 3´	2kb pLjSYMREM1	HindIII	pGEM-T
LjsymREM1prom1k_1F	5´AAGCTTCGCATGTAGATTCTCTGAGG 3´	975bp pLjSYMREM1	HindIII	pGEM-T
LjsymREM1prom_1R	5´GTGTGTGCTAGTTAACATAGGATCC 3´	pLjSYMREM1	BamHI	pGEM-T
LjsymREM1prom1k_FwTopo	5´caccCGCATGTAGATTCTCTGA 3´	975bp pLjSYMREM1	no	pENTR/D-TOPO
LjsymREM1prom_Rev	5´TATGTTAACTAGCACACACTTAGA 3´	pLjSYMREM1	no	pENTR/D-TOPO
LjSYMREM1_TOPO1F	5´caccATGGGAGAAGAAGAGACCAAAC 3´	LjSYMREM1	no	pENTR/D-TOPO
LjSYMREM1_TOPO1R	5´TTAAAAGCTGAAGTTGAAGCAT 3´	LjSYMREM1	no	pENTR/D-TOPO
LjSymrem1_Topo2R	5´AAAGCTGAAGTTGAAGCATGAC 3´	LjSYMREM1	no	pENTR/D-TOPO
LjSYMREM1_pDSL-Nx Fw	5´TAGGCCATTACGGCCATGGGAGAAGAAGA GACCAAA 3´	LjSYMREM1	SfiI	pDSL-Nx and pBT3-N ; SUS vectors
LjSYMREM1_pDSL-Nx Rev	5´TAGGCCGAGGCGGCCGTTAAAAGCTGAAGTTG AAGCATG 3´	LjSYMREM1	SfiI	pDSL-Nx ; SUS vector
LjSYMR1_Rev_SfiI	5´TTGGCCGAGGCGGCCTTTTAAAAGCTGAAGTT GAAGCATGA 3´	LjSYMREM1	SfiI	pBT3-N ; SUS vector
GWYmOrange_FwXbaI	5´TTGTCTAGAACAAGTTTGTACAAAAAAGCTGA AC 3´	GWYcasette:mOrange	XbaI	pUb-gwy-HYG binary plant vector
GWYmOrange_RevKpnI	5´TTGGTACCTTACTTGTACAGCTCGTCCATGC 3´	GWYcasette:mOrange	KpnI	pUb-gwy-HYG binary plant vector
LjATPase_pDSL-NxFw	5´TAGGCCATTACGGCCATGGCGCCAATCGTTC AGA 3´	AAA+ATPase core domain	SfiI	pDSL-Nx ; SUS vector
LjATPase_pDSL-NxRev	5´TAGGCCGAGGCGGCCGTCAGGTCCTTGAAGAA ATGTGAGA 3 ´	AAA+ATPase core domain	SfiI	pDSL-Nx ; SUS vector

Primers used in this study

Primer name	Sequence	Amplicon	Restriction site included	Cloned into vector
LjN5_pDSL-NxFw	5´TAGGCCATTACGGCCATGGCACAGTCTA GTGGCA 3´	MtN5-like	SfiI	pDSL-Nx ; SUS vector
LjN5_pDSL-NxRev	5´TAGGCCGAGGCGGCCGTCACTGACATTC CGGAGGT 3´	MtN5-like	SfiI	pDSL-Nx ; SUS vector
LjPEPT_pDSL-NxFw	5´TAGGCCATTACGGCCATGAATTTCAAGTT TTTTACTGCT 3´	PeptidaseA1	SfiI	pDSL-Nx ; SUS vector
LjPEPT_pDSL-NxRev	5´TAGGCCGAGGCGGCCGCTAGTTACAAAG TTCACGGGCT 3´	PeptidaseA1	SfiI	pDSL-Nx ; SUS vector
LjLTP_pDSL-NxFw	5´TAGGCCATTACGGCCATGGCTTCCAAGG CTGCTAT 3´	LTP	SfiI	pDSL-Nx ; SUS vector
LjLTP_pDSL-NxRev	5´TAGGCCGAGGCGGCCGTTAATAGCATAC GAATCCCTTAG 3´	LTP	SfiI	pDSL-Nx ; SUS vector
LjPhosphatase_pDSL-NxFw	5´TAGGCCATTACGGCCATGGATCCCGCCGT ACCGT 3´	Phosphatase	SfiI	pDSL-Nx ; SUS vector
LjPhosphatase_pDSL-NxRev	5´TAGGCCGAGGCGGCCGTTAAGAAATATA ATACATTGGGTT 3´	Phosphatase	SfiI	pDSL-Nx ; SUS vector
LjGPX_pDSL-NxFw	5´TAGGCCATTACGGCCATGGCTGAACAAA CCTCCAAATCT 3´	GPX	SfiI	pDSL-Nx ; SUS vector
LjGPX_pDSL-NxRev	5´TAGGCCGAGGCGGCCGTCAAGAAGATTG TAAGAGCTTCT 3´	GPX	SfiI	pDSL-Nx ; SUS vector

Primers used in this study

Primer name	Sequence	Purpose of use
dslNx_seqFw	5´AGTCGAAAATTCAAGACAAGG 3´	Forward sequencing of inserts in SUS vectors : pDSL-Nx and pDL2-Nx
dslNx_seqRev	5´GTGAATGTAAGCGTGACATAACT 3´	Reverse sequencing of inserts in SUS vectors : pDSL-Nx, pDL2-Nx and pBT3-N
pBT3-N_seqFw	5´CAGAAGGAGTCCACCTTACA 3´	Forward sequencing of inserts in SUS vectors : pBT3-N
LjSYMREM1_TOPO1F	5´caccATGGGAGAAGAAGAGACCAAAC 3´	Genotyping of *pLjSYMREM1:gLjSYMREM1:YFP* Lj lines and EMS mutagenized Lj lines
YFP_rev	5´GTTTAAACTTACTTGTCAGCTCGTCCATGC 3´	Genotyping of *pLjSYMREM1:gLjSYMREM1:YFP* Lj lines
LjSYMREM1_TOPO1R	5´TTAAAAGCTGAAGTTGAAGCAT 3´	Genotyping of EMS mutagenized Lj lines
M13Fw	5´GTAAAACGACGGCCAG 3´	Colony PCR and sequencing of TOPO entry clones
M13Rev	5´CAGGAAACAGCTATGAC 3´	Colony PCR and sequencing of TOPO entry clones
SP6 (fw)	5´ATTTAGGTGACACTATAG 3´	Sequencing of pGEM-T clones
T7 (rev)	5´TAATACGACTCACTATAGGG 3´	Sequencing of pGEM-T clones